

Electronic Thesis and Dissertation Repository

2-7-2013 12:00 AM

Carboxylic Acid Functionalized Butyl Rubber: From Synthesis to Applications

Matthew John McEachran
The University of Western Ontario

Supervisor
Dr. Elizabeth R. Gillies
The University of Western Ontario

Graduate Program in Chemistry
A thesis submitted in partial fulfillment of the requirements for the degree in Master of Science
© Matthew John McEachran 2013

Follow this and additional works at: <https://ir.lib.uwo.ca/etd>

 Part of the [Materials Chemistry Commons](#), [Medicinal-Pharmaceutical Chemistry Commons](#), and the [Polymer Chemistry Commons](#)

Recommended Citation

McEachran, Matthew John, "Carboxylic Acid Functionalized Butyl Rubber: From Synthesis to Applications" (2013). *Electronic Thesis and Dissertation Repository*. 1117.
<https://ir.lib.uwo.ca/etd/1117>

This Dissertation/Thesis is brought to you for free and open access by Scholarship@Western. It has been accepted for inclusion in Electronic Thesis and Dissertation Repository by an authorized administrator of Scholarship@Western. For more information, please contact wlsadmin@uwo.ca.

Carboxylic Acid Functionalized Butyl Rubber: From Synthesis to Applications

(Spine title: Carboxylic Acid Functionalized Butyl Rubber)

(Thesis format: Integrated Article)

by

Matthew John McEachran

Graduate Program in Chemistry

A thesis submitted in partial fulfillment
of the requirements for the degree of
Master of Science

The School of Graduate and Postdoctoral Studies
The University of Western Ontario
London, Ontario, Canada

© Matthew John McEachran 2013

THE UNIVERSITY OF WESTERN ONTARIO
School of Graduate and Postdoctoral Studies

CERTIFICATE OF EXAMINATION

Supervisor

Examiners

Dr. Elizabeth Gillies

Dr. Leonard Luyt

Dr. Martin Stillman

Dr. Paul Charpentier

The thesis by

Matthew John McEachran

entitled:

Carboxylic Acid Functionalized Butyl Rubber: From Synthesis to Applications

is accepted in partial fulfillment of the
requirements for the degree of
Master of Science

Date

Chair of the Thesis Examination Board

Abstract

Butyl Rubber (RB) is a copolymer of isobutylene (IB) with small percentages of isoprene (IP). Typically these IP units serve as sites for the covalent cross-linking of the rubber, but they can also serve as sites to further functionalize RB. These modifications can expand the potential applications of RB. This thesis describes the synthesis of carboxylic acid functionalized RB and some properties and applications of these materials. Several avenues of RB functionalization were studied such as cyclic anhydride ring opening, thiol-ene chemistry, ring opening polymerization and ATRP graft polymerizations to provide RB with varying carboxylic acid content. The most successful methods were the cyclic anhydride ring opening and ATRP polymerization of *tert*-butyl methacrylate followed by removal of the *tert*-butyl group. The adhesion of the resulting polymers to metal surfaces was studied and it was found that the carboxylic acids as well as other oxygenated rubber derivatives leading up to them led to enhanced adhesion. They also provided compatibilization properties that allowed for the deposition of hydrophilic polymers on butyl rubber. Lastly, the anti-proliferative drug Paclitaxel was covalently conjugated to the carboxylic acid functionalized rubber to provide a sustained release in comparison to physically encapsulated drug, leading to promising potential in stent coating applications.

Keywords

butyl rubber, cyclic anhydride ring opening, thiol-ene, ATRP, paclitaxel, drug release, surface adhesion, compatibilization, stent coating

Acknowledgments

First and foremost I would like to thank Dr. Elizabeth Gillies for her guidance and motivation throughout my graduate career. A special thanks Dr. Gillies for her constant support through my leave of absence after my accident. The research and life skills learned within the Gillies lab will surely carry with me in my career. I would also like to thank LANXESS Inc. for their financial support as well as their guidance in research. A special thanks goes to Lorenzo Ferrari for his constant positivity and support of the research from the Gillies lab. Also, a thanks is required to Brianna Binder at LANXESS Inc. for her assistance with the surface adhesion testing. I would also like to thank the many LANXESS Inc. employees that came in and out of the project; all of you have impacted this research project.

I would like to thank all of the past and current members of the Gillies group for making my graduate career a truly memorable experience. I would like to thank Dr. Colin Bonduelle for my training and support at the beginning of my Masters. From the group I would also like to thank Solmaz Karamadoust, Bethany Turowec (cell work) and our technician, Aneta Borecki (HPLC and SEC).

I also want to thank my thesis examiners Dr. Luyt, Dr. Stillman and Dr. Charpentier, for taking the time to read my thesis. I would also like to thank the support staff here at Western: Dr. Wilans in the NMR room for his continued assistance, Dr. Nie at Surface Science Western for his assistant in imaging and training on the AFM, Dr. Ragogna and group for use/training of his instruments, all of the chemstores staff, and our graduate secretary, Darlene McDonald for making sure I was up to date on things.

On a personal note I would like to thank my family for their continued support and words of encouragement. My study and work habits were learned from you and I know you are very proud of me and my accomplishments, without you none of this would have been possible. Lastly I would like to thank my better half, Lenka, you are there everyday listening to my ramblings and giving me advice. You make me a better person and that is shown everyday. Lubim ta.

Table of Contents

CERTIFICATE OF EXAMINATION	ii
Abstract	iii
Acknowledgments	iv
Table of Contents	v
List of Tables	viii
List of Figures	ix
List of Schemes	xii
List of Appendices	xiii
List of Abbreviations	xv
Chapter 1	1
Polymers used in the production in biomaterials	1
1.1 General Introduction	1
1.2 Vascular Stents	2
1.3 Butyl Rubber	8
1.3.1 Introduction	8
1.3.2 Synthesis	9
1.3.3 Chemical & Physical Properties	10
1.3.4 Modifications of Butyl Rubber	12
1.3.5 Applications	15
1.4 Motivation and Goals of Thesis	18
1.5 References	19
Chapter 2	28
2 Synthesis of Acid functionalized Butyl Rubber	28
2.1 Introduction	28

2.2 Results and Discussion	32
2.2.1 Cyclic Anhydride Ring-Opening	32
2.2.2 Thiol-ene “Click” Chemistry	35
2.2.3 Synthesis of Poly(carboxylic acid) Functionalized RB	39
2.3 Conclusions	43
2.4 Experimental	44
2.5 References	47
Chapter 3	50
3 Improvements to the Physical Properties of Butyl Rubber	50
3.1 Introduction	50
3.2 Results and Discussion	52
3.2.1 The application of oxygenated RBs as compatibilizing layers	52
3.2.2 Measurement of the adhesion of RB derivatives to a stainless steel substrate	57
3.3 Conclusions	58
3.4 Experimental	59
3.5 References	61
Chapter 4	64
4 Conjugation and Release of Paclitaxel from Butyl Rubber films	64
4.1 Introduction	64
4.2 Results and Discussion	65
4.3 Conclusions	75
4.4 Experimental	76
4.5 References	79
Chapter 5	82
5 Conclusions	82

5.1 Concluding remarks and future directions.....	82
Appendices.....	84
Curriculum Vitae	99

List of Tables

Table 1.3.1 Physical properties of RB ⁵⁶	11
Table 1.3.2 Diffusivity of several gases in RB and NR at 25 °C ⁵⁷	11
Table 2.2.1 A summary of the cyclic anhydrides used to create carboxylic acid modified RB. Each anhydride has different electronics, ring sizes and degrees of saturation.....	32
Table 2.2.2 Reaction conditions and results for the photoinitiated thiol-ene reaction between polymer 2.3 and TGAc.	37
Table 2.2.3 Molecular weight data collected using SEC for the various equivalents of <i>tert</i> -butyl methacrylate co-polymers polymerized from initiator 2.8. M _w and M _n are given relative to polystyrene standards.....	41
Table 2.2.4 Data collected from TGA analysis and converted to degree of polymerization..	41
Table 3.2.1 Tabulated data of static contact angles, film thickness and roughness from AFM for the laminates of 3.2a, 3.3a, 3.4a coated on 3.1a.....	55
Table 3.2.2 Tabulated data of static contact angles, film thickness and roughness from AFM for the PEO coated onto RB samples.....	56
Table 3.2.3 Surface adhesion data obtained on the Tel-Tak system with a stainless steel substrate for the different oxygenated RBs.....	58
Table 4.2.1 Description of the samples used in the release study.....	69

List of Figures

Figure 1.2.1 Cross-sectional images of porcine coronary arteries with stent explants, a) a polycarbonate urethane-coated stent exhibiting substantial inflammation and proliferation (2 months), b) a bare metal stent at 3 months showing some restenosis and c) poly(styrene)-co-poly(isobutylene)-co-poly(styrene) (SIBS) coated stent at 180 days showing resilience ⁹	3
Figure 1.2.2 Function of Sirolimus and Paclitaxel in halting cell proliferation and different points of the cell cycle as the body identifies the arterial injury ¹⁷	4
Figure 1.2.3 Control of drug release via a) control of wt.% of drug to polymer ²⁴ and b) manipulation of the SIBS backbone by the introduction of hydrophilic entities i.e. poly(styrene-co-maleic anhydride (SMA) ²⁶	6
Figure 1.2.4 Chemical composition of drug/polymer for the two commercialized DES a) TAXUS and b) CYPHER. c) through e) show SEMs of a DES coated with 25% PTx/ 30% SMA/ 45% SIBS c) unexpanded stent at X40 magnification d) X40 magnification of an expanded stent e) X200 magnification of an expanded stent ²⁶	7
Figure 1.3.1 Fluorescence confocal microscopy images (543nm) of thin films (spin-cast at 20 mg/mL from CH ₂ Cl ₂) following adsorption of a rhodamine-fibrinogen conjugate. Images represent different wt.% of PEO grafted to the RB backbone; a) 2%, b) 4%, c) 6%, d) 12%, e) 24% and f) 34% ⁷⁸	16
Figure 1.3.2 a) Evaluation of cell growth on surfaces. (a) RB, (b) epoxidized RB coated with PEO, (c) control surface of silane-functionalized PEO grafted on glass, (d) PEO-coated silicon wafer following HHIC b) Relative fluorescence obtained by confocal microscopy corresponding to the adsorption of a fluorescently labeled fibrinogen on surfaces following HHIC. (a) RB, (b) epoxidized RB, (c) epoxidized RB coated with PEO, (d) PEO on clean silicon wafer, (e) control surface of silane functionalized PEO grafted on glass (0.01 μg/cm ²). Error bars represent the standard deviation of 10 measurements on each of 3 samples ⁸⁶	17
Figure 2.2.1 ¹ H NMR spectra of a) polymer 2.3a; b) after reacting with to form 2.4a (CDCl ₃ , 400 MHz).	34

Figure 2.2.2 IR trace of acid modified RB 2.4a, the acid confirmed with the appearance of two carbonyl peaks at 1728 and 1748 cm^{-1}	35
Figure 2.2.3 ^1H NMR spectra of a) polymer 1; b) reaction product after 10 minutes of UV irradiation; c) reaction product after 1 hour of irradiation (3 equiv. of TGAc, DMPA photoinitiator). (CDCl_3 , 400 MHz)	38
Figure 2.2.4 ^1H NMR spectra of a) polymer 2.8 the bromo-initiator; b) after polymerization with tBMA 2.9 (CDCl_3 , 400 MHz)	40
Figure 2.2.5 SEC traces of the co-polymers created with varying equivalents of <i>tert</i> -butyl methacrylate	42
Figure 2.2.6 IR traces of copolymer 2.9 & deprotected copolymer 2.13, the carbonyl region to show a broadening of the carbonyl stretch, suggestive of the emergence of a new peak corresponding to the carboxylic acid at 1701 cm^{-1}	43
Figure 3.2.1 Thin film preparation of RB/PEO films using spin casting and HHIC	53
Figure 3.2.2 Visual depiction how molecules form radicals and recombine to form cross-linked films via HHIC	53
Figure 3.2.3 a) AFM image (topography) of 3.1a b) AFM image of 3.2a spin coated on 3.1a. AFM images correspond to a 5 μm x 5 μm area	54
Figure 3.2.4 a) AFM image (topography) of PEO coated on 3.1a b) AFM image of PEO spin coated on 3.2a c) AFM image of PEO spin coated on 3.3a d) AFM image of PEO spin coated on 3.4a. AFM images correspond to a 5 μm x 5 μm area	56
Figure 4.2.1 ^1H NMR spectra of the 4.3a showing all the peaks corresponding to both PTx and RB, the key peaks are assigned for PTx	67
Figure 4.2.2 ^1H NMR spectra illustrating the key peak changes observed a) a mixture of PTx with 4.2a/b b) after conjugation of PTx to 4.3a/b	68
Figure 4.2.3 Release study of PTx from the polymeric substrates completed using HPLC. Note: 2C and 7C overlap for much of the study	70

Figure 4.2.4 a) left- S1 after 35 days showing delamination right- 2C at 35 days showing little or no delamination b) left- 2P at 35 days showing slight delamination right- 2C at 35 days showing resilience with no or little delamination..... 71

Figure 4.2.5 SEM images of polymer surfaces before and after the degradation study: a) S1 before degradation; b) S1 at 35 days; c) 2P before degradation; d) 2P at 35 days; e) 7C before degradation; f) 7C at 35 days; g) 2C before degradation; h) 2C at 35 days. 72

Figure 4.2.6 AFM topography images of polymer surfaces before and after the degradation study: a) S1 before degradation; b) S1 at 35 days; c) 2C before degradation; d) 2C at 35 days; e) 7C before degradation; f) 7C at 35 days; g) 2P before degradation; h) 2P at 35 days. 73

Figure 4.2.7 MTT assay in evaluation of the toxicity of the polymeric surfaces. 75

List of Schemes

Scheme 1.3.1 Generic scheme of the cationic polymerization of RB.	9
Scheme 1.3.2 Synthetic pathway to yield bromo-butyl/ chloro-butyl using elemental halogens to yield three potential isomers.	12
Scheme 1.3.3 Synthetic pathway in the production of cationic ionmers and conjugated dienes through reactions with bromo-butyl.....	13
Scheme 1.3.4 Cycloaddition in a Diels Alder fashion to yield a grafted acid functionalized RB.	14
Scheme 1.3.5 Synthetic pathway to yield PEO co-polymers grafted off of RB through manipulation of the RB backbone.....	15
Scheme 2.1.1 Proposed general route towards carboxylic acid functionalized butyl rubber.	29
Scheme 2.1.2 Proposed reaction of butyl rubber derivative 2.3 and TGAc in the presence of a photochemical initiator.	30
Scheme 2.1.3 Proposed reaction of butyl rubber derivative 2.3 to produce a graft copolymer containing protected carboxylic acids via ring-opening polymerization of a cyclic carbonate.	31
Scheme 2.1.4 Proposed reaction of butyl rubber derivative 2.3a to form an ATRP initiator, followed by subsequent synthesis of a RB-co-poly(<i>tert</i> -butyl methacrylate) and its deprotection to yield the target RB-co-poly(methacrylic acid).	32
Scheme 3.1.1 The oxygenated RBs synthesized from commercially available RB (3.1); epoxide (3.2), alcohol (3.3) and carboxylic acid (3.4).....	51
Scheme 4.2.1 Schematic representation of the conjugation of PTx to the RB backbone.....	66

List of Appendices

Appendix A ¹ H NMR (400 MHz, CDCl ₃) of polymer 2.4b with the 7.0% IP RB.	84
Appendix B IR trace for polymer 2.4b with higher IP content (7%) RB.	85
Appendix C left-DSC and right-TGA for polymer 2.4b.	85
Appendix D left-DSC and right-TGA for polymer 2.4a.	86
Appendix E ¹ H NMR (400 MHz, CDCl ₃) of thiol-ene attempts with dodecanethiol with polymer 2.3a.	87
Appendix F ¹ H NMR (400 MHz, CDCl ₃) of copolymer 2.10.	88
Appendix G ¹ H NMR (400 MHz, CDCl ₃) of copolymer 2.11.	88
Appendix H ¹ H NMR (400 MHz, CDCl ₃) of copolymer 2.12.	89
Appendix I TGA analysis of polymer 2.8.	90
Appendix J TGA analysis of polymer 2.9.	91
Appendix K TGA analysis of polymer 2.10.	92
Appendix L TGA analysis of 2.11.	93
Appendix M ¹ H NMR (400 MHz, CDCl ₃) of polymer 4.3b.	94
Appendix N SEC traces for the PTx conjugates 4.3a/b.	95
Appendix O Calibration curve for the release study of paclitaxel via HPLC.	96
Appendix P Representative HPLC trace for release study.	97
Appendix Q TGA analysis of PTx conjugate 4.3b.	97
Appendix R TGA analysis of PTx conjugate 4.3a.	97

Appendix S IR trace of PTx conjugate of 4.3a..... 98

List of Abbreviations

AFM	Atomic Force Microscopy
ATRP	Atom Transfer Radical Polymerization
BMS	bare metal stents
brs	broad singlet
d	doublet
DCC	dicyclohexylcarbodiimide
DES	drug eluting stents
DMAP	4-dimethylaminopyridine
DMOA	N,N- dimethyloctylamine
DSC	differential scanning calorimetry
EDC•HCl	1-Ethyl-3-(3-dimethylaminopropyl)carbodiimide
IB	isobutylene
IP	isoprene
IR	infrared spectroscopy
HHIC	Hyperthermal Hydrogen Induced Cross-Linking
HMTETA	1,1,4,7,10,10- hexamethyltriethylenetetramine
HPLC	high performance liquid chromatography
m	multiplet
m-CPBA	meta-chloroperoxybenzoic acid
M_n	number average molecular weight
M_p	peak molecular weight
MTT	3-(4,5-dimethylthiazol-2-yl)-2,5-diphenyltetrazolium bromide
M_w	weight average molecular weight
MW	molecular weight (g/mol)

NMR	nuclear magnetic resonance
NR	natural rubber
PDI	polydispersity index
PEO	poly(ethylene oxide)
PEVA	poly(ethylene-co-vinyl acetate)
PBMA	poly(n-butyl methacrylate)
PIB	poly(isobutylene)
PMMA	poly(methyl methacrylate)
PPh ₃	triphenylphosphine
PTx	paclitaxel
RB	butyl rubber/ poly(isobutylene-co-isoprene)
ROP	ring-opening polymerization
s	singlet
SEC	size exclusion chromatography
SEM	scanning electron microscopy
SIBS	poly(styrene)-co-poly(isobutylene)-co-poly(styrene)
SMA	poly(styrene-co-maleic anhydride)
tBMA	<i>tert</i> -butyl methacrylate
TFA	trifluoroacetic acid
TGA	thermal gravimetric analysis
TGAc	thioglycolic acid
T _g	glass transition (°C)
THF	tetrahydrofuran
UV	ultraviolet
wt. %	weight percentage

Chapter 1

Polymers used in the production in biomaterials

1.1 General Introduction

The field of biomaterials is a vast and ever changing field that encompasses the improvement and extension of life through materials. There are many different definitions of biomaterials, but a common theme is the use of materials to improve or replace function within a biological system. These materials vary in function, structure and importance. Early examples of biomaterials like wooden teeth and glass eyes were crude but served their purpose¹. Upon the advent of polymers at the end of the nineteenth century, polymers became increasingly integrated within medical applications². Some early examples were the use of poly(methyl methacrylate) (PMMA), in dentistry³ as well as in coatings for hip-replacements. Another example was the use of polyether urethanes in the production of artificial hearts^{1,3}.

Examples of biomaterials can be both medical and non-medical and also these materials can be either natural or synthetic. Thus for simplicity, biomaterials can be divided into two-sub groups, which are not mutually exclusive - structural and functional biomaterials. An example of structural biomaterials is the glass eye that fills the cavity in which the eye used to be, but does not replace sight. This material fulfills the structural requirements for the eye to protect the eye socket from the outside surroundings. Other examples of structural biomaterials include artificial bone and artificial limbs. Functional biomaterials on the other hand interact with the biological system to replace or enhance function other than structural support. Such materials can serve many functions but some examples are artificial organs⁴, pacemakers and controlled release implants¹.

Common issues have been addressed within all biomaterials. These issues are critical to the improvement and expansion of biomaterials for explicit applications. They include improved biocompatibility, mechanical properties and degradation⁵. The synthetic modification of polymer microstructures can create new classes of materials that can reduce or eliminate the above-mentioned concerns. Using new methodologies,

materials can be created that are more biocompatible, responsive, stealthy and specific. Research is plentiful in researching materials for specific applications for both medical and non-medical materials.

1.2 Vascular Stents

An excellent example of the evolution of a biomaterial from purely structural to functional is the advancement in medical implants, especially coronary stents. In 1977 the use of balloon inflations to reduce coronary lesions was a medical breakthrough, but this only served as a temporary solution⁶. Restenosis rates were very high after treatment with balloon angioplasty due to the recoil effect of the vessels and constrictive remodeling. It became quite evident that the insertion of a structural scaffold was needed to ensure the vessel remained open. The insertion of metallic stents reduced the recoil phenomenon at both acute and chronic levels. However, the bare metal stents (BMS) caused unavoidable vessel damage due to the pathological biological cascade, which caused thickening of the blood vessel (Figure 1.2.1b)⁷. The late luminal loss limits the long-term efficacy of BMS. This also caused issues of thrombosis and blood clotting. The restenosis rates for BMS ranged between 20 and 40%, which was an improvement from rates of 40 to 60% for vessels not stented⁸. These rates are also very dependent on the patient and previous/current medical conditions such as diabetes.

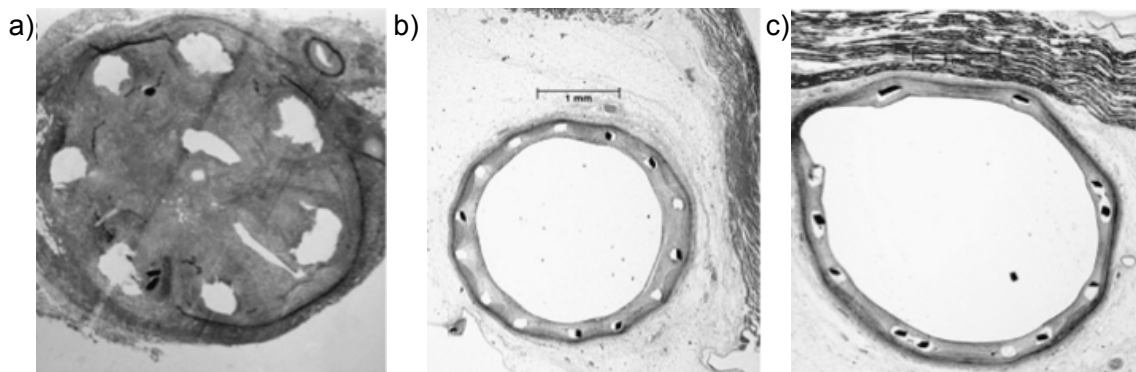


Figure 1.2.1 Cross-sectional images of porcine coronary arteries with stent explants, a) a polycarbonate urethane-coated stent exhibiting substantial inflammation and proliferation (2 months), b) a bare metal stent at 3 months showing some restenosis and c) poly(styrene)-co-poly(isobutylene)-co-poly(styrene) (SIBS) coated stent at 180 days showing resilience⁹.

Drug-eluting stents (DES) are a means of providing mechanical integrity to the blood vessel but retain blood flow by means of pharmacotherapy to inhibit in-stent restenosis response as well as early thrombosis (Figure 1.2.1c). A decade of clinical use of the first generation DES has afforded overwhelming support of the clear benefits DES exhibit over their BMS counterparts^{10, 11}. There are two first generation DES that are based on two different drugs, sirolimus and paclitaxel. These stents have been commercialized under the name CYPHER (sirolimus) and TAXUS (paclitaxel-PTx). As a result of the numerous clinical trials that have been completed, there are some concerns involving DES^{12, 13}. Restenosis has still been observed as well as poor re-endothelialization¹⁴, delayed healing¹⁵ and tissue growth¹⁶ behind the polymeric film causing thrombosis.

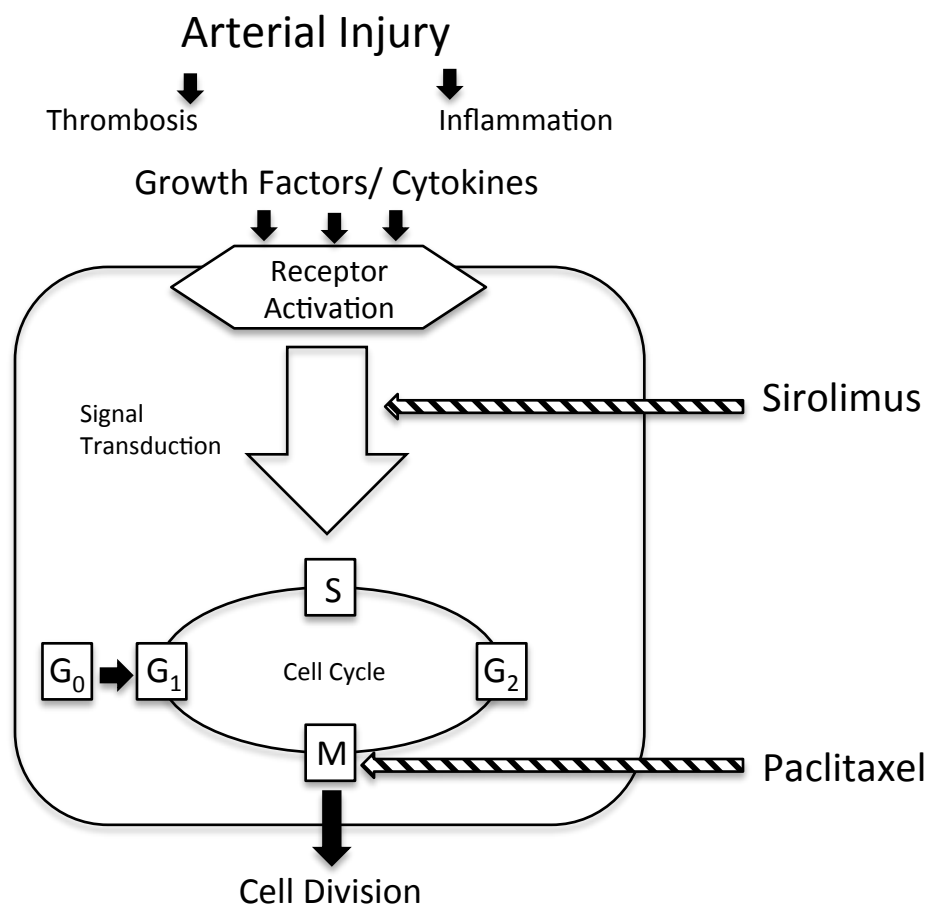


Figure 1.2.2 Function of Sirolimus and Paclitaxel in halting cell proliferation and different points of the cell cycle as the body identifies the arterial injury¹⁷.

When constructing a DES, there are several parameters to consider such as the choice of drug, polymer, and scaffold composition. The drugs used in the two DES that are approved for clinical use are sirolimus and paclitaxel (PTx), which have very different mechanisms. The drugs selected interfere with cell proliferation at different steps, but yield a similar result, which is inhibition of cell proliferation. Sirolimus (rapamycin) is a natural macrocyclic, lipophilic lactone with immunosuppressive antibiotic activity. The molecule was initially isolated in the mid-1970's from *Streptomyces hygroscopicus* found in soil samples from the Easter Islands¹⁸. Sirolimus showed excellent antimicrobial and antifungal activity but this was further exceeded by its immunosuppressive properties. From a therapeutic point of view, the sirolimus molecule binds to a specific class of cytosolic proteins called immunophiles. The receptor

is the FK binding protein 12 and this results in inhibition of regulatory signal transduction kinase. This in essence shuts down cell proliferation at the G1-S checkpoint (Figure 1.2.2)¹⁹⁻²¹. Alternatively, paclitaxel is a diterpenoid with a taxane skeleton. The drug inhibits the cell proliferation by stabilizing the microtubules, thus the cell is not released, which halts the cell cycle in the M phase (Figure 1.2.2)¹⁵. PTx inhibits the growth of cells by its cytotoxic and antineoplastic properties. Paclitaxel gave a remarkable reduction in neointimal hyperplasia in animal studies and this led to its use in DES^{22, 23}. The aforementioned DES drug release profiles have been studied thoroughly and release has been controlled to some degree, through loading of different weight percentages²⁴ (wt.%) of drugs and modifications of the drug carrier^{25, 26}. The resultant release profiles can be seen in Figure 1.1.3a where the release is tuned from slow to rapid through altering the wt.% of PTx relative to the amount of SIBS utilized²⁴. Alternatively, as seen in Figure 1.1.3b the release profile can be modified by the introduction of more hydrophilicity. This was accomplished by the introduction of poly(styrene-co-maleic anhydride) (SMA) as part of the polymer mixture²⁶. As seen in the release profile, upon increasing the amount of SMA the release of PTx is much quicker than its only SIBS counterpart (Figure 1.2.3).

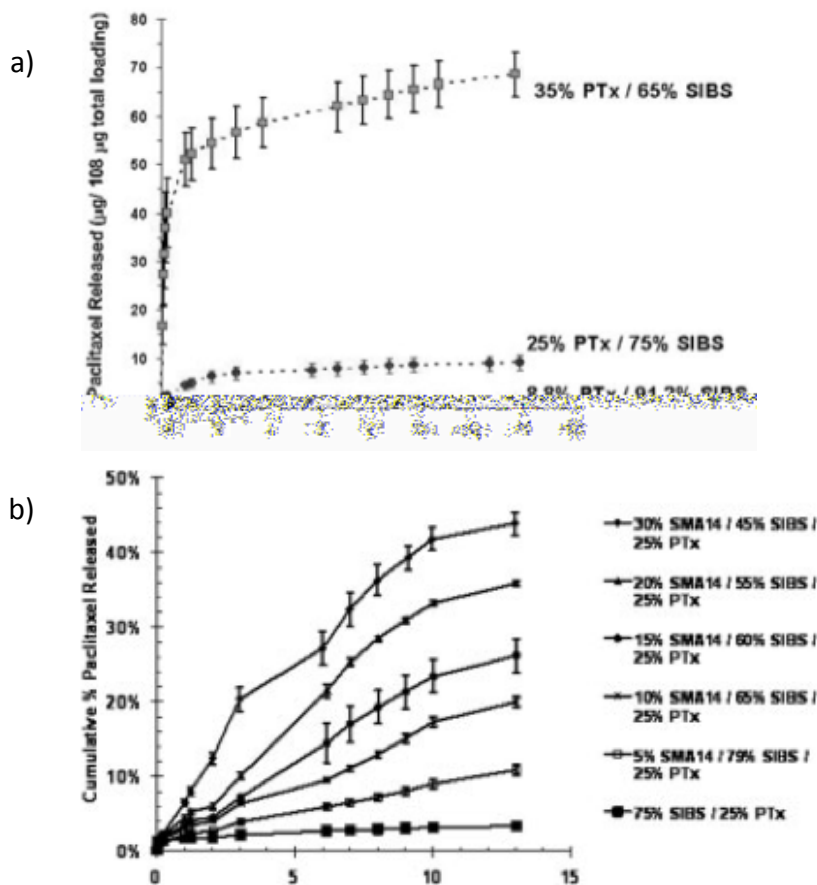


Figure 1.2.3 Control of drug release via a) control of wt.% of drug to polymer²⁴ and b) manipulation of the SIBS backbone by the introduction of hydrophilic entities i.e. poly(styrene-co-maleic anhydride (SMA))²⁶.

The TAXUS stent platform uses a robust mechanically tough elastomer to support the enormous stresses within a biological system. The TAXUS DES utilizes a triblock copolymer, poly(styrene)-co-poly(isobutylene)-co-poly(styrene) (SIBS) that exhibits the required mechanical properties for use *in vivo* (Figure 1.2.4a)²⁷. The CYPHER DES employs a poly(ethylene-co-vinyl acetate) (PEVA) and poly(n-butyl methacrylate) (PBMA) mixture, which is also a robust polymer much like PS-PIB (Figure 1.2.4b)¹⁷. SEM images show the compressed and expanded stent structures and why an elastomeric polymer is needed for such movements (Figure 1.2.4c-e)²⁶. These materials are known to be durable, but they are limited by low adhesion to the metal, which can cause delamination of the polymer from the metal stent, causing thrombosis^{28,29}. Also, it has been illustrated that such materials can exhibit erratic release profiles^{30,31}. Alternative

DES systems have been studied such as biodegradable polymer systems. These materials have several advantages but again several limitations. An example is the JACTAX HD DES, which uses polylactide³². This polymer undergoes degradation by hydrolysis and enzymatic activity. The degradation products are eventually metabolized to water and carbon dioxide. The limitation with ester hydrolysis is the random cleavage sites that cause burst release of drug. Once significant degradation has occurred, the bottom layer is a BMS, which will cause the problems outlined above. Lastly, the biodegradable polymers do not have the ideal mechanical properties needed for the constant wear *in vivo*³³. These stents have similar rates of restenosis as the durable elastomeric DES^{32, 34, 35}. Similar rates of restenosis have also been seen for the polymer free versions of DES^{34, 36}.

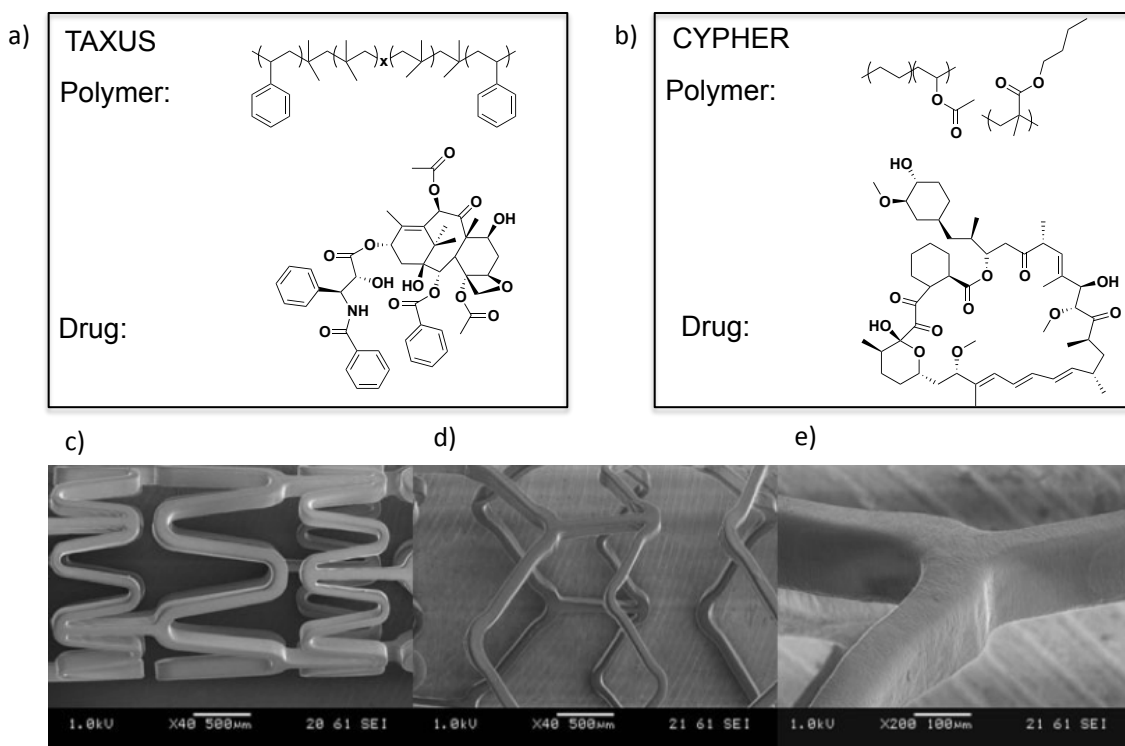


Figure 1.2.4 Chemical composition of drug/polymer for the two commercialized DES a) TAXUS and b) CYPHER. c) through e) show SEMs of a DES coated with 25% PTx/ 30% SMA/ 45% SIBS c) unexpanded stent at X40 magnification d) X40 magnification of an expanded stent e) X200 magnification of an expanded stent²⁶.

The studies of DES are multi-faceted and very intricate in terms of polymer and drug selection. Each decision alters the way the stent affects the therapeutics of the DES. The current commercial DES has disadvantages such as delamination and burst release, but these issues can be optimized. Through optimization, the DES should be able to capitalize on its excellent mechanical properties.

1.3 Butyl Rubber

1.3.1 Introduction

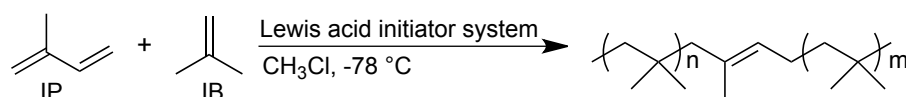
Butyl rubber (RB) is a synthetic elastomer that is a copolymer of isobutylene and a small amount of isoprene. The IP units serve as sites for cross-linking. The most common commercial method of cross-linking is the process of vulcanization, which entails treatment with sulfur and heat. The first polymerizations of isobutylene were completed in 1873 but only produced low M_w polymers until I. G. Farben in Germany synthesized higher M_w poly(isobutylene) (PIB) by lowering the polymerization temperature. PIB was synthesized at $-75\text{ }^\circ\text{C}$ and using boron trifluoride as a catalyst. PIB had no commercialization potential because it was fully saturated and could not be cross-linked³⁷. Poly(isobutylene-co-isoprene) (RB) was synthesized by Standard Oil Development Co. in 1937. The polymer was first synthesized using 1,3 butadiene but it was later found that isoprene was a better comonomer. The technologies developed played great importance during World War II because of the curtailed supply of natural rubber. For its time, the commercialization of RB was a scientific and engineering marvel due to the complexity of the technology.

RB possesses many attractive properties such as gas/water impermeability, chemical stability, excellent mechanical properties and biocompatibility^{38,39}. Many of these properties arise from the low degree of unsaturation amongst the long PIB chains. The first major commercial use of RB was in tires, due to its gas/water impermeability and this continues to be a major market. In addition to the tire industry, RB is used in other applications such as pharmaceutical stoppers, sealants, bladders, and adhesives. These applications take advantage of the other attractive properties of RB such as

resistance to UV degradation, oxidation and ozone but also its dampening and thermal stability.

1.3.2 Synthesis

Butyl rubber is synthesized from very pure monomers, isobutylene (IB) (2-methylpropene, >95%) and isoprene (2-methyl-1,3-butadiene, >98%) (IP). The mechanism is consistent with a highly complex cationic polymerization⁴⁰⁻⁴². Water and oxygenated organic molecules are minimized due to their interference with the cationic polymerization process. The reaction utilizes a Lewis acid catalyst system (co-initiator and initiator). Typical Lewis acid co-initiators include aluminum trichloride, alkylaluminum dichloride, boron trifluoride, tin tetrachloride and titanium tetrachloride. Initiators used are commonly Brønsted acids such as water, hydrochloric acid, organic acids, though alkyl halides can also be used.



Scheme 1.3.1 Generic scheme of the cationic polymerization of RB.

Initiation occurs when an isobutylene monomer reacts with the Lewis acid to produce a carbenium ion. Monomer and comonomer units are added to the carbenium ion as the propagation continues. Various parameters such as solvent polarity, temperature and counter ions must be considered due to the way they affect the propagation. The rate of propagation has been determined to be around 108 L/(mol•s), essentially diffusion limited^{43, 44}. Low polymerization temperatures give higher polymerization rates in either hydrocarbon or halogenated solvents. The propagation step continues until there is a chain transfer or termination.

For chain transfer to occur, the carbenium ion end must react with isobutylene, isoprene, or species with unshared electrons. These species could include solvents, counterions and olefins. Once the carbenium reacts with these species, it terminates the growth of the macromolecule and facilitates a new chain. Activation energy of chain transfer is larger than propagation. Therefore molecular weight (MW) is strongly

influenced by temperature. The issue of chain transfer is more evident upon synthesizing higher IP content RB. Upon raising the IP content, lower MW co-polymers are observed due to the comonomers' own affinity to chain transfer⁴⁵. Alternatively, in chain termination the carbenium ion and its counter ion collapse, which results in destruction of the active chain. Termination can occur through several avenues such as hydride abstraction from comonomer, formation of stable allylic carbenium ions or reactions with the carbenium ion involving nucleophiles.

1.3.3 Chemical & Physical Properties

Isobutylene polymerizes in a regular head-to-tail fashion to produce a polymer with quaternary carbons atoms with two-pendant methyl groups', which produces steric strain between other polymerized portions of isobutylene. This is partially relieved by distortion of the methylene carbon to 124° as compared to 110° for a tetrahedral carbon and also through the dihedral angle of the carbon-carbon bond by approximately 25°⁴⁶⁻⁴⁸. The isoprene is polymerized in a head-to-tail arrangement leading to a predominantly 1,4-addition (90-95%)⁴⁹. The other IP species are identified spectroscopically as 1,2 enchain⁴⁹ or as branched 1,4-addition^{50, 51}. The percentage of IP can be tuned from low (0.5%) to high (7.0%). With these low amounts of IP and similar reactivity ratios, a random distribution of IP is found throughout RB. Polydispersity indices (PDI) for these copolymers are typically in the range of 2-5 (M_w/M_n). Also, the typical glass transition point of RB has been found to be -65 °C⁵² (Table 1.3.1). Due to the very hydrophobic nature of the polymer, this affords the polymer excellent chemical inertness especially to UV degradation and oxidation. RB has been known to be degraded by atmospheric ozone over extended periods of time but this can be prevented by introduction of antioxidants. The chemical properties make this polymer relevant for its current and future applications.

The physical properties of PIB and its copolymers such as RB allow it to be used in many commercial products. RB and other variations show low permeability to small molecule diffusants such as He, H₂, O₂, N₂, and CO₂. This is a result of the efficient intermolecular packing, which leads to a relatively high density⁵³⁻⁵⁵. The efficient packing of the isobutylene portions allows for low fractional volumes and low diffusion

coefficients for penetrants. Table 1.3.1 shows tabulated data of some important physical properties of RB.

Table 1.3.1 Physical properties of RB ⁵⁶.

Property	Value
Density (g/cm ³)	0.917
Glass Transition, T _g (°C)	-75 to -67
Heat Capacity, C _p (kJ/kgK) ^b	1.95
Refractive Index, n _p	1.5081

The low diffusion rates for various gases are shown in Table 1.3.2. The differences can be seen when comparing RB to NR, which is a polymer of cis-1,4-polyisoprene. The increase in diffusivity of gases can be rationalized by looking at the structures of RB compared to NR. NR cannot pack as efficiently as RB due to the lack of flexibility of the backbone. This makes RB and its associated co-polymers especially useful in some commercial applications.

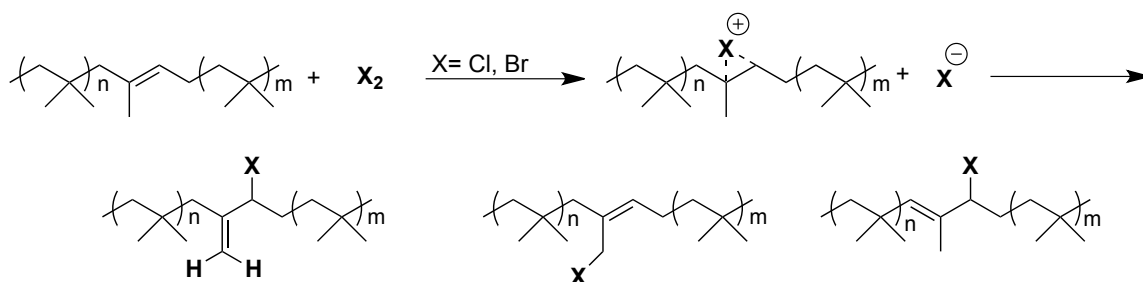
Table 1.3.2 Diffusivity of several gases in RB and NR at 25 °C ⁵⁷.

Gas	Diffusivity (cm ² /s) x 10 ⁶	
	Butyl Rubber	Natural Rubber
He	5.93	21.6
H ₂	1.52	10.2
O ₂	0.081	1.6
N ₂	0.045	1.1
CO ₂	0.058	1.1

Another attractive property is RB's biocompatibility and being inert to various tissues^{38,39}. RB and its derivatives are used in numerous applications such as chewing gum, pharmaceutical stoppers and DES, where it comes into direct contact with different biological environments⁵⁸. The bioinert property arises from the very hydrophobic nature of the polymer itself and again its low diffusivity. Thus the material being bioinert comes from the RB backbone being chemically inert and stable. However, there are some fundamental limitations to using RB for biomaterials, such as protein adsorption and growth of pathogenic species in certain applications⁵⁹.

1.3.4 Modifications of Butyl Rubber

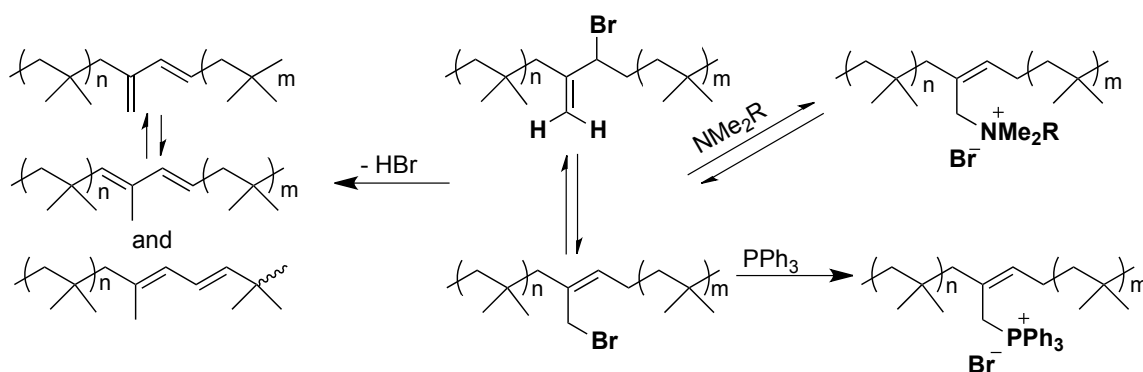
Shortly after the advent of RB, there were investigations into how to instill increased polarity and the ability to cross-link it, referred to as curing, with other elastomers. Goodrich first synthesized halogenated RBs in the mid 1950's by reacting RB with N-bromosuccinimide⁶⁰. Eventually this method was improved to use elemental bromine by Polymer Co. of Canada (Scheme 1.3.2). Also, in 1961 chlorinated RB was commercialized by Exxon and was synthesized by continuous chlorination of a solution of butyl rubber⁶¹. The production of halogenated butyls expanded the application of butyl rubber due to its increased vulcanization rates and improved compatibility with other highly unsaturated elastomers (NR).



Scheme 1.3.2 Synthetic pathway to yield bromo-butyl/ chloro-butyl using elemental halogens to yield three potential isomers.

With the synthesis of these halogenated RBs, further modification and alternatives to cross-linking were investigated. Cross-linking can be completed with halogenated RBs in other ways than the conventional vulcanization⁶². These halogenated RBs can be

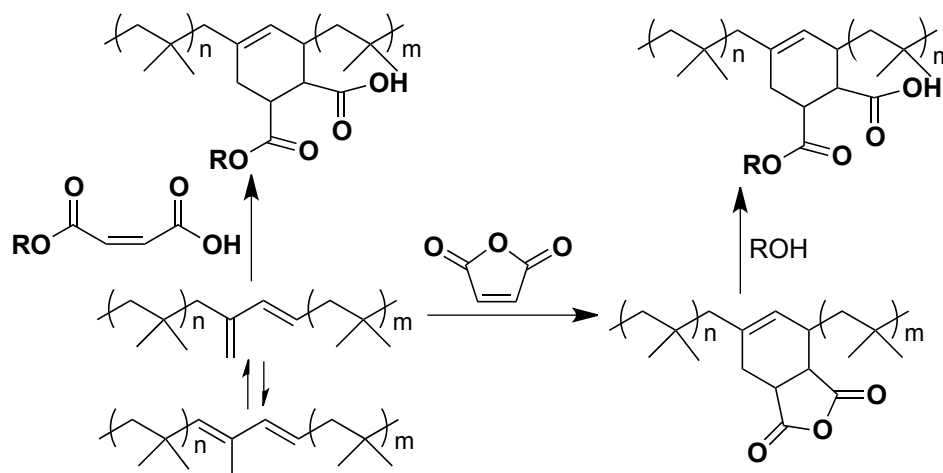
cross-linked using hydrogen peroxide⁶³, moisture curing⁶⁴ and transition metals like zinc oxide⁶⁵. Beyond alternatives to conventional cross-linking, there was also a focus on manipulation of the butyl backbone to modify the chemical/physical properties. The halogenated RBs have been used in numerous examples to produce various functionalities off the RB backbone. Through the manipulation of the halogenated RB the installation of amine^{66, 67}, esters^{68, 69}, ether⁷⁰, acids⁷¹, sulfuration⁷² and ammonium/phosphonium bromide ionomers⁷³⁻⁷⁶ have been successfully achieved. The installations of ionmeric molecules are of specific interest due to their altered properties. To install the ammonium/phosphonium bromide ionomers either triphenylphosphine (PPh₃) or N,N-dimethyloctylamine (DMOA)⁷⁶ displaces the bromine to form the corresponding salt (Scheme 1.3.3). These polymers have shown interesting properties in terms of increased antimicrobial efficacy and increased adhesion to various substrates compared to its starting bromo-butyl.



Scheme 1.3.3 Synthetic pathway in the production of cationic ionomers and conjugated dienes through reactions with bromo-butyl.

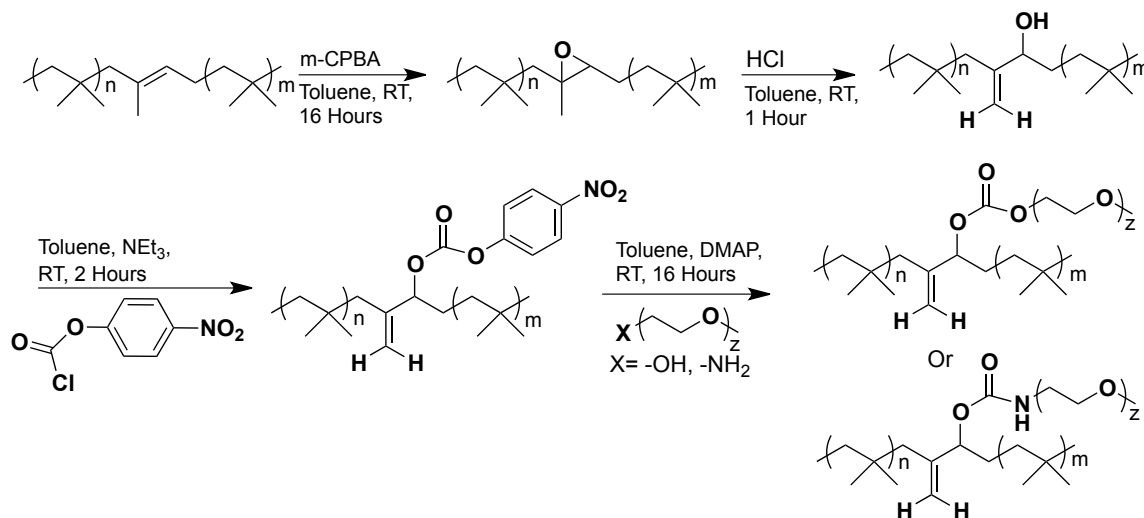
The installation of acid moieties should increase some properties required for certain applications like increased surface adhesion to metal substrates. Dehydrohalogenation of the allylic bromo-butyl yielded the conjugated diene that can be used in the Diels-Alder cycloaddition of maleic anhydride⁷¹. The cyclo adduct can be attacked by an alcohol to yield an ester and an acid. The use of hydroxyl terminated polymers yielded graft copolymers with acid functionalities (Scheme 1.3.4). This reaction

was limited due to the number of steps, the extreme conditions that were used, and also the mixture of resulting products as the conversion was not clean.



Scheme 1.3.4 Cycloaddition in a Diels Alder fashion to yield a grafted acid functionalized RB.

Work has also been completed on modification of the RB backbone directly. There have been numerous methods of epoxidation reported in the literature⁷⁷⁻⁷⁹. Recently a synthetic pathway in which poly(ethylene oxide) (PEO) was attached to RB using a clean and mild synthetic pathway^{78, 79}. Graft copolymers had previously been synthesized using halogenated RB but these reactions required halide substitution, a reaction that requires high temperatures and yields multiple products^{70, 80, 81}. The newer synthetic pathway involved the introduction of an epoxide utilizing *m*-chloroperoxybenzoic acid (*m*-CPBA), which cleanly yielded the epoxide ring. Upon treatment of the epoxide under acidic conditions, the ring opened giving an alcohol. The surprising result was the structure of the alcohol, which was a product of the elimination reaction to yield an alkene. In contrast to Saytzeff's law, the less substituted product was formed. This alcohol was then activated with 4-nitrophenylchloroformate and reacted with either hydroxyl or amine terminated PEO to yield the resultant graft copolymers (Scheme 1.3.5)^{78, 79}.



Scheme 1.3.5 Synthetic pathway to yield PEO co-polymers grafted off of RB through manipulation of the RB backbone.

1.3.5 Applications

The majority of RB applications are tied closely with the automotive industry, involving tires and other automotive parts. RB and its modified polymers are used extensively in the innerliner. The tire innerliner typically consists of halobutyl due to its excellent air and moisture impermeability, fatigue resistance and durability. Bromobutyl is advantageous over chlorobutyl for many reasons, including superior adhesion to steel, better balance properties, fuel efficiency and lower costs⁵². RB is commonly used in innertubes. This is due to incompatibility with other rubbers such as NR. The sidewalls and treads generally consist of mixtures of NR and butadiene rubber. RB is also commonly used in many automotive parts that require RB's special blend of properties. In terms of hosing in an automobile, it requires an elastomer that is resistant to the material it is transporting, possesses low permeability and thermal stability. RB based applications include air conditioning hoses, coolant hoses, fuel line hoses and brake line hoses. RB is also utilized in dynamic parts within an automobile, many of the mounts use RB due to its ability to damp vibrations⁵². These vibrations can come from the road or engine and help protect essential parts from damage. These polymers must be extremely durable and very thermally stable for such applications.

RB has also been utilized in other applications outside the spectrum of the automotive industry. RB is commonly used in chewing gum and pharmaceutical stoppers. RB and its copolymers have been used in DES as described earlier^{39, 59, 82}. Recently, there has been more focus on using RB as a viable biomaterial and improving its properties. The graft copolymers with PEO mentioned above have shown intriguing surface patterning but more interesting is the resistance to protein adsorption when higher weight percentages of PEO were attached⁷⁸. This was demonstrated by examining the fluorescent confocal microscopy images of the increasing amounts of PEO content. As seen in Figure 1.3.1e & f, which have 24 and 34 wt.% PEO, there is no fluorescence and this is consistent with no detectable protein adsorption.

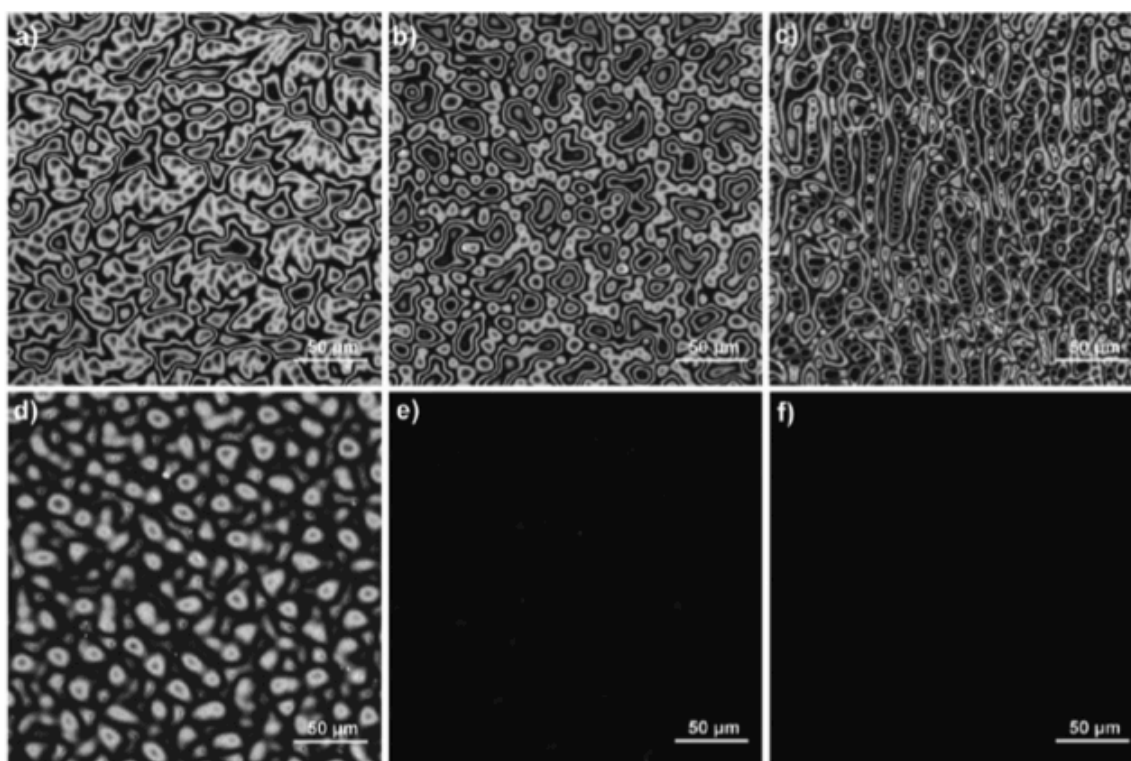


Figure 1.3.1 Fluorescence confocal microscopy images (543nm) of thin films (spin-cast at 20 mg/mL from CH_2Cl_2) following adsorption of a rhodamine-fibrinogen conjugate. Images represent different wt.% of PEO grafted to the RB backbone; a) 2%, b) 4%, c) 6%, d) 12%, e) 24% and f) 34%⁷⁸.

The use of PEO to eliminate protein adsorption on RB has been used in a laminate surface. In this work RB and epoxidized RB were spin cast, cross-linked using a new technique called Hyperthermal Hydrogen Induced Cross-Linking (HHIC)⁸³⁻⁸⁵. The cross-linked RB was then spin coated with PEO and cross-linked by HHIC. These surfaces were then subjected to fluorescently labeled fibrinogen to evaluate protein adsorption and cell studies were also performed. As seen in Figure 1.3.2a, RB supports well the growth of cells. Upon coating of RB with PEO a significant reduction in the number of cells was observed, a result attributed to their resistance to protein adsorption, which is thought to be the first step in the adhesion of cells to a surface. Figure 1.3.2b illustrates the effect PEO has on RB surfaces in terms of decreased protein adsorption. Epoxidized-RB showed a substantial decrease in protein adsorption upon coating the RB surface with PEO⁸⁶.

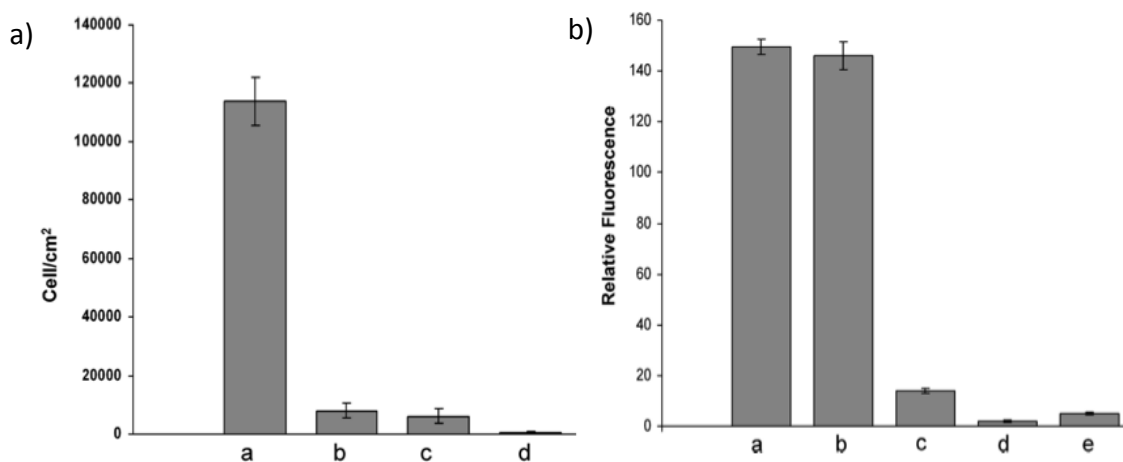


Figure 1.3.2 a) Evaluation of cell growth on surfaces. (a) RB, (b) epoxidized RB coated with PEO, (c) control surface of silane-functionalized PEO grafted on glass, (d) PEO-coated silicon wafer following HHIC b) Relative fluorescence obtained by confocal microscopy corresponding to the adsorption of a fluorescently labeled fibrinogen on surfaces following HHIC. (a) RB, (b) epoxidized RB, (c) epoxidized RB coated with PEO, (d) PEO on clean silicon wafer, (e) control surface of silane functionalized PEO grafted on glass (0.01 $\mu\text{g}/\text{cm}^2$). Error bars represent the standard deviation of 10 measurements on each of 3 samples⁸⁶.

1.4 Motivation and Goals of Thesis

With the synthetic knowledge for the preparation of the allylic alcohol derivative of RB^{79, 87}, it can be further modified to yield other materials that may improve certain properties. In the case of coronary stent coating applications, a polymer is required to adhere well to the metal. This reduces the chances of delamination of the coating, which has been reported in the commercial TAXUS stents^{28, 29}. This could lead to adverse events in vivo such as uncontrolled/altered drug release from the coating that could cause thrombosis. Lack of surface adhesion to metal surfaces is an issue in the case of RB due to its overall hydrophobicity and lack of polar groups. To tackle this issue, the introduction of more polar groups, specifically carboxylic acids may be useful. Carboxylic acid groups have been shown to exhibit increased surface adhesion to stainless steel surfaces⁸⁸. Also, the current commercial DES based on a SIBS coating has an initial burst release of the drug, paclitaxel followed by a long sustained release⁵⁸. The successful introduction of carboxylic acid groups can serve as a site for covalent immobilization of drugs via ester linkages. The covalent immobilization should eliminate the burst release^{30, 31}, creating a slower more controlled release of drug. Finally, these acid moieties on the PIB may serve to enhance adhesion to other materials than metal, such as bone^{89, 90}, which would be beneficial in applications such as bone cements⁹¹.

The first goal of this thesis, described in Chapter 2, is to synthesize and study new PIB materials containing carboxylic acid functionalities. The starting material will be the allylic alcohol functionalized polymer (Scheme 1.3.5). The hydroxyl cannot undergo oxidation directly to the acid because it is a secondary alcohol. However, it should be possible to perform a ring opening of a cyclic anhydride to yield the acid product. There are literature examples of these cyclic anhydride ring openings with the use of 4-dimethylaminopyridine (DMAP) as a catalyst⁹²⁻⁹⁵. The initial allylic alcohol has an exo alkene present which could be used in thiol-ene “click” reaction^{96, 97}. It could also be possible to directly conjugate a thiol-acid, which would eliminate the double bond. These reactions will first be attempted with the RB containing 2.2% IP. If this does not yield a sufficient amount of acid functionality, then a higher 7.0% IP-RB can be utilized. Another possibility if this again does not provide a sufficient number of carboxylic acids

is to increase the carboxylic acid content significantly through a ring-opening polymerization (ROP) of a cyclic carbonate containing pendant carboxylic acids on the side chain, initiated by the hydroxyls along the RB backbone⁹⁸⁻¹⁰⁰. Another alternative is to synthesize a poly(carboxylic acid) is the use of atom transfer radical polymerization (ATRP), which can polymerize many different monomers with varying functionality. ATRP has been completed on PIB but only reacting on the terminus of the polymer¹⁰¹⁻¹⁰⁴. The resulting number of acid groups in this case would be equal to the number of monomer units polymerized. Thus, the first goal of this project will attempt to create acid functionalized RBs through the described methods.

The second goal of this thesis, described in Chapter 3, will be to explore the enhanced functionality of the carboxylic acid functionalized RB. The carboxylic functionality installed should allow for flexibility in the properties of the polymer. It is proposed that polar groups on the RB backbone will increase its surface adhesion to substrates especially stainless steel. Also it was shown that the introduction of an epoxide ring increased the compatibilization of a hydrophilic polymer like PEO⁸⁶ when producing laminates. Hence the allylic alcohol and acid functionality should further introduce compatibilization of PEO. Lastly, as described in Chapter 4, to address the issue of burst release inherent with DES, PTx will be conjugated to the RB backbone and be tested as drug delivery substrate. This thesis will be focused on the production of carboxylic acid moieties on the RB backbone and their potential applications.

1.5 References

- (1) Ratner, B. D. In *Biomaterials science :an introduction to materials in medicine*; Academic Press: San Diego, 1996; , pp 484.
- (2) Langer, R. *Nature* **1998**, *392*, 5.
- (3) Peppas, N.; Langer, R. *Science* **1994**, *263*, 1715.
- (4) Vacanti, J.; Langer, R. *Lancet* **1999**, *354*, SI32.

- (5) Langer, R.; Tirrell, D. *Nature* **2004**, *428*, 487.
- (6) Gruentzig, A.; King, S.; Schlumpf, M.; Siegenthaler, W. *N. Engl. J. Med.* **1987**, *316*, 1127-1132.
- (7) Scott, N. *Adv. Drug Deliv. Rev.* **2006**, *58*, 358.
- (8) Abizaid, A.; Kornowski, R.; Mintz, G.; Hong, M.; Abizaid, A.; Mehran, R.; Pichard, A.; Kent, K.; Satler, L.; Wu, H.; Popma, J.; Leon, M. *J. Am. Coll. Cardiol.* **1998**, *32*, 584.
- (9) Pinchuk, L.; Wilson, G. J.; Barry, J. J.; Schoepfoerster, R. T.; Parel, J.; Kennedy, J. P. *Biomaterials* **2008**, *29*, 448.
- (10) James, S. K.; Stenestrand, U.; Lindback, J.; Carlsson, J.; Schersten, F.; Nilsson, T.; Wallentin, L.; Lagerqvist, B. *N. Engl. J. Med.* **2009**, *360*, 1933.
- (11) Moreno, R.; Fernandez, C.; Sanchez-Recalde, A.; Galeote, G.; Calvo, L.; Alfonso, F.; Hernandez, R.; Sanchez-Aquino, R.; Angiolillo, D. J.; Villarreal, S.; Macaya, C.; Lopez-Sendon, J. L. *Eur. Heart J.* **2007**, *28*, 1583.
- (12) Alfonso, F. *J. Am. Coll. Cardiol.* **2010**, *55*, 2717.
- (13) Lotan, C.; Meredith, I. T.; Mauri, L.; Liu, M.; Rothman, M. T. *JACC Cardiovasc. Interv.* **2009**, *2*, 1227.
- (14) Jimenez-Valero, S.; Moreno, R.; Sanchez-Recalde, A. *J. Invasive Cardiol.* **2009**, *21*, 488.
- (15) Farb, A.; Heller, P.; Shroff, S.; Cheng, L.; Kolodgie, F.; Carter, A.; Scott, D.; Froehlich, J.; Virmani, R. *Circulation* **2001**, *104*, 473.
- (16) Hong, M.; Mintz, G.; Lee, C.; Park, D.; Park, K.; Lee, B.; Kim, Y.; Song, J.; Han, K.; Kang, D.; Cheong, S.; Song, J.; Kim, J.; Park, S.; Park, S. *Circulation* **2006**, *113*, 414.

- (17) Duda, S.; Poerner, T.; Wiesinger, B.; Rundback, J.; Tepe, G.; Wiskirchen, J.; Haase, K. *J. Vasc. Interv. Radiol.* **2003**, *14*, 291.
- (18) Teirstein, P. *Circulation* **2001**, *104*, 1996.
- (19) Rogue, M.; Cordon-Cardo, C.; Fuster, V.; Reis, E.; Drobnjak, M.; Badimon, J. *Atherosclerosis* **2000**, *153*, 315.
- (20) Gallo, R.; Padurean, A.; Jayaraman, T.; Marx, S.; Rogue, M.; Adelman, S.; Chesebro, J.; Fallon, J.; Fuster, V.; Marks, A.; Badimon, J. *Circulation* **1999**, *99*, 2164.
- (21) Groth, C.; Backman, L.; Morales, J.; Calne, R.; Kreis, H.; Lang, P.; Touraine, J.; Claesson, K.; Campistol, J.; Durand, D.; Wramner, L.; Brattstrom, C.; Charpentier, B. *Transplantation* **1999**, *67*, 1036.
- (22) Heldman, A.; Cheng, L.; Jenkins, G.; Heller, P.; Kim, D.; Ware, M.; Nater, C.; Hruban, R.; Rezai, B.; Abella, B.; Bunge, K.; Kinsella, J.; Sollott, S.; Lakatta, E.; Brinker, J.; Hunter, W.; Froehlich, J. *Circulation* **2001**, *103*, 2289.
- (23) Hong, M.; Kornowski, R.; Bramwell, O.; Ragheb, A.; Leon, M. *Coron. Artery Dis.* **2001**, *12*, 513.
- (24) Ranade, S.; Miller, K.; Richard, R.; Chan, A.; Allen, M.; Helmus, M. *J. Biomed. Mater. Res. Part A* **2004**, *71A*, 625.
- (25) Sipos, L.; Som, A.; Faust, R. *Biomacromolecules* **2005**, *6*, 2570.
- (26) Richard, R.; Schwarz, M.; Chan, K.; Teigen, N.; Boden, M. *J. Biomed. Mater. Res. Part A*. **2009**, *90A*, 522.
- (27) Strickler, F.; Richard, R.; McFadden, S.; Lindquist, J.; Schwarz, M. C.; Faust, R.; Wilson, G. J.; Boden, M. *J. Biomed. Mater. Res. Part A* **2010**, *92A*, 773.
- (28) Levy, Y.; Mandler, D.; Weinberger, J.; Domb, A. J. *J. Biomed. Mater. Res. B Appl. Biomater.* **2009**, *91B*, 441.

- (29) Ormiston, J.; Currie, E.; Webster, M.; Kay, P.; Ruygrok, P.; Stewart, J.; Padgett, R.; Panther, M. *Catheter. Cardio. Inte.* **2004**, *63*, 332.
- (30) Yoo, H.; Oh, J.; Lee, K.; Park, T. *Pharm. Res.* **1999**, *16*, 1114.
- (31) Tong, R.; Cheng, J. *Angew. Chem. Int. Ed.* **2008**, *47*, 4830.
- (32) Grube, E.; Schofer, J.; Hauptmann, K. E.; Nickenig, G.; Curzen, N.; Allocco, D. J.; Dawkins, K. D. A. *JACC Cardiovasc. Interv.* **2010**, *3*, 431.
- (33) Papafaklis, M. I.; Chatzizisis, Y. S.; Naka, K. K.; Giannoglou, G. D.; Michalis, L. K. *Pharmacol. Ther.* **2012**, *134*, 43.
- (34) Mehilli, J.; Byrne, R. A.; Wieczorek, A.; Iijima, R.; Schulz, S.; Bruskina, O.; Pache, J.; Wessely, R.; Schoemig, A.; Kastrati, A.; *Eur. Heart J.* **2008**, *29*, 1975.
- (35) Windecker, S.; Serruys, P. W.; Wandel, S.; Buszman, P.; Trznadel, S.; Linke, A.; Lenk, K.; Ischinger, T.; Klaus, V.; Eberli, F.; Corti, R.; Wijns, W.; Morice, M. C.; di Mario, C.; Davies, S.; van Geuns, R.; Eerdmans, P.; van Es, G.; Meier, B.; Jueni, P. *Lancet* **2008**, *372*, 1163.
- (36) Grube, E.; Mueller, R.; Schuler, G.; Hauptmann, K.; Schofer, J. *J. Am. Coll. Cardiol.* **2012**, *60*, B14.
- (37) Paul, K., Joseph; Tarnqvist, E. G. M. In *Polymer chemistry of synthetic elastomers; High polymers* ; Interscience Publishers: New York, 1968; Vol. 23, pp 1044.
- (38) Puskas, J.; Chen, Y. *Biomacromolecules* **2004**, *5*, 1141.
- (39) Puskas, J.; Chen, Y.; Dahman, Y.; Padavan, D. *J. Polym. Sci., Part A: Polym. Chem.* **2004**, *42*, 3091-3109.
- (40) Paul, K. J. In *Cationic polymerization of olefins: a critical inventory*; New York; Toronto : Wiley, 1975. pp 337.

- (41) Kennedy, J. P. In *Cationic graft copolymerization editor: J.P. Kennedy*; Applied polymer symposia ; New York : Wiley, 1977, Vol. 30, pp 193.
- (42) Matyjaszewski, K. In *Cationic polymerizations :mechanisms, synthesis, and applications*; Plastics engineering ; Marcel Dekker: New York, 1996; Vol. 35, pp 768.
- (43) Roth, M.; Mayr, H. *Macromolecules* **1996**, *29*, 6104.
- (44) Schlaad, H.; Kwon, Y.; Sipos, L.; Faust, R.; Charleux, B. *Macromolecules* **2000**, *33*, 8225.
- (45) American Chemical Society; *Advances in chemistry series* ; American Chemical Society: Washington, 1962; Vol. 34, pp 260.
- (46) Boyd, R.; Breitlin S. *Macromolecules* **1972**, *5*, 1.
- (47) Suter, U.; Saiz, E.; Flory, P. *Macromolecules* **1983**, *16*, 1317.
- (48) Cho, D.; Neuburger, N.; Mattice, W. *Macromolecules* **1992**, *25*, 322.
- (49) Cheng, D.; Gardner, I.; Wang, H.; Frederick, C.; Dekmezian, A.; Hous, P. *Rubber Chem. Technol.* **1990**, *63*, 265.
- (50) Puskas, J.; Wilds, C. *Rubber Chem. Technol.* **1994**, *67*, 329.
- (51) White, J.; Shaffer, T.; Ruff, C.; Cross, J. *Macromolecules* **1995**, *28*, 3290.
- (52) Rodgers, B. In *Rubber compounding: chemistry and applications*; Marcel Dekker: New York, N.Y., 2004; , pp 645.
- (53) Pant, P.; Boyd, R. *Macromolecules* **1992**, *25*, 494.
- (54) Pant, P.; Boyd, R. *Macromolecules* **1993**, *26*, 679.
- (55) Boyd, R.; Pant, P. *Macromolecules* **1991**, *24*, 6325.

- (56) Mark, H. F.; Kroschwitz, J. I. In *Encyclopedia of polymer science and engineering*; Wiley: New York ;; Toronto, 1985; .
- (57) Hopfenberg, H. B.; Stannett, V.; *Polymer science and technology* ; Plenum Press: New York, 1974; Vol. 6, pp 482.
- (58) Pinchuk, L.; Wilson, G. J.; Barry, J. J.; Schoephoerster, R. T.; Parel, J.; Kennedy, J. *P. Biomaterials* **2008**, *29*, 448.
- (59) Cadieux, P.; Watterson, J.; Denstedt, J.; Harbottle, R.; Puskas, J.; Howard, J.; Gan, B.; Reid, G. *Colloids Surf., B* **2003**, *28*, 95.
- (60) Morrissey, R. *Ind. Eng. Chem.* **1955**, *47*, 1562.
- (61) Baldwin, F. *Rubber Chem. Technol.* **1979**, *52*, G77.
- (62) Hendrikse, K.; McGill, W. *J Appl Polym Sci* **2000**, *78*, 2302.
- (63) Takenaka, K.; Suzuki, M.; Takeshita, H.; Miya, M.; Shiomi, T.; Tamamitsu, K.; Konda, T. *J. Polym. Sci., Part A: Polym. Chem.* **2012**, *50*, 659.
- (64) Yamashita, S.; Yamada, A.; Oohata, M.; Kohjiya, S. *Makromol. Chem.* **1985**, *186*, 1373.
- (65) Vukov, R. *Elastomerics* **1983**, *115*, 25.
- (66) Whitney, R.; Penciu, A.; Parent, J.; Resendes, R.; Hopkins, W. *Macromolecules* **2005**, *38*, 4625.
- (67) Parent, J.; White, G.; Whitney, R.; Hopkins, W. *Macromolecules* **2002**, *35*, 3374.
- (68) Xiao, S.; Parent, J. S.; Whitney, R. A.; Knight, L. K. *J. Polym. Sci., Part A: Polym. Chem.* **2010**, *48*, 4691.
- (69) Malmberg, S. M.; Parent, J. S.; Pratt, D. A.; Whitney, R. A. *Macromolecules* **2010**, *43*, 8456.

- (70) Guillen-Castellanos, S.; Parent, J.; Whitney, R. *J. Polym. Sci., Part A: Polym. Chem.* **2006**, *44*, 983.
- (71) McLean, J. K.; Guillen-Castellanos, S. A.; Parent, J. S.; Whitney, R. A.; Resendes, R. *Eur. Polym. J.* **2007**, *43*, 4619.
- (72) Parent, J.; White, G.; Thom, D.; Whitney, R.; Hopkins, W. *J. Polym. Sci., Part A: Polym. Chem.* **2003**, *41*, 1915.
- (73) Parent, J.; Liskova, A.; Resendes, R. *Polymer* **2004**, *45*, 8091.
- (74) Parent, J.; Liskova, A.; Whitney, R.; Resendes, R. *J. Polym. Sci., Part A: Polym. Chem.* **2005**, *43*, 5671.
- (75) Parent, J. S.; Porter, A. M. J.; Kleczek, M. R.; Whitney, R. A. *Polymer* **2011**, *52*, 5410.
- (76) Parent, J.; Penciu, A.; Guillen-Castellanos, S.; Liskova, A.; Whitney, R. *Macromolecules* **2004**, *37*, 7477.
- (77) Jian, X.; Hay, A. *J. Polym. Sci., Part A: Polym. Chem.* **1991**, *29*, 547.
- (78) Gillies, E.; Bonduelle, C.; McEachran, M.; Arsenault, G.; Stojcevic, G. WO 2012/019303A1, 2012
- (79) Bonduelle, C. V.; Gillies, E. R. *Macromolecules* **2010**, *43*, 9230.
- (80) Yamashita, S.; Kodama, K.; Ikeda, Y.; Kohjia, S. *J. Polym. Sci., Part A: Polym. Chem.* **1993**, *31*, 2437.
- (81) Ikeda, Y.; Kodama, K.; Kajiwara, K.; Kohjia, S. *J. Polym. Sci., Part B: Polym. Phys.* **1995**, *33*, 387.
- (82) Puskas, J. E.; Munoz-Robledo, L. G.; Hoerr, R. A.; Foley, J.; Schmidt, S. P.; Evancho-Chapman, M.; Dong, J.; Frethem, C.; Haugstad, G. *Wiley Interdiscip. Rev. Nanomed. Nanobiotechnol.* **2009**, *1*, 451.

- (83) Zheng, Z.; Kwok, W. M.; Lau, W. M. *Chem. Commun.* **2006**, 3122.
- (84) Zheng, Z.; Xu, X.; Fan, X.; Lau, W.; Kwok, R. *J. Am. Chem. Soc.* **2004**, *126*, 12336.
- (85) Zheng, Z.; Wong, K. W.; Lau, W. C.; Kwok, R. W. M.; Lau, W. M. *Chem. Eur. J.* **2007**, *13*, 3187.
- (86) Bonduelle, C. V.; Lau, W. M.; Gillies, E. R. *ACS Appl. Mater. Interfaces*, **2011**, *3*, 1740.
- (87) Bonduelle, C. V.; Karamdoust, S.; Gillies, E. R. *Macromolecules* **2011**, *44*, 6405.
- (88) Sahoo, R. R.; Biswas, S. K. *J. Colloid Interface Sci.* **2009**, *333*, 707.
- (89) Yoshioka, M.; Yoshida, Y.; Inoue, S.; Lambrechts, P.; Vanherle, G.; Nomura, Y.; Okazaki, M.; Shintani, H.; Van Meerbeek, B. *J. Biomed. Mater. Res.* **2002**, *59*, 56.
- (90) Shin, Y. N.; Kim, B. S.; Ahn, H. H.; Lee, J. H.; Kim, K. S.; Lee, J. Y.; Kim, M. S.; Khang, G.; Lee, H. B. *Appl. Surf. Sci.* **2008**, *255*, 293.
- (91) Kennedy, J.; Askew, M.; Richard, G. *J. Biomater. Sci., Polym. Ed.* **1993**, *4*, 445.
- (92) Chen, Y.; McDaid, P.; Deng, L. *Chem. Rev.* **2003**, *103*, 2965.
- (93) Atodiresei, L.; Schiffers, I.; Bolm, C. *Chem. Rev.* **2007**, *107*, 5683.
- (94) Theisen, P.; Heathcock, C. *J. Org. Chem.* **1988**, *53*, 2374.
- (95) Theisen, P.; Heathcock, C. *J. Org. Chem.* **1993**, *58*, 142.
- (96) Magenau, A. J. D.; Hartlage, T. R.; Storey, R. F. *J. Polym. Sci., Part A: Polym. Chem.* **2010**, *48*, 5505.
- (97) Magenau, A. J. D.; Chan, J. W.; Hoyle, C. E.; Storey, R. F. *Polym. Chem.* **2010**, *1*, 831.

- (98) Suriano, F.; Coulembier, O.; Hedrick, J. L.; Dubois, P. *Polym. Chem.* **2011**, *2*, 528-533.
- (99) Pratt, R. C.; Nederberg, F.; Waymouth, R. M.; Hedrick, J. L. *Chem. Commun.* **2008**, 114.
- (100) Sanders, D. P.; Fukushima, K.; Coady, D. J.; Nelson, A.; Fujiwara, M.; Yasumoto, M.; Hedrick, J. L. *J. Am. Chem. Soc.* **2010**, *132*, 14724.
- (101) Storey, R.; Scheuer, A.; Achord, B. *Polymer* **2005**, *46*, 2141.
- (102) Breland, L. K.; Storey, R. F. *Polymer* **2008**, *49*, 1154.
- (103) Fang, Z.; Kennedy, J. J. *Polym. Sci., Part A: Polym. Chem.* **2002**, *40*, 3662.
- (104) Zhu, Y.; Storey, R. F. *Macromolecules* **2012**, *45*, 5347.
- (105) Resendes, R.; Krista, R.; Hickey, J. N. US Patent 7,662,480, 2010.

Chapter 2

2 Synthesis of Acid functionalized Butyl Rubber

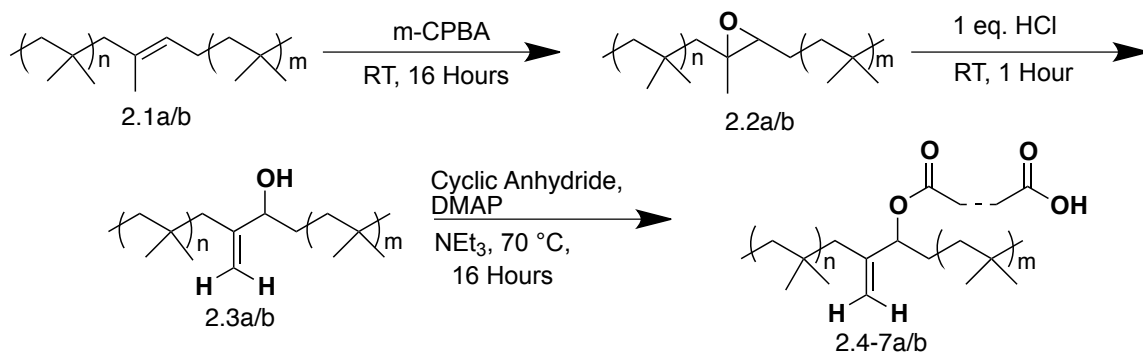
2.1 Introduction

Butyl Rubber (RB) is a synthetic elastomer, which is used in many high performance applications due to its many attractive properties. These properties include water/gas impermeability, chemical stability, high elasticity and biocompatibility. Commercial RB is a co-polymer of isobutylene with small amounts of isoprene (IP). RB and its co-polymers are important components in many commercial products such as innerliners for automobile tires, sporting equipment, sealants and even chewing gum. One property of RB that is currently being investigated further is its biocompatibility. This is due to the growth of the aging populations with a growing demand for products to enhance life expectancy and quality.

There has been some recent research in RB-based materials that are highly promising for a number of biomedical applications¹⁻³. A prime example is polyisobutylene-co-polystyrene (SIBS) triblock copolymers, which are currently being used for drug eluting coatings on TAXUS® vascular stents. Boston Scientific (U.S.A.) has commercialized this technology¹. This class of polymers has also been investigated as synthetic aortic valves⁴ and as shunts for glaucoma⁵. However, even the commercialized polymers have exhibited problems when integrated into implants. For example, SIBS was investigated as an implant in the urinary tract but there was significant attachment of uropathogenic species such as *E. coli* 67⁶. Also, in the stent application there was coating delamination in vivo^{7,8}. This indicates that the adhesion of SIBS polymers to the metal should be strengthened. The other major issue identified is a burst-release of the physically encapsulated drug from the laminate surface^{9,10}, this causes a decrease in the life of the stent. There is a need for new materials and chemical synthesis to provide functionalized RB's that will be better suited for medical applications. With the above issues in mind, it was proposed that the installation of carboxylic acid moieties on the RB backbone may reduce or eliminate these issues. Acid

groups have shown increased surface adhesion to stainless steel and other substrates in certain applications¹¹⁻¹³. Also, the acid group can act as a functional handle to covalently link a drug to the polymer reducing the burst release.

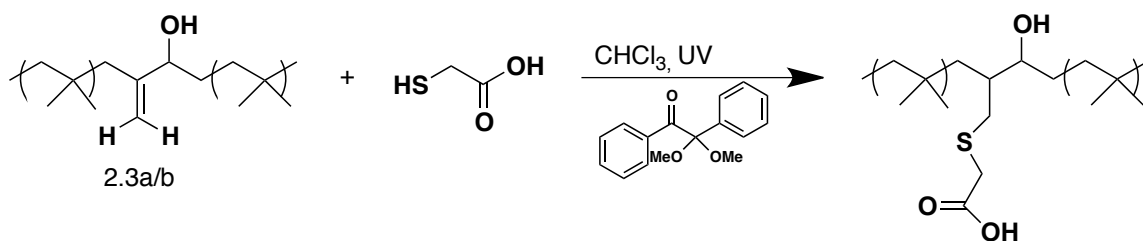
The target product of an acid functionalized RB should be scalable, cheap and reliable for industrial purposes. Cyclic anhydrides have been known to ring open upon attack from alcohols¹⁴⁻¹⁷. As shown in Scheme 2.1.1, upon treatment of RB (2.1) with *m*-chloroperoxybenzoic acid (*m*-CPBA), an epoxide functionalized RB (2.2) is yielded^{18, 19}. The epoxide can then be treated with aqueous hydrochloric acid to provide an allylic alcohol functionalized polymer 2.3²⁰. The allylic alcohol serves as a perfect substrate for cyclic anhydride ring opening to yield the target carboxylic acid products. This avenue fills the desired criteria for a potential industrial application. The reaction utilizes inexpensive cyclic anhydrides and only requires three steps to yield the desired product (Scheme 2.1.1). This chemistry has been recently utilized to functionalize hydroxylated poly(ethylene glycol) and then this acid was used as a functional handle to covalently attach a drug²¹.



Scheme 2.1.1 Proposed general route towards carboxylic acid functionalized butyl rubber.

Another potential way of synthesizing carboxylic acid functionalized RB would be utilizing 2.3 and performing a thiol-ene click reaction (Scheme 2.1.2). Thiol-ene chemistry, the reaction of a thiol with an alkene moiety under free radical conditions, has proven to be an effective synthetic tool in small molecule and polymer chemistry in recent years^{22, 23}. It can provide numerous advantages including high chemoselectivity,

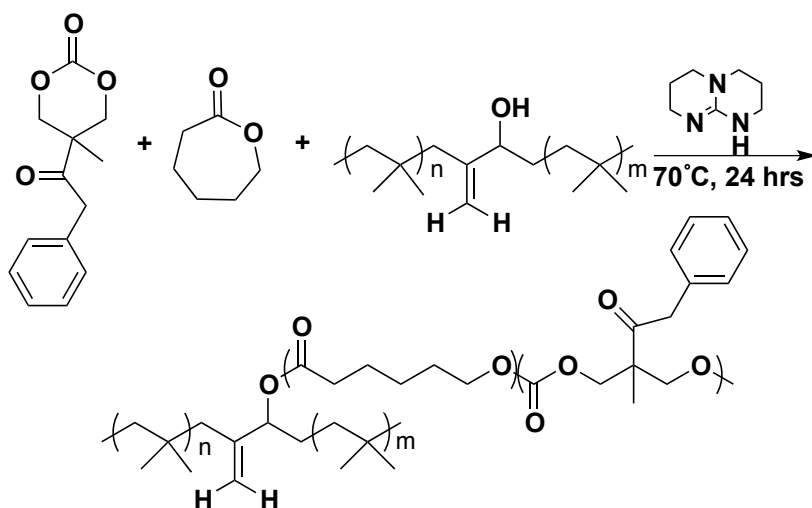
tolerance to oxygen, water, and a wide range of functional groups, relatively simple purification, high rates of reaction and quantitative conversion. These advantages, combined with the presence of double bond moieties throughout the backbone of butyl rubber make this reaction attractive for the introduction of various functionalities to RB. Along with the introduction of functional groups, this reaction should also result in the conversion of unsaturated to saturated moieties, potentially improving the chemical, oxidative, and biological stability of the butyl rubber backbone. Thus far, there are a very limited number of examples involving the use of thiol-ene chemistry with polyisobutylene derivatives²⁴⁻²⁶; these examples have much lower molecular weights than the commercialized RBs. The polymers reported involved the modification of terminal exo-alkene units of telechelic RB (a polymer in which both ends contain the same functionality) by *Storey* and coworkers.



Scheme 2.1.2 Proposed reaction of butyl rubber derivative 2.3 and TGAc in the presence of a photochemical initiator.

Another possibility is to introduce multiple carboxylic acids on the backbone by polymerization from the hydroxyl groups on the modified RB backbone. This would allow for tuning of surface adhesion as well as drug loading by tuning the length of the poly(carboxylic acid) chains. There are several potential avenues to produce a poly(carboxylic acid) functionalized RB. Ring-opening polymerizations (ROP) of cyclic carbonates have been performed from alcohol initiators. Hedrick *et al.* have demonstrated polymerization of cyclic carbonates from simple alcohols to yield various co-polymers²⁷⁻²⁹. The monomers have flexibility in terms of the types of functional groups that can be incorporated. To produce an acid functionalized RB, the monomer was

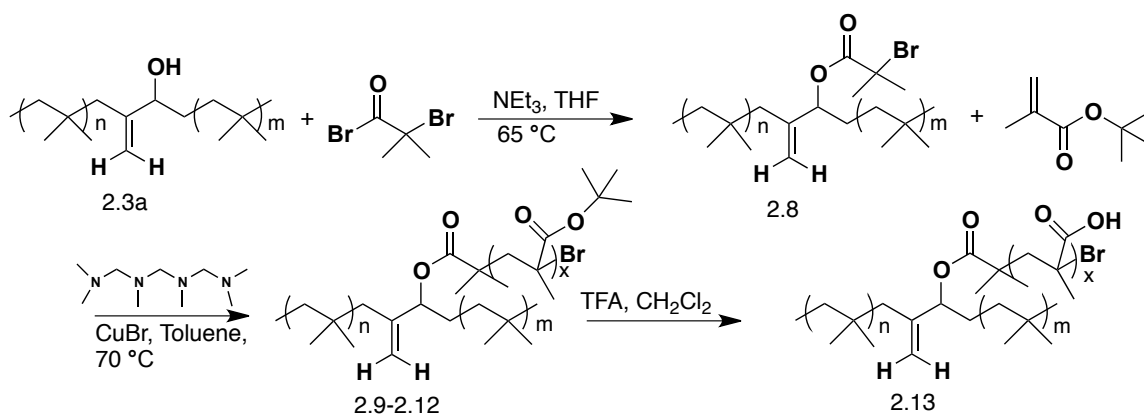
protected, then deprotected after polymerization. The proposed polymerization is shown in Scheme 2.1.3.



Scheme 2.1.3 Proposed reaction of butyl rubber derivative 2.3 to produce a graft copolymer containing protected carboxylic acids via ring-opening polymerization of a cyclic carbonate.

Atom-Transfer Radical Polymerization (ATRP) is an alternative approach to yield a poly(carboxylic acid) functionalized RB. Previous work has involved the use of standard ATRP conditions to polymerize various methacrylate/acrylate monomers to produce relatively low molecular weight copolymers of PIB³⁰⁻³³. They successfully incorporated an ATRP initiator to PIB by coupling α -bromoisobutyryl bromide to the terminus of hydroxyl functionalized PIB under basic conditions. For the current work polymer 2.3a is proposed as a suitable substrate for the production of the required bromide initiator followed by ATRP (Scheme 2.1.4). *Tert*-butyl methacrylate is proposed as the monomer due to the ease of its polymerization, deprotection and its commercial

availability³⁰.



Scheme 2.1.4 Proposed reaction of butyl rubber derivative 2.3a to form an ATRP initiator, followed by subsequent synthesis of a RB-co-poly(*tert*-butyl methacrylate) and its deprotection to yield the target RB-co-poly(methacrylic acid).

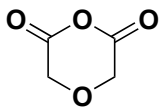
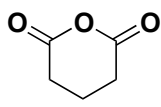
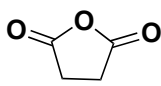
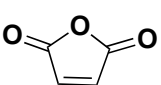
This chapter will describe the investigation of several approaches to the synthesis of carboxylic acid functionalized RB. The ring opening of cyclic anhydrides, thiol-ene coupling, the ring opening polymerization, and ATRP of protected poly(carboxylic acids) from the hydroxyl functionalized butyl rubber derivative 2.3a was studied and the products were characterized chemically by techniques including NMR, IR, SEC, TGA and DSC.

2.2 Results and Discussion

2.2.1 Cyclic Anhydride Ring-Opening

The study began by evaluating the reaction of RB derivative 2.3a/b with various cyclic anhydrides that are commercially available and inexpensive (Table 2.2.1). The anhydrides all differed in either ring size, degrees of unsaturation or electronics; this gave a suitable cross-section of the anhydrides that would be most advantageous for ring opening.

Table 2.2.1 A summary of the cyclic anhydrides used to create carboxylic acid modified RB. Each anhydride has different electronics, ring sizes and degrees of saturation.

Anhydride	Target Product	Equivalents	% Conversion
	2.4a/b	10-20	100%
	2.5	20	~50%
	2.6	20	5-6%
	2.7	20	NA

Using ^1H NMR spectroscopy, the conversion was calculated relative to the initial alcohol functionalized polymer 2.3a/b and differences in reactivity were observed (Table 2.2.1). The six-membered anhydrides worked with the highest conversions, diglycolic anhydride having complete conversion to the corresponding acid. The ^1H NMR spectrum after reaction of 2.3a/b with diglycolic anhydride (2.4) showed no starting allylic alcohol (Figure 2.2.1). The structure of the expected product was also supported by IR spectroscopy (Figure 2.2.2), with the appearance of two peaks in the carbonyl region at 1728 and 1748 cm^{-1} . These peaks correspond to the acid as well as the ester. In contrast, the five-membered anhydrides worked only to a small extent, if at all, to yield the desired carboxylic acid products. Succinic anhydride (2.6) showed minimal conversion whereas maleic anhydride (2.7) reacted rapidly to yield an insoluble product³⁴. These results were rationalized by the ring strain within the six-membered anhydride causing them to be more reactive than the five-membered counterparts. Diglycolic anhydride went to completion (2.4) and was more reactive than glutaric anhydride (2.5) due to the electron withdrawing effects of the extra oxygen. The scalability was also tested using diglycolic anhydride. These reactions were completed on two different isoprene contents a-2.2 & b-7.0%, which represents 2.4a/b respectively. The reaction can be successfully synthesized

in a greater than 10 g scale. This was an encouraging sign for testing in larger scale reactors.

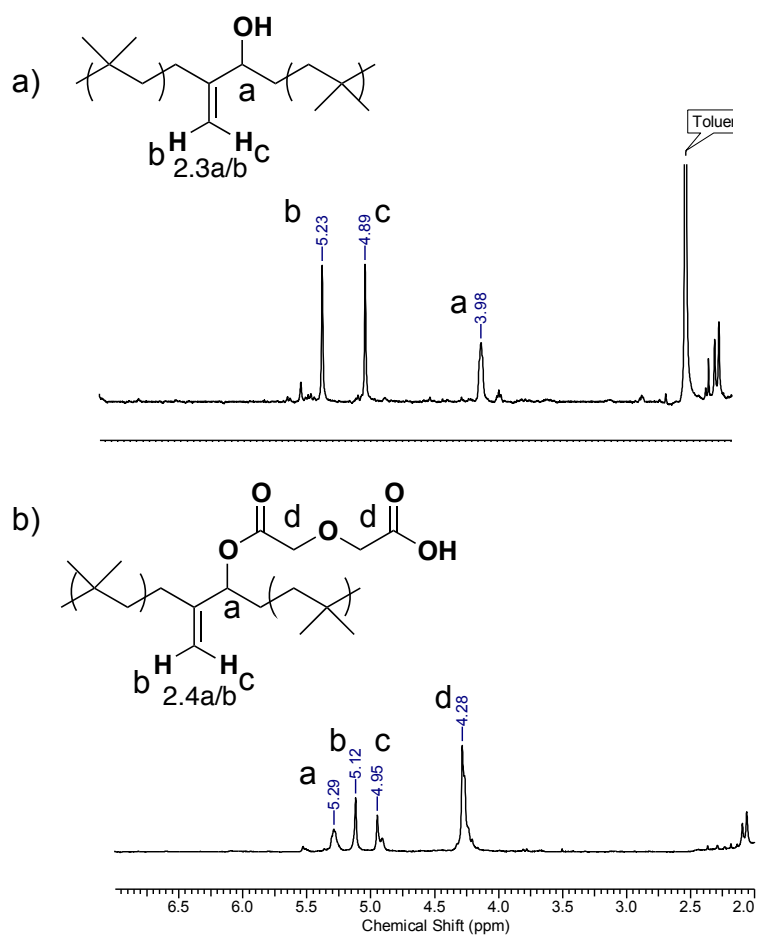


Figure 2.2.1 ^1H NMR spectra of a) polymer 2.3a; b) after reacting with to form 2.4a (CDCl_3 , 400 MHz).

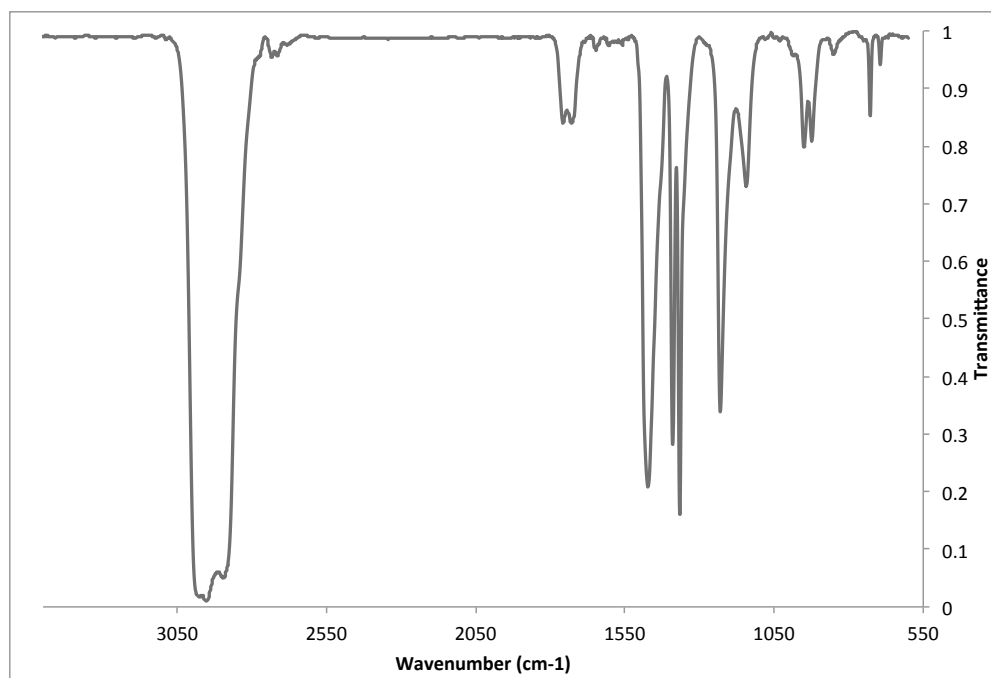


Figure 2.2.2 IR trace of acid modified RB 2.4a, the acid confirmed with the appearance of two carbonyl peaks at 1728 and 1748 cm⁻¹.

2.2.2 Thiol-ene “Click” Chemistry

Initial attempts to directly functionalize polymer 2.1 via thiol-ene chemistry did not lead to any detectable conversion. This is consistent with the lower reactivity of endo double bonds in the thiol-ene chemistry and the low accessibility of these bonds along the backbone of this high molecular weight polymer. The allylic alcohol 2.3 has an exo-alkene that would be more accessible for thiol-ene chemistries. Storey and coworkers were able to successfully perform thiol-ene chemistry on the terminal exo-alkene of telechelic RB^{22,23}; hence 2.3 might be more amenable to functionalization by thiol-ene chemistry. Using the reaction conditions previously reported for telechelic RB as a starting point²⁴, a number of reaction conditions were explored. Storey and coworkers used 2,2-dimethoxy-2-phenyl acetophenone (DMPA) as the photo-initiator and the reactions were performed with photochemical irradiation in CHCl₃. Following literature precedent, reactions were carried out under inert conditions, degassing for a minimum of 15 minutes to ensure that no oxygen is present. We selected thioglycolic acid (TGAc) as our thiol in initial work in order to introduce carboxylic acid moieties.

Table 2.2.2 summarizes the results of reaction attempts that involved different equivalents of thiols (relative to the double bond on the rubber) and different irradiation times. First, to ensure the stability of polymer 2.3 under the reaction conditions, control experiments were performed. Polymer 2.3 was exposed for various increments of time to UV light and it was observed that it was stable beyond one hour of irradiation. Next, the photoinitiator DMPA was added and the mixture was exposed for similar time periods. Again similar stability was observed. In contrast, upon the addition of 3 equivalents of TGAc to the reaction mixture and exposure to UV irradiation in the presence of DMPA some significant changes were observed in the ^1H NMR spectrum. Figure 2.2.3 shows the spectrum of the starting polymer 2.3. As shown in Figure 2.2.3, after 10 minutes of irradiation, new peaks were observed in the NMR spectrum, though it was difficult to assign these peaks entirely to the expected product, suggesting the presence of byproducts. After 60 min of irradiation, the starting material peaks in the NMR spectrum had almost entirely disappeared but again the spectrum was messy and it appeared that a number of byproducts were generated in the reaction.

Table 2.2.2 Reaction conditions and results for the photoinitiated thiol-ene reaction between polymer 2.3 and TGAc.

Thiol	Initiator (Y/N)	UV Exposure (min.)	Result
None	N	60	No detectable changes in the NMR spectrum
None	Y	60	No detectable changes in the NMR spectrum
TGAc (3 equiv.)	Y	10	Partial conversion with byproduct generation
TGAc (3 equiv.)	Y	60	Near complete conversion with byproduct generation
Dodecanethiol (5 equiv.)	Y	60	Near complete conversion but possible byproduct generation and difficulties removing excess thiol

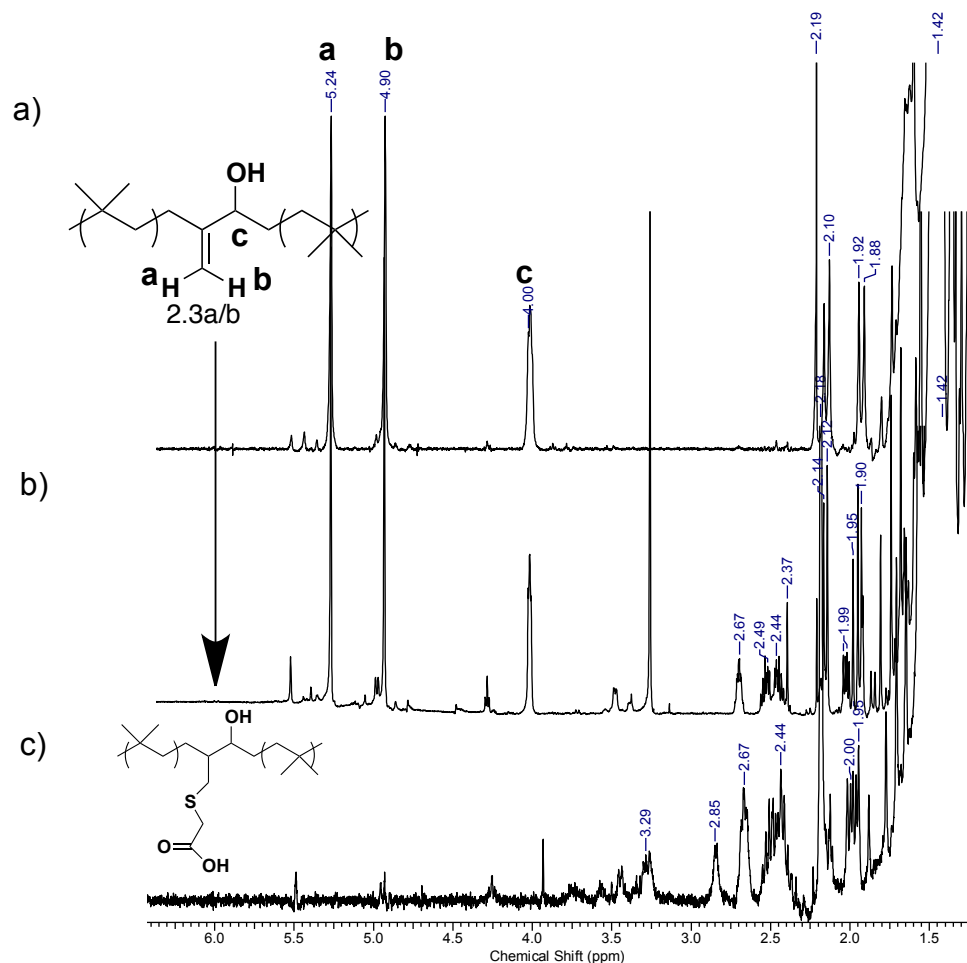


Figure 2.2.3 ^1H NMR spectra of a) polymer 2.3a; b) reaction product after 10 minutes of UV irradiation; c) reaction product after 1 hour of irradiation (3 equiv. of TGAc, DMPA photoinitiator). (CDCl_3 , 400 MHz)

At this stage it was proposed that byproducts might have resulted from the presence of the acidic carboxylic acid moiety on TGAc. Thus, the reaction was repeated with 1-dodecanethiol. The NMR spectrum (Appendix E) suggested that at least partial conversion to the product may have occurred, but again the reaction was not clean and was not complete. Furthermore, it was difficult to separate the excess 1-dodecanethiol from the product rubber.

2.2.3 Synthesis of Poly(carboxylic acid) Functionalized RB

This study began by using polymer 2.3 as the initiator and the benzyl protected cyclic carbonate as the monomer^{27, 28, 35}. The cyclic carbonate was copolymerized with ϵ -caprolactone as per literature protocol³⁶. The polymerization was relatively successful but the major issue was removal of the benzyl-protecting group via hydrogenation. Upon many attempts with various different conditions and monomer modification this polymerization technique was deemed not suitable and was abandoned.

Controlled radical polymerization techniques have been abundant in the literature as a means of producing functional co-polymers. The polymerization technique chosen was atom transfer radical polymerization (ATRP). This technique utilizes a copper/ligand system as a catalyst for polymerization. This technique was also chosen due to the easy installation of a bromo-initiator required for polymerization^{30, 32, 33, 37}. Polymer 2.3 was reacted with α -bromoisobutyryl bromide in the presence of triethylamine to yield the required bromo-initiator with a simple one step reaction. The ¹H NMR validated that the reaction went to completion yielding initiator 2.8 (Figure 2.2.4a).

The polymerization conditions followed literature precedent using copper bromide (CuBr) with the ligand 1,1,4,7,10,10- hexamethyltriethylenetetramine (HMTETA) as the catalyst³⁰. The monomer selected was *tert*-butyl methacrylate (tBMA) due to the ease of removal of the *tert*-butyl group to yield the final grafted poly(carboxylic acid).

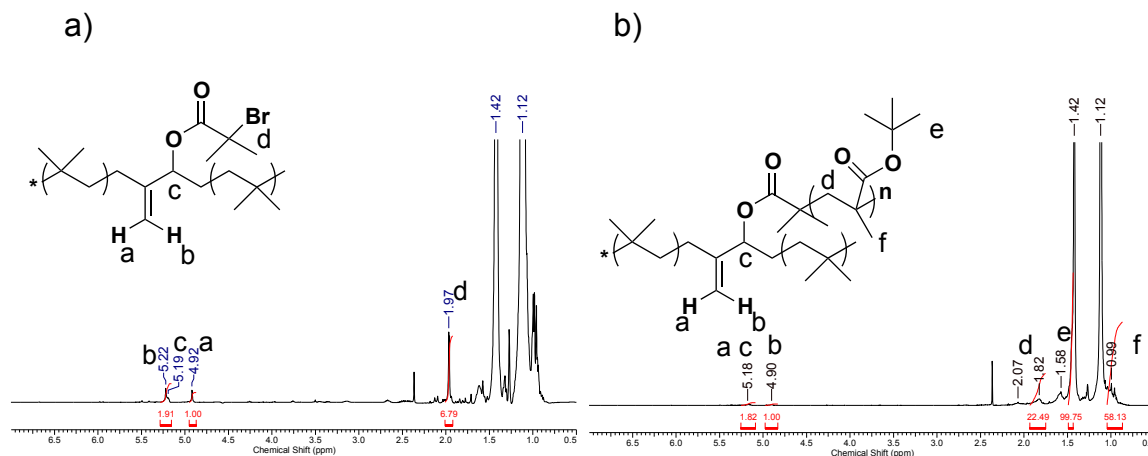


Figure 2.2.4 ^1H NMR spectra of a) polymer 2.8 the bromo-initiator; b) after polymerization with tBMA 2.9 (CDCl_3 , 400 MHz).

The polymerization was completed with tBMA and a small library of copolymers was prepared by tuning the degree of polymerization of tBMA (Table 2.2.3). The ^1H NMR spectrum (Figure 2.2.4b) shows conversion from 2.8 to the graft copolymer with broad polymeric peaks belonging to poly(*tert*-butyl methacrylate). It is interesting to note that at longer grafted chain lengths the polymer acted more like the arms than the core. Thus, the polymer became soluble in non-conventional solvents of RB such as acetone. Upon shortening the arms, the copolymer was observed to behave more like RB. This made purification very challenging for the longer chain polymers, so homopolymer poly(*tert*-butyl methacrylate) remained in the samples that could not be removed by conventional methods (Figure 2.2.5). The change in M_n can be seen in Table 2.2.3 and the SEC traces indicated the issue of homopolymerization. The grafting of shorter chains was investigated to see if it would eliminate the issue of purification. Upon reacting 2.8 with 15-50 equivalents of monomer (2.9/2.10), it was observed that there was no longer a side peak in the SEC trace. The resulting copolymer acted more like standard RB, allowing it to be precipitated in acetone. Thermogravimetric analysis (TGA) was then performed on several of the copolymers synthesized. The *tert*-butyl group begins degrading at ~ 210 $^\circ\text{C}$ which is prior to the degradation of the polymer backbone. These values allow for degree of polymerization to be calculated and these results can be seen in Table 2.2.4.

Table 2.2.3 Molecular weight data collected using SEC for the various equivalents of *tert*-butyl methacrylate co-polymers polymerized from initiator 2.8. M_w and M_n are given relative to polystyrene standards.

	Equivalents	M_w (g/mol)	M_n (g/mol)	PDI
2.8	0	397,000	139,900	2.8
2.9	15	195,000	86,500	2.3
2.10	50	285,000	96,000	3.0
2.11	100	566,000	185,000	3.6
2.12	300	817,000	225,000	3.7

Table 2.2.4 Data collected from TGA analysis and converted to degree of polymerization.

	Equivalents	Wt.% <i>tert</i> butyl group	Degree of Polymerization
2.9	15	9.0	5
2.10	50	19	17
2.11	100	33	89

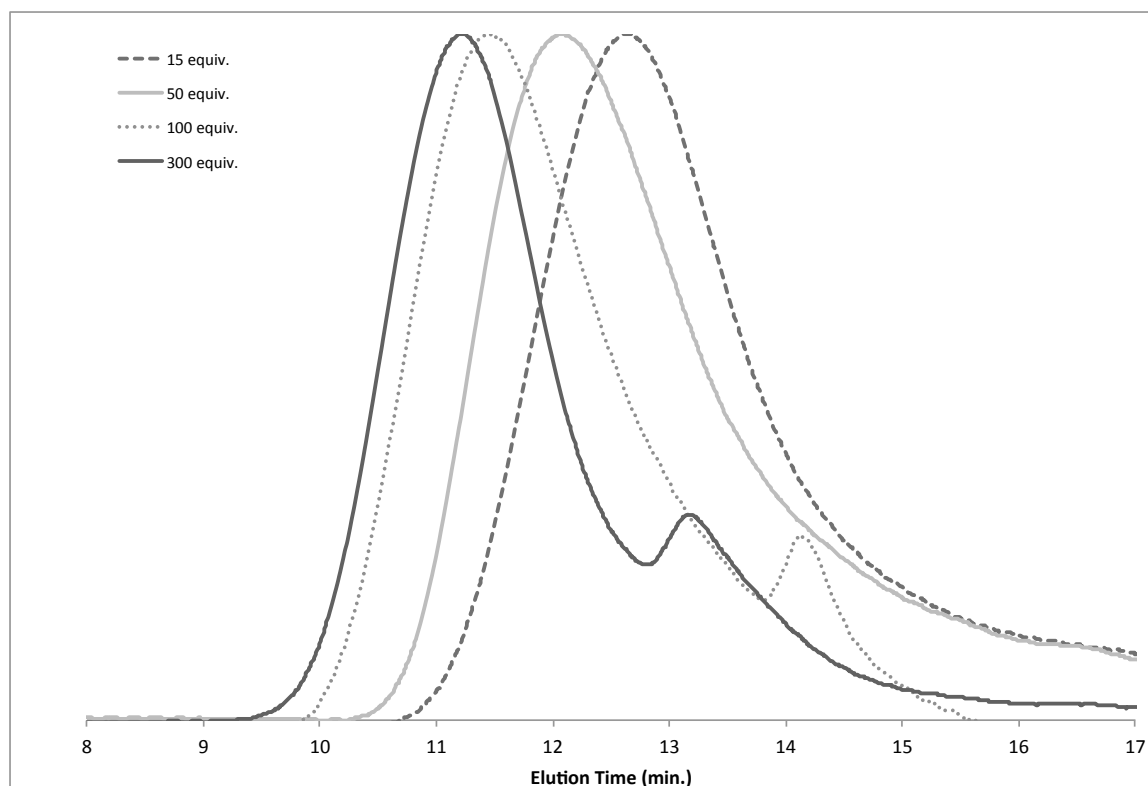


Figure 2.2.5 SEC traces of the co-polymers created with varying equivalents of *tert*-butyl methacrylate.

Deprotection of copolymer 2.9 was then investigated to yield the target poly(carboxylic acid) functionalized RB. In the literature there are many routes to deprotection. The three most common are 1) thermolysis^{32, 33} 2) heating in the presence of hydrochloric acid³⁰ & 3) use of trifluoroacetic acid (TFA) at room temperature³⁷. We attempted thermolysis first due to its simplicity and the avoidance of strong acids. Upon exposure in the vacuum oven at 150 °C and 30 mbar it was observed that deprotection was not close to completion. This was rationalized by RB's gas impermeability, so the focus was shifted to the use of TFA as a means of deprotection. First a control reaction was done to demonstrate the stability of RB to TFA treatment. After stirring RB in TFA for 2 h, an NMR spectrum was obtained which showed no changes relative to the starting polymer. SEC also showed no change in the polymer molecular weight. The copolymer was very soluble in dichloromethane (CH₂Cl₂) and upon adding TFA the polymer did not precipitate, meaning the reaction should be viable. However, after two hours the polymer

precipitated out of the CH_2Cl_2 and aggregated. Once the TFA was removed the polymer was not soluble in any common NMR solvents therefore, deprotection was followed using IR spectroscopy³⁰. The IR spectra suggested the emergence of a new peak corresponding to the carboxylic acid moiety at $\sim 1700\text{ cm}^{-1}$. Though it was difficult from the spectrum to determine whether complete deprotection was achieved, certainly a significant portion of the carboxylic acid moieties appeared to be unmasked (Figure 2.2.6).

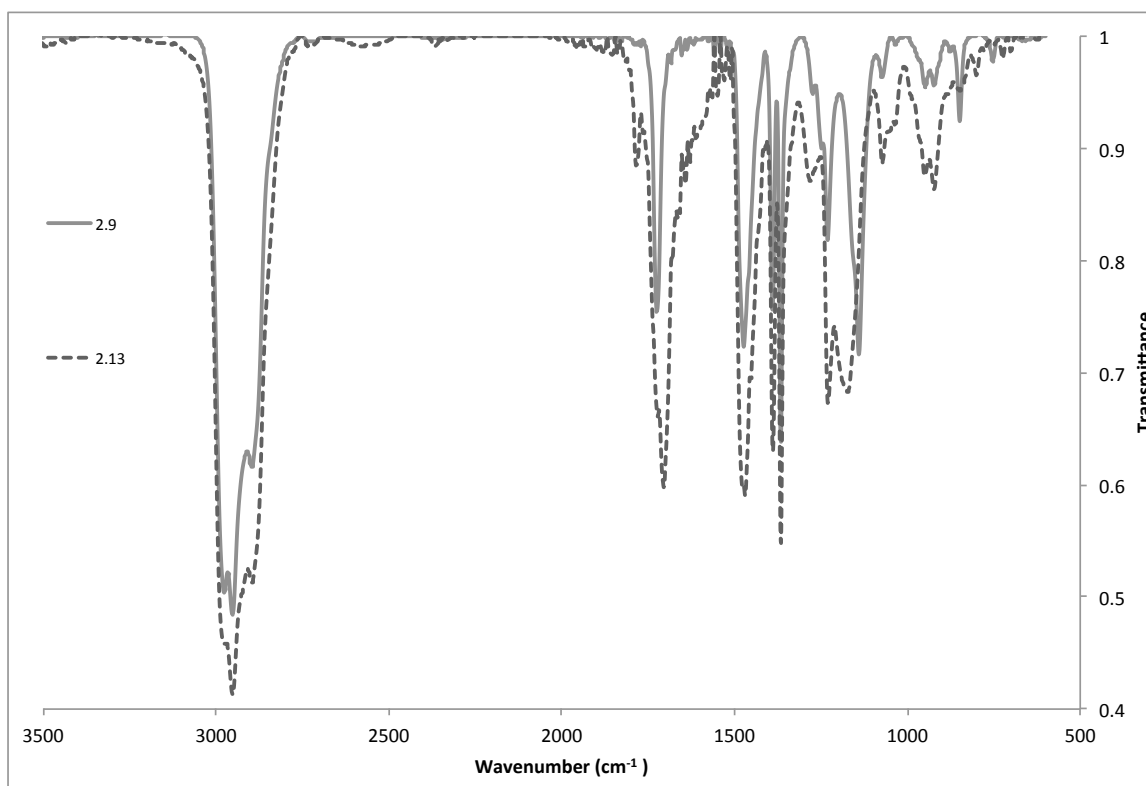


Figure 2.2.6 IR traces of copolymer 2.9 & deprotected copolymer 2.13, the carbonyl region to show a broadening of the carbonyl stretch, suggestive of the emergence of a new peak corresponding to the carboxylic acid at 1701 cm^{-1} .

2.3 Conclusions

Several methods of producing carboxylic acid functionalized RBs were investigated. Installation of the acid moieties on the backbone was successfully completed using ring opening of a cyclic anhydride and using ATRP polymerization

conditions. Diglycolic anhydride was ring opened to yield a full conversion to the carboxylic acid product. Also, polymerization of *tert*-butyl methacrylate under ATRP conditions provided a copolymer that could be deprotected using TFA to yield a poly(carboxylic acid). Other investigated approaches yielded no straightforward route to the desired product. Thiol-ene chemistry had too many side reactions while ring-opening polymerization was successful but deprotection of the benzyl-protecting group was not possible.

2.4 Experimental

General

LANXESS Butyl 402 ($M_w = 4.69 \times 10^5$ g/mol, PDI = 2.4) and butyl rubber containing 7 mol% ($M_w = 1.05 \times 10^6$ g/mol, PDI = 3.3) isoprene were provided by LANXESS Inc. Silicon wafers were purchased from University Wafer (Boston, MA). Solvents were purchased from Caledon and all other chemicals were purchased from Sigma-Aldrich and were used without further purification unless otherwise noted. Dry toluene was obtained from a solvent purification system. ^1H NMR spectra were obtained in CDCl_3 at 400 MHz. NMR chemical shifts (δ) are reported in ppm and are calibrated against residual solvent signals of CDCl_3 (δ 7.26). Infrared spectra were obtained as films from CH_2Cl_2 on NaCl plates using a Bruker Tensor 27 instrument. Differential scanning calorimetry (DSC) and thermal gravimetric analysis (TGA) was performed on a Mettler Toledo DSC 822e at a heating rate of 10 $^\circ\text{C}/\text{min}$ from -120 to +150 $^\circ\text{C}$.

Synthesis of polymer 2.4a

RB derivative 2.3a (10 g, 3.9 mmol of $-\text{OH}$) was dissolved in 350 mL of toluene. The solution was heated to 70 $^\circ\text{C}$, then 20 equivalents of triethylamine (10.9 mL, 78 mmol) was added followed by 2 equivalents of 4-(dimethylamino)pyridine (0.99 g, 7.8 mmol). A solution of diglycolic anhydride (10 equivalents, 4.5 g, 39 mmol) dissolved in toluene was then added via syringe and the reaction mixture was stirred at 70 $^\circ\text{C}$ overnight. The product was then washed with distilled water and 6 M HCl twice, followed by concentration under reduced pressure. The product was further purified by precipitation

(2:1 Acetone/Toluene) and then dried under vacuum. Conversion = 100% Yield = 90%
 ^1H NMR (400 MHz, CDCl_3) 5.29 (br s, 1H), 5.12 (s, 1H), 4.95 (s, 1H), 4.20-4.40 (m, 4H),
 1.42 (s, 145H), 1.12 (s, 431H). SEC: $M_w = 308900$ g/mol, PDI = 2.52. IR: 1230, 1365.
 1390, 1475, 1733, 1758, 2974 cm^{-1} . $T_g = -61$ °C

Synthesis of polymer 2.4b

RB derivative 2.2b (10 g, 12.1 mmol of epoxide) was dissolved in 350 mL toluene. The solution was treated with one equivalent HCl (1.0 mL, 12.1 mmol) and allowed to react at room temperature for 1 hour. Due to solubility issues 3b was not isolated. Instead the HCl was neutralized with Sodium Carbonate and then dried with MgSO_4 . The mixture was then centrifuged and 3 was decanted from the MgSO_4 . The solution was heated to 70 °C, then 20 equivalents of triethylamine (33.7 mL, 242 mmol) was added followed by 2 equivalents of 4-(dimethylamino)pyridine (3.1 g, 24.2 mmol). A solution of diglycolic anhydride (10 equivalents, 14.0 g, 121 mmol) dissolved in toluene was then added via syringe and the reaction mixture was stirred at 70 °C overnight. The product was then washed with distilled water and 6 M HCl twice, followed by concentration under reduced pressure. The product was further purified by precipitation (2:1 Acetone/Toluene) and then dried under vacuum. Conversion = 100% Yield = 90% ^1H NMR (400 MHz, CDCl_3) 5.29 (br s, 1H), 5.12 (s, 1H), 4.95 (s, 1H), 4.20-4.40 (m, 4H), 1.42 (s, 69H), 1.12 (s, 209H). IR: 1230, 1365. 1390, 1475, 1733, 1758, 2974 cm^{-1} . $T_g = -53$ °C

Ring opening polymerization from polymer 2.3a

Polymer 2.3a was dissolved in dry toluene under nitrogen. Bn-MTC was dissolved in dry toluene and was added to the solution followed by ϵ -caprolactone. The mixture was heated to 70° C. The catalyst 1,5,7 triazabicyclo[4,4,0] dec-5-ene was added and the solution was allowed to react overnight. The resultant mixture was then washed twice with water and precipitated using 2:1 Acetone/Toluene. Polymer was dried under vacuum. ^1H NMR (400 MHz, CDCl_3): 7.36 (Bn-MTC br m, 5H), 5.24 (s, 1H), 5.12-5.16 (Bn-MTC s, 2H), 4.90 (s, 1H), 4.24 (br m, 4H), 4.06-4.11 (CL, m, 8H) 2.31 (CL m, 8H), 1.42 (CH₂, 143H), 1.12 (s, CH₃, 424H). SEC: $M_w = 489000$ g/mol, PDI = 1.73.

Synthesis of polymer 2.8

Butyl rubber derivative 2.3 (10 g, 3.9 mmol of –OH) was dissolved in 350 mL of toluene. The solution was heated to 70 °C, then 14 equivalents of triethylamine (7.60 mL, 54.6 mmol) was added followed by 14 equivalents of 2-bromoisobutyl bromide (6.95 mL, 54.6 mmol). The solution was stirred overnight at 70 °C, then the reaction mixture was washed with distilled water three times, then concentrated under reduced pressure. The product was further purified by precipitation (2:1 Acetone/Toluene) and then dried under vacuum. Conversion = 100% Yield = 80% ¹H NMR (400 MHz, CDCl₃) 5.22 (s, 1H), 5.19 (br s, 1H), 4.92 (s, 1H), 1.97 (s, 6H), 1.42 (s, 290H), 1.12 (s, 913H). SEC: M_w = 396900 g/mol, PDI = 2.84. IR: 1232, 1367, 1390, 1479, 1736, 2977 cm⁻¹.

Synthesis of polymer 2.9

In a predried Schlenk tube under a nitrogen atmosphere at room temperature were placed 1 eq. CuBr (0.13 mmol, 0.187 g), a stirring bar, 2 eq. of the ligand 1,1,4,7,10,10-hexamethyltriethylenetetramine (HMTETA) (0.26 mmol, 0.071 mL), 15 eq. of deoxygenated *tert*-butyl methacrylate (1.95 mmol, 0.316 mL), and toluene. The tube was tightly sealed with a rubber septum and degassed by three freeze–pump–thaw cycles. Right after the addition of 2.8 (0.13 mmol, 0.356 g) initiator by a syringe, the tube was immersed in a thermostated oil bath maintained at 70 °C. After twelve hours the solution was exposed to the atmosphere and concentrated using rotary evaporation. The crude mixture was then precipitated in methanol and washed with water. ¹H NMR (400 MHz, CDCl₃) 5.16 (br s, 2H), 4.92 (s, 1H), 1.82 (tBMA, brs, 22.49H), 1.44 (tBMA, brs, 99.75H) 1.42 (s, 290H), 1.12 (s, 913H), 1.05 (tBMA, m, 58.13H),). SEC: M_w = 195000 g/mol, PDI = 2.26. IR: 1253, 1367, 1392, 1483, 1728, 2981 cm⁻¹.

Synthesis of polymer 2.13

The poly *tert*-butyl methacrylate- RB co-polymer was dissolved in CH₂Cl₂ in a round bottom with a magnetic stir-bar. Upon dissolution of the polymer a 10-molar excess TFA was added to the solution. The reaction was then left for twenty-four hours at 25 °C. The

solvent and TFA was removed via evaporation, the polymer was re-dissolved and evaporated for three cycles. IR: 1203, 1280, 1390, 1450, 1488, 1701, 2603, 2972, 3471 cm^{-1} .

2.5 References

- (1) Pinchuk, L.; Wilson, G. J.; Barry, J. J.; Schoephoerster, R. T.; Parel, J.; Kennedy, J. P. *Biomaterials* **2008**, *29*, 448.
- (2) Puskas, J.; Chen, Y. *Biomacromolecules* **2004**, *5*, 1141.
- (3) Puskas, J.; Chen, Y.; Dahman, Y.; Padavan, D. *J. Polym. Sci., Part A: Polym. Chem.* **2004**, *42*, 3091.
- (4) Gallocher, S. L.; Aguirre, A. F.; Kasyanov, V.; Pinchuk, L.; Schoephoerster, R. T. *J. Biomed. Mater. Res. B Appl. Biomater.* **2006**, *79B*, 325.
- (5) Acosta, A. C.; Espana, E. M.; Yamamoto, H.; Davis, S.; Pinchuk, L.; Weber, B. A.; Orozco, M.; Dubovy, S.; Fantes, F.; Parel, J. *Arch. Ophthalmol.* **2006**, *124*, 1742.
- (6) Cadieux, P.; Watterson, J.; Denstedt, J.; Harbottle, R.; Puskas, J.; Howard, J.; Gan, B.; Reid, G. *Colloids Surf., B* **2003**, *28*, 95.
- (7) Levy, Y.; Mandler, D.; Weinberger, J.; Domb, A. J. *J. Biomed. Mater. Res. B Appl. Biomater.* **2009**, *91B*, 441.
- (8) Ormiston, J.; Currie, E.; Webster, M.; Kay, P.; Ruygrok, P.; Stewart, J.; Padgett, R.; Panther, M. *Catheter. Cardio. Inte.* **2004**, *63*, 332-336.
- (9) Yoo, H.; Oh, J.; Lee, K.; Park, T. *Pharm. Res.* **1999**, *16*, 1114.
- (10) Tong, R.; Cheng, J. *Angew. Chem. Int. Ed.* **2008**, *47*, 4830.
- (11) Yoshioka, M.; Yoshida, Y.; Inoue, S.; Lambrechts, P.; Vanherle, G.; Nomura, Y.; Okazaki, M.; Shintani, H.; Van Meerbeek, B. *J. Biomed. Mater. Res.* **2002**, *59*, 56.

- (12) Shin, Y. N.; Kim, B. S.; Ahn, H. H.; Lee, J. H.; Kim, K. S.; Lee, J. Y.; Kim, M. S.; Khang, G.; Lee, H. B. *Appl. Surf. Sci.* **2008**, *255*, 293.
- (13) Kennedy, J.; Askew, M.; Richard, G. *J. Biomater. Sci., Polym. Ed.* **1993**, *4*, 445.
- (14) Chen, Y.; McDaid, P.; Deng, L. *Chem. Rev.* **2003**, *103*, 2965.
- (15) Atodiresei, L.; Schiffers, I.; Bolm, C. *Chem. Rev.* **2007**, *107*, 5683.
- (16) Theisen, P.; Heathcock, C. *J. Org. Chem.* **1988**, *53*, 2374.
- (17) Theisen, P.; Heathcock, C. *J. Org. Chem.* **1993**, *58*, 142.
- (18) Puskas, J.; Wilds, C. *Rubber Chem. Technol.* **1994**, *67*, 329.
- (19) Jian, X.; Hay, A. *J. Polym. Sci., Part A: Polym. Chem.* **1991**, *29*, 547.
- (20) Bonduelle, C. V.; Gillies, E. R. *Macromolecules* **2010**, *43*, 9230.
- (21) Zhang, X.; Li, Y.; Chen, X.; Wang, X.; Xu, X.; Liang, Q.; Hu, J.; Jing, X. *Biomaterials* **2005**, *26*, 2121.
- (22) Hoyle, C. E.; Bowman, C. N. *Angew. Chem. Int. Ed.* **2010**, *49*, 1540.
- (23) Hoyle, C. E.; Lowe, A. B.; Bowman, C. N. *Chem. Soc. Rev.* **2010**, *39*, 1355.
- (24) Magenau, A. J. D.; Chan, J. W.; Hoyle, C. E.; Storey, R. F. *Polym. Chem.* **2010**, *1*, 831.
- (25) Magenau, A. J. D.; Hartlage, T. R.; Storey, R. F. *J. Polym. Sci., Part A: Polym. Chem.* **2010**, *48*, 5505.
- (26) Mazzolini, J.; Boyron, O.; Monteil, V.; Gignes, D.; Bertin, D.; D'Agosto, F.; Boisson, C. *Macromolecules* **2011**, *44*, 3381.
- (27) Sanders, D. P.; Fukushima, K.; Coady, D. J.; Nelson, A.; Fujiwara, M.; Yasumoto, M.; Hedrick, J. L. *J. Am. Chem. Soc.* **2010**, *132*, 14724.

- (28) Pratt, R. C.; Nederberg, F.; Waymouth, R. M.; Hedrick, J. L. *Chem. Commun.* **2008**, 114.
- (29) Suriano, F.; Coulembier, O.; Hedrick, J. L.; Dubois, P. *Polymer Chemistry* **2011**, 2, 528.
- (30) Fang, Z.; Kennedy, J. J. *J. Polym. Sci., Part A: Polym. Chem.* **2002**, 40, 3662.
- (31) Storey, R.; Scheuer, A.; Achord, B. *Polymer* **2005**, 46, 2141.
- (32) Breland, L. K.; Storey, R. F. *Polymer* **2008**, 49, 1154.
- (33) Zhu, Y.; Storey, R. F. *Macromolecules* **2012**, 45, 5347.
- (34) Saelao, J.; Phinyocheep, P. *J Appl Polym Sci* **2005**, 95, 28-38.
- (35) Kim, S. H.; Tan, J. P. K.; Fukushima, K.; Nederberg, F.; Yang, Y. Y.; Waymouth, R. M.; Hedrick, J. L. *Biomaterials* **2011**, 32, 5505.
- (36) Lu, J.; Shoichet, M. S. *Macromolecules* **2010**, 43, 4943.
- (37) Storey, R.; Scheuer, A.; Achord, B. *Polymer* **2005**, 46, 2141.

Chapter 3

3 Improvements to the Physical Properties of Butyl Rubber

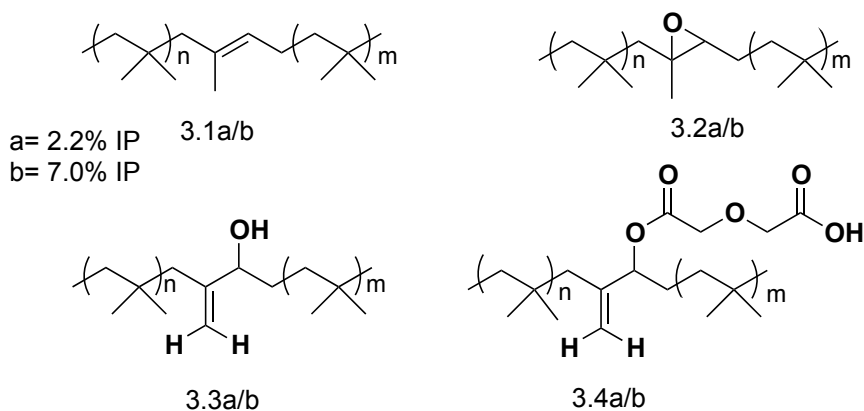
Contribution Statement: Surface adhesion testing was completed in collaboration with LANXESS Inc. and was performed by Brianna Binder. Dr. Heng-Yong Nie at Surface Science Western assisted with AFM training and imaging

3.1 Introduction

Butyl Rubber (RB) is a synthetic elastomer that contains many attractive properties such as gas/water impermeability, chemical stability, excellent mechanical properties and biocompatibility^{1,2}. With all of these attributes there are still some limitations. One limitation is the ability to create homogeneous coatings of hydrophilic/polar materials or polymers such as poly(ethylene oxide) (PEO) on a RB surface³. Surface homogeneity is crucial to expand the applications of RB to biomedical devices, especially *in-vivo*. This incompatibility is due to the very hydrophobic nature of RB and is evidenced by a relatively high contact angle of $\sim 90^\circ$. This creates a surface that is difficult to coat due to the incompatibility of polar materials with a non-polar surface. Such incompatibility hinders the wettability of the polar material and thus yields a partially coated surface^{4,5}. The resultant surfaces are not appropriate for high-end applications like biomaterials where a high degree of surface uniformity is needed. Thus, there is a need to investigate potential compatibilization approaches to create much more homogeneous surfaces.

The other inherent problem with RB as a biomaterial is delamination of RB coatings from substrates such as stainless steel^{6,7}. This again limits the use of such polymers in bio-medical applications because once delamination occurs it can cause major implications *in vivo* and is of particular relevance to RB-based copolymers used clinically as coatings on drug-eluting stents⁸. The surface adhesion of RB to metallic substrates should ideally be improved. Both of these surface compatibility issues can be addressed by modification of the polymer backbone and introducing different

functionalities along the RB backbone. Recently, as shown in Scheme 3.1.1, modifications have been made along the RB backbone that can yield multiple oxygen-containing functionalities including an epoxide, an alcohol and a carboxylic acid⁹. In previous work it was noted that there was increased compatibilization between butyl rubber and polar polymers when an oxygen-containing butyl rubber derivative was used as the substrate¹⁰. For example, it was found that it was possible to prepare uniform, cross-linked films of PEO on epoxidized butyl rubber (3.2a), but not on butyl rubber itself (3.1a). However, the other oxygenated butyl rubber derivatives such as 3.3a and 3.4a were not previously investigated. It was also anticipated that such oxygenated butyl rubber derivatives might provide enhanced adhesion to metal substrates¹¹⁻¹³, a property that could significantly enhance their performance in applications such as stent coatings.



Scheme 3.1.1 The oxygenated RBs synthesized from commercially available RB (3.1); epoxide (3.2), alcohol (3.3) and carboxylic acid (3.4).

In this chapter, the performance of oxygenated butyl rubber derivatives including 3.2a, 3.3a, and 3.4a as compatibilizing layers to enable the coating of butyl rubber with more hydrophilic polymers such as PEO is described. The surfaces are characterized by static contact angle measurements and atomic force microscopy (AFM). In addition, the adhesion properties of these polymers (3.2a/b, 3.3a/b, and 3.4a/b) to stainless steel are also described.

3.2 Results and Discussion

3.2.1 The application of oxygenated RBs as compatibilizing layers

The previously reported approach for investigating the compatibilization properties of epoxidized butyl rubber was used for the current work. A silicon wafer was selected as the underlying substrate due to its flat nature. A cleaned 1 cm x 1 cm silicon wafer was spin coated with 3.1a (5 mg/mL in toluene) (Figure 3.2.1). In order to prevent dissolution of each polymer layer during the deposition of subsequent layers, each layer was cross-linked by a method termed hyperthermal hydrogen induced cross-linking (HHIC). This is an alternative to conventional plasma treatments¹⁴⁻¹⁷. Briefly, when a lightweight projectile such as an atom or molecule, possessing elevated kinetic energy collides with the atoms of organic molecules on a substrate, there is a transfer of kinetic energy. The projectile is generally H^+ ^{15, 16} or H_2 ¹⁴. It has been demonstrated through molecular dynamics simulations and experiments, that the collision is only effective if it collides with a hydrogen atom of the organic molecule as opposed to a heavier atom such as carbon or oxygen. This mechanism depends on mass-dependent kinematic energy transfer, which is readily understood when it is simplified to the framework of hard-sphere collision theory. A hydrogen projectile can transfer 100% of its kinetic energy to a hydrogen target but the maximum drops to 28% when the target is carbon. This allows for selective breaking of C-H bonds without breaking other bonds. Thus, HHIC is functional group tolerant, which is not the case for most traditional plasma techniques^{18, 19}. Once radicals are produced on the surface molecules, they can recombine and form a cross-linked layer, thus providing an elegant means of preparing chemically grafted,

cross-linked surfaces (Figure 3.2.2). There are limited examples of using HHIC but all have thus far demonstrated functional group tolerance^{3, 20, 21}.

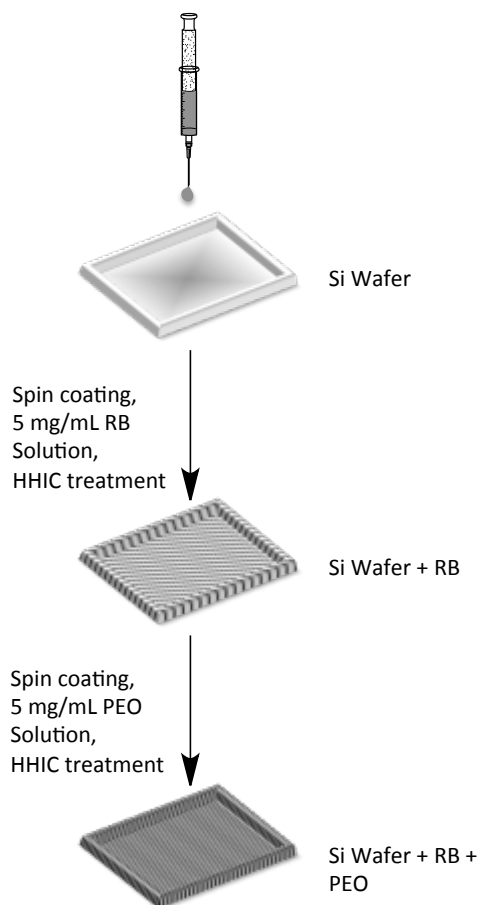


Figure 3.2.1 Thin film preparation of RB/PEO films using spin casting and HHIC.

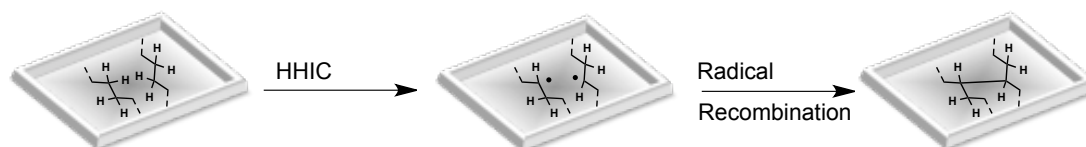


Figure 3.2.2 Visual depiction how molecules form radicals and recombine to form cross-linked films via HHIC.

Following cross-linking by HHIC, the butyl rubber layer was characterized by AFM to measure film thickness and surface uniformity, and contact angle measurements were performed. It was found that upon coating RB onto the silicon substrate, a very homogenous film was obtained. The surface was visualized using AFM, as shown in Figure 3.2.3a and AFM was also used to quantify the average surface roughness, which was 1.5 nm. The oxygenated butyl rubbers 3.2a, 3.3a, or 3.4a, were then deposited on top of the butyl rubber layer by spin coating and cross-linked by HHIC. As shown in Table 3.2.1, it was found that the thickness increased upon coating the oxygenated RBs, which was expected. Also seen was the same surface roughness as the RB under layer, as well as similar contact angles. Upon visualization with AFM it was seen that a homogenous film was obtained for these laminates.

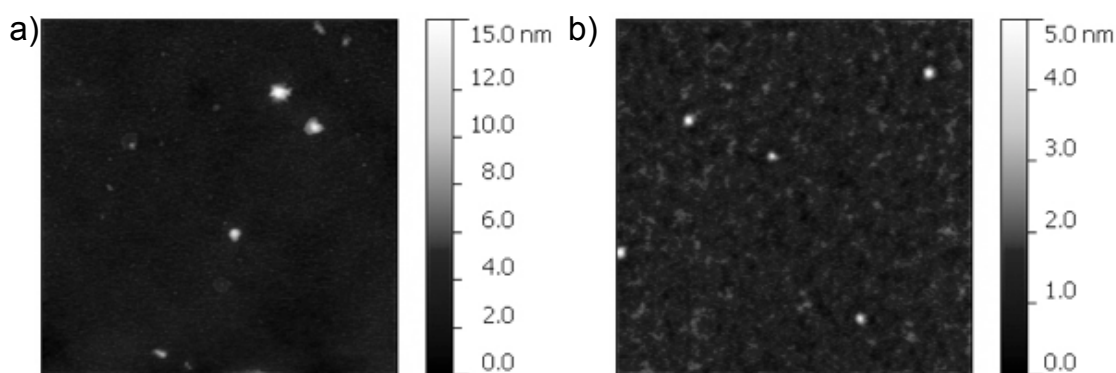


Figure 3.2.3 a) AFM image (topography) of 3.1a b) AFM image of 3.2a spin coated on 3.1a. AFM images correspond to a 5 μm x 5 μm area.

Table 3.2.1 Tabulated data of static contact angles, film thickness and roughness from AFM for the laminates of 3.2a, 3.3a, 3.4a coated on 3.1a.

Sample	Film Thickness (nm)	Film Roughness (nm)	Static CA(°)
Butyl 402 3.1a	28	2	91.5 ± 1
Epoxidized Butyl 3.2a on 3.1a	43	2	87.7 ± 2
Hydroxyl functionalized butyl 3.3a on 3.1a	45	2	87.0 ± 0.4
Acid functionalized butyl 3.4a on 3.1a	41	2	85.9 ± 3

In order to investigate the capabilities of the various oxygenated butyl rubber derivatives to compatibilize butyl rubber towards more hydrophilic polymers, PEO was selected as the coating material. It was chosen due to its many desirable properties such as resistance to protein adsorption as well as its biocompatibility²²⁻²⁶. Hydrophobic elastomers like RB are known to strongly adsorb proteins^{1,3}, which limits their use in biomedical applications. PEO was spin coated from CH₂Cl₂ onto butyl rubber as well as the oxygenated rubber surfaces described above. Upon coating PEO on native butyl rubber (3.1a) it was found using AFM that the resulting layer was very non-uniform (Figure 3.2.4). In contrast, when 3.2a was coated prior to coating of PEO there was a remarkable difference in the surface homogeneity. This has been described previously³ but upon coating with 3.3a & 3.4a homogenous films were also obtained (Figure 3.2.4 b-d). The laminate formed with 3.3a showed no improvement to surface roughness or static contact angles relative to 3.2a. 3.4a showed slight improvement in surface roughness and decreases in the contact angles, though the differences were not statistically significant (Table 3.2.2). It has been shown with 3.2a that the increased homogeneity of the PEO

film relative to that on unmodified butyl rubber translates into a substantial decrease in the amount of protein absorption³. Based on the results for 3.3a and 3.4a, it can also be inferred that such PEO coatings would resist the adsorption of proteins.

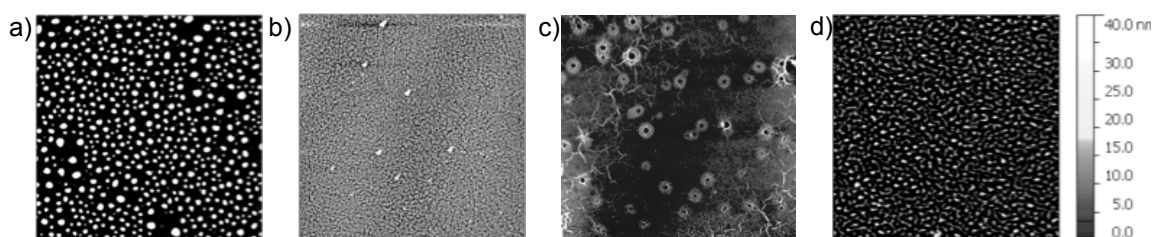


Figure 3.2.4 a) AFM image (topography) of PEO coated on 3.1a b) AFM image of PEO spin coated on 3.2a c) AFM image of PEO spin coated on 3.3a d) AFM image of PEO spin coated on 3.4a. AFM images correspond to a 5 μm x 5 μm area.

Table 3.2.2 Tabulated data of static contact angles, film thickness and roughness from AFM for the PEO coated onto RB samples.

Sample	Film Thickness (from AFM) (nm)	Film Roughness (from AFM) (nm)	Static CA ($^{\circ}$)
PEO on RB 3.1a	32	18	59 ± 1
PEO on Epoxidized RB 3.2a on 3.1a	56	5	49 ± 3
PEO on Hydroxyl functionalized RB 3.3a on 3.1a	53	6	51 ± 3
Acid functionalized RB 3.4a on 3.1a	53	5	48 ± 3

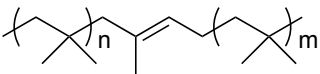
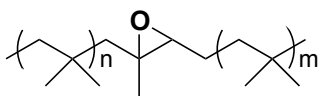
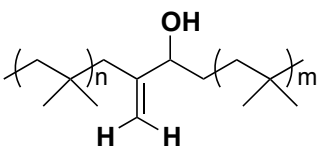
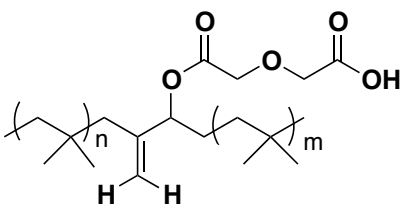
3.2.2 Measurement of the adhesion of RB derivatives to a stainless steel substrate

The synthesis of polymers 3.2a/b, 3.3a/b, and 3.4a/b was performed on a 5-10 g scale as described in Chapter 2. Surface adhesion or stickiness was determined by the amount of force required to remove the sample from the substrate. In the current work, a stainless steel substrate was selected due to the interest in the adhesion of RB copolymers to stainless steel stents²⁷. The experiments were completed in collaboration with LANXESS Inc. by measuring the force required to separate the material and the substrate. The test specimens consisted of 6.4 X 50.8 mm reinforced strips with a thickness between 0.5 and 3.3 mm. They were produced by pressing the material in a square mold at 100 °C for five minutes between Mylar and Teflon. From these sheets the samples were cut and tested. The test specimens were placed in the apparatus at right angles to each other, which defined the area of contact. Once the two specimens came into contact with each other, force was then applied in the opposite direction, and the amount of energy required to separate the two plates was measured. This energy was defined as the surface adhesion.

The adhesion of the commercially available RB 3.1a/b is well known and the various oxygenated RBs (3.2a/b, 3.3a/b, 3.4a/b) were tested and compared to 3.1a/b. All of the oxygenated RBs showed significant improvements in adhesion to the stainless steel substrate. The largest improvement in adhesion was seen with 3.4a, which took 32.8 ± 1.3 psi to separate (Table 3.2.3.) This can be attributed to the installation of the acidic group on the backbone. It was believed that increasing the amount of IP from 2.2 to 7.0% would increase the adhesion accordingly in 3.4b versus 3.4a due to the increase in acidic groups, but this was not observed. This was attributed to the material being highly ionomeric in nature, which limited its flow. The reduction in flow made it exceedingly difficult to process the sample for this test. Hence the value observed for 3.4b was not indicative of what the adhesion should be for such a material. These values can also be compared to previously reported values for cationic ionomers of RB such as those containing pendant phosphonium groups²⁸. These polymers provided a remarkable increase in the amount of adhesion to stainless steel; they observed an increase to 30.3 psi

with an IP content of 6.5%²⁹. The results for the oxygenated butyl rubber derivatives are very similar to these, making them very promising materials to eliminate the issue of delamination and provide better coating adhesion to stainless steel.

Table 3.2.3 Surface adhesion data obtained on the Tel-Tak system with a stainless steel substrate for the different oxygenated RBs.

Variations of RB	Force to separate (psi)	
	2.2%	7%
 3.1a/b	14.6 ± 0.3	12.1 ± 0.2
 3.2a/b	22.2 ± 2.2	25.2 ± 1.6
 3.3a/b	29.6 ± 0.6	20.5 ± 2.1
 3.4a/b	32.8 ± 1.3	28.3 ± 2.7

3.3 Conclusions

Compatibilization of polar materials on butyl rubber surfaces was improved by using oxygenated butyl rubber derivatives as compatibilizing layers. To demonstrate this,

PEO was coated on the compatibilizer layers providing more uniform coatings, as measured by AFM and contact angle measurements in comparison with the deposition of PEO directly on butyl rubber. The uniformity of these coatings is expected to translate into functional properties of the PEO, such as resistance to protein adsorption. In addition, the issue of delamination of RB from stainless steel surfaces was addressed by the introduction of the oxygenated functionalities. Specifically, the acid functionality increased the surface adhesion the greatest, demonstrating the promise of these materials in stent coating applications.

3.4 Experimental

Preparation of Films

Silicon wafers (1 cm X 1 cm) were cleaned by immersion in H₂O₂/H₂SO₄ solution (3:1). They were then rinsed with deionized distilled water and dried at 100 °C. Polymer **1** in hexane (5 mg/mL) was spin coated onto a clean silicon wafer and then cross-linked by HHIC (see below). Polymer 3.2a, 3.3a, or 3.4a in hexane (5 mg/mL) was then spin coated onto the cross-linked butyl rubber (3.1a) surface and was then cross-linked by HHIC. PEO was then spin coated from CH₂Cl₂ onto cross-linked 3.1a, 3.2a, 3.3a or 3.4a and was then cross-linked by HHIC. In each of the above cases the polymer concentration was 5 mg/mL and the spin coating conditions were 100 μL of polymer solution per cm², at a spin rate of 6000 rpm for 30 seconds.

*Hyperthermal Hydrogen Induced Cross-linking (HHIC)*¹⁴

Samples were inserted into a homemade HHIC reactor and pumped down to a background pressure of 2×10^{-6} Torr. Hydrogen gas was then introduced inside the reactor until a pressure of 8×10^{-4} Torr was reached and maintained throughout the experiment. An electron-cyclotron- resonance microwave plasma (87.5 mT, 2.45 GHz) was set up in a semi-permeable region of the reactor, enclosing the plasma with zero potential. Positive hydrogen ions were extracted through an applied potential difference of -96 V and accelerated into a drift zone, which is a 50 cm long electric field-free region. There they

underwent a series of binary collisions with molecular hydrogen in a stochastic manner. In order to calculate an average number of collision centers in the drift zone, the diameter of the hydrogen molecule was assumed to be 2.72 Å. For the given pressure and temperature = 20 °C, the average number of collision centers was calculated to be 4.3. Residual electrons and positive ions were repelled in two stages with an applied voltage of +60 V and -40 V respectively. Based on these values and an extraction current of 7 mA, the fluence of hyperthermal neutrals was calculated to be 3×10^{16} per cm^2 , sufficient to cross-link the polymer by physical means. Under this set of conditions, the surface was exposed to hyperthermal molecular hydrogen with a nominal average kinetic energy of 5×10^2 eV, an appropriate kinetic energy to break C-H bonds but not other bonds undesirably. The surfaces were treated for 30 to 100 seconds.

Atomic Force Microscopy

Surface morphology of the samples was imaged with the dynamic force mode using a Park Systems XE-100 atomic force microscope. A rectangular-shaped silicon cantilever (T300, VISTAprobes) was used, which has a nominal tip apex radius of 10 nm; spring constant of 40 N/m and resonant frequency of 300 kHz. The cantilever was vibrated around its resonant frequency and its reduced amplitude was used as the feedback parameter to image the sample surface. The measurements were carried out in air at room temperature. Film thickness was measured by scratching the laminate to the substrate and measuring the height difference from the top of the laminate to the substrate.

Contact Angle Measurements

A contact angle goniometer (Ramé-Hart's Model 100-00 or Kruss DSA 100) was used. Surfaces were first loaded onto the stage and drops of distilled water (10 μL) were placed on the specimens. The reported static angles were calculated by averaging the angles from both the left and right sides of the droplet. Advanced and receding contact angles were also evaluated. At least 10 measurements on each surface were obtained for each experimental condition.

Surface Adhesion

Sample sheets were prepared by pressing a sheet of the same compound into a square woven fabric (canvas) in a mould for 5 minutes at 100 °C between Mylar and Teflon. The test strips were then died from the sheet and tested. The test specimens consisted of 6.35 X 50.8 mm reinforced strips, the thickness of which varied from 0.5 to 3.3 mm. The test specimens were placed in the apparatus at right angles to each other and thus defined the area of contact. A 450 g weight was placed on the weight support, the dwell time was set to 60 seconds, and strips were died out with the Tel-Tak die. The stainless steel specimen was placed in the top platen; the Mylar was removed from the rubber surface and placed in the lower platen. The force gauge was zeroed. The lower platen was raised to make contact with the specimen in the upper platen. At the end of the dwell time period the drive motor began to pull the specimens apart and the force required for separation was recorded.

3.5 References

- (1) Puskas, J.; Chen, Y. *Biomacromolecules* **2004**, *5*, 1141.
- (2) Puskas, J.; Chen, Y.; Dahman, Y.; Padavan, D. *J. Polym. Sci., Part A: Polym. Chem.* **2004**, *42*, 3091.
- (3) Bonduelle, C. V.; Lau, W. M.; Gillies, E. R. *ACS Appl. Mater. Interfaces*, **2011**, *3*, 1740.
- (4) Reiter, G. *Phys. Rev. Lett.* **2001**, *87*, 186101.
- (5) Sharma, A.; Reiter, G. *J. Colloid Interface Sci.* **1996**, *178*, 383.
- (6) Ormiston, J.; Currie, E.; Webster, M.; Kay, P.; Ruygrok, P.; Stewart, J.; Padgett, R.; Panther, M. *Catheter Cardio. Inte.* **2004**, *63*, 332.
- (7) Levy, Y.; Mandler, D.; Weinberger, J.; Domb, A. J. *J. Biomed. Mater. Res. Part B.* **2009**, *91B*, 441.
- (8) Horbett, T. *Cardiovasc. Pathol.* **1993**, *2*, S137.

- (9) Gillies, E.; Bonduelle, C.; McEachran, M.; Arsenault, G.; Stojcevic, G. WO 2012/019303A1, **2012**.
- (10) Ocando, C.; Tercjak, A.; Serrano, E.; Ramos, J. A.; Corona-Galvan, S.; Parellada, M. D.; Fernandez-Berridi, M. J.; Mondragon, I. *Polym. Int.* **2008**, *57*, 1333.
- (11) Yoshioka, M.; Yoshida, Y.; Inoue, S.; Lambrechts, P.; Vanherle, G.; Nomura, Y.; Okazaki, M.; Shintani, H.; Van Meerbeek, B. *J. Biomed. Mater. Res.* **2002**, *59*, 56.
- (12) Shin, Y. N.; Kim, B. S.; Ahn, H. H.; Lee, J. H.; Kim, K. S.; Lee, J. Y.; Kim, M. S.; Khang, G.; Lee, H. B.. *Appl. Surf. Sci.* **2008**, *255*, 293.
- (13) Kennedy, J.; Askew, M.; Richard, G. *J. Biomater. Sci., Polym. Ed.* **1993**, *4*, 445.
- (14) Liu, Y.; Yang, D. Q.; Nie, H. -.; Lau, W. M.; Yang, J. *J. Chem. Phys.* **2011**, *134*, 074704.
- (15) Zheng, Z.; Xu, X.; Fan, X.; Lau, W.; Kwok, R. *J. Am. Chem. Soc.* **2004**, *126*, 12336.
- (16) Zheng, Z.; Kwok, W. M.; Lau, W. M. *Chem. Commun.* **2006**, 3122.
- (17) Zheng, Z.; Wong, K. W.; Lau, W. C.; Kwok, R. W. M.; Lau, W. M. *Chem. Eur. J.* **2007**, *13*, 3187.
- (18) Chilkoti, A.; Ratner, B.; Briggs, D. *Chemistry of Materials* **1991**, *3*, 51.
- (19) Guruvenket, S.; Rao, G.; Komath, M.; Raichur, A. *Appl. Surf. Sci.* **2004**, *236*, 278.
- (20) Karamdoust, S.; Yu, B.; Bonduelle, C. V.; Liu, Y.; Davidson, G.; Stojcevic, G.; Yang, J.; Lau, W. M.; Gillies, E. R. *Chem. Mater.* **2012**, *22*, 4881.
- (21) Thompson, D. B.; Trebicky, T.; Crewdson, P.; McEachran, M. J.; Stojcevic, G.; Arsenault, G.; Lau, W. M.; Gillies, E. R. *Langmuir* **2011**, *27*, 14820.
- (22) Prime, K.; Whitesides, G. *Science* **1991**, *252*, 1164.
- (23) Lee, J.; Lee, H.; Andrade, J. *Prog. Polym. Sci.* **1995**, *20*, 1043.

- (24) Andrade, J.; Hlady, V.; Jeon, S. *Hydrophilic Polymers: Performance with Environmental Acceptance* **1996**, 248, 51.
- (25) Kingshott, P.; Griesser, H. *Curr. Opin. Solid State Mater. Sci.* **1999**, 4, 403.
- (26) Leckband, D.; Sheth, S.; Halperin, A. *J. Biomater. Sci., Polym. Ed.* **1999**, 10, 1125.
- (27) Pinchuk, L.; Wilson, G. J.; Barry, J. J.; Schoephoerster, R. T.; Parel, J.; Kennedy, J. P.. *Biomaterials* **2008**, 29, 448.
- (28) Parent, J.; Penciu, A.; Guillen-Castellanos, S.; Liskova, A.; Whitney, R. *Macromolecules* **2004**, 37, 7477.
- (29) Resendes, R.; Krista, R.; Hickey, J. N. US Patent 7,662,480, **2010**.

Chapter 4

4 Conjugation and Release of Paclitaxel from Butyl Rubber films

Contribution Statement: Toxicity testing was completed in collaboration with Bethany Turowec.

4.1 Introduction

Poly(isobutylene) (PIB) and its copolymers such as butyl rubber (RB) have been used for years in a number of different applications. Conventionally these synthetic elastomers have been used in the production of tires and various automotive parts due to desirable properties such as water/gas impermeability, chemical stability, high elasticity and thermal stability. Recently PIB and its copolymers have been identified for use in biomaterials. Currently these elastomers are used in chewing gum, pharmaceutical stoppers, and vascular stents¹⁻³.

Vascular stents are employed when balloon angioplasty is used to clear blood vessels to retain the open form of the blood vessel. Without insertion of a stent, rapid restenosis occurs causing health implications⁴. Bare metal stents (BMS) have been utilized to prevent the rapid restenosis but there have been long-term complications common with BMS such as restenosis and thrombosis^{5,6}. Recently, drug-eluting stents (DES) were developed in the hope that these long-term implications would be resolved. The metallic stent was coated with a durable elastomer and mixed with a loading of drug to eliminate cell growth on the surfaces of the stent. Boston Scientific commercialized the TAXUS stent, which has passed FDA regulations and is in clinical use today¹. The stent utilizes poly(styrene)-co-poly(isobutylene)-co-poly(styrene) (SIBS) as the polymeric coating and paclitaxel (PTx) as drug. Over the past decade since they have been approved for clinical use, all of the studies have shown the drastic improvement in preventing events like restenosis and thrombosis⁷⁻⁹. However, there are still issues in real world applications. Events of late thrombosis and restenosis are still observed in these DES, which has been accredited to delamination of the film from the stainless steel substrate as

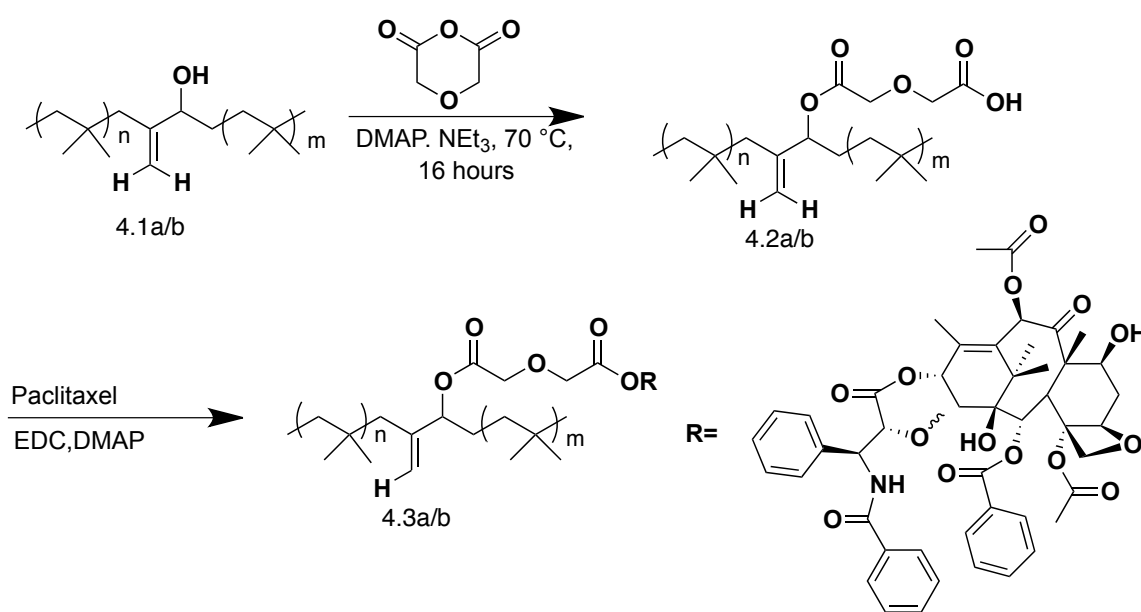
well as erratic release of drug. Various weight percentages (wt.%) of SIBS compared to PTx have shown slow to fast release this however did not address the issue of delamination¹⁰. Recently Faustus' group has synthesized modified SIBS polymers in the hope to control release. They synthesized styrene maleic anhydride (SMA) copolymers and blended it with traditional SIBS¹¹. Upon studying the release of PTx they found that the higher amounts of SMA blended relative to SIBS gave an accelerated release of PTx. They also studied the synthesis of poly(methyl methacrylate-*b*-isobutylene-*b*-methyl methacrylate) and poly(hydroxystyrene-*b*-isobutylene-*b*-hydroxystyrene), which yielded a similar result to the SMA derivative studied^{12, 13}.

Work has been completed on the modification of butyl rubber (RB) as a potential alternative to SIBS^{2, 3, 14}. RB is typically polymerized with small amounts of isoprene (IP) (2.2-7%). Various functionalities have been installed along the RB backbone through its bromo-RB derivative but recently RB itself has been functionalized¹⁵⁻¹⁷. Poly(ethylene oxide) (PEO) graft copolymers were synthesized using mild conditions and in high purity^{18, 19}. One intermediate of specific interest is the allylic alcohol produced upon the ring opening of an epoxide. The allylic alcohol can be treated with a cyclic anhydride to a carboxylic acid functionalized RB as described in Chapter 2. This acid derivative should serve as an excellent polymeric backbone to eliminate the issues inherent with the current TAXUS DES. Carboxylic acid moieties have shown increased adhesion to various substrates, metallic and natural. Also, the functional handle can be used to conjugate PTx to eliminate early burst release of drug. The following chapter will discuss the use of carboxylic acid functionalized RB to synthesize PTx conjugates as well as a preliminary drug release. The conjugates were studied chemically via NMR, IR, SEC, TGA and DSC. The release study was followed using HPLC, and surfaces were imaged using SEM and AFM.

4.2 Results and Discussion

As described in Chapter 2, reacting 4.1 with a cyclic anhydride can synthesize an acid functionalized RB. Diglycolic anhydride reacts to complete conversion to yield 4.2 bearing carboxylic acid moieties to which PTx can be conjugated (Scheme 4.2.1). A similar approach has been used to produce monomethoxy-poly(ethylene glycol)-*b*-

poly(lactide) conjugated with paclitaxel²⁰. The conjugation of paclitaxel occurred through the use of dicyclohexylcarbodiimide (DCC) but in this study 1-ethyl-3-(3-dimethylaminopropyl)carbodiimide (EDC•HCl) was employed. DCC byproducts were very problematic to remove due to their limited solubilities in comparison to those obtained using EDC•HCl. To modify the wt.% of PTx two different IP content polymers were used in this study – a-2.2 mol% and b-7.0 mol%. These variations in the IP content will affect the wt.% of drug loaded onto the RB.



Scheme 4.2.1 Schematic representation of the conjugation of PTx to the RB backbone.

Conjugation was successful of PTx was confirmed by ¹H NMR spectroscopy (Figure 4.2.1). The spectrum illustrates the characteristic PTx and RB peaks. Upon closer examination of the RB-PTx conjugate, some very characteristic shifts were observed. The most obvious change was the disappearance of the peak at 4.81 ppm, which corresponds to the proton adjacent to the hydroxyl to which conjugation occurs. After conjugation this peak shifts to 5.60 ppm. Furthermore the peak at 5.80 ppm, which corresponds to the proton adjacent to the benzyl ring, shifts to 6.05 ppm (Figure 4.2.2). These peak assignments were assisted by comparison with previously reported PTx ester prodrugs²¹. There is still some unreacted acids remaining on the RB backbone but conjugation was

greater than >80%. Based on NMR analysis, the conjugate with the RB acid prepared from RB with 2.2 mol% IP containing ~24 wt.% PTx, while that prepared from the RB containing 7.0 mol% IP contained ~48 wt.% PTx. These samples are denoted as 2C and 7C respectively.

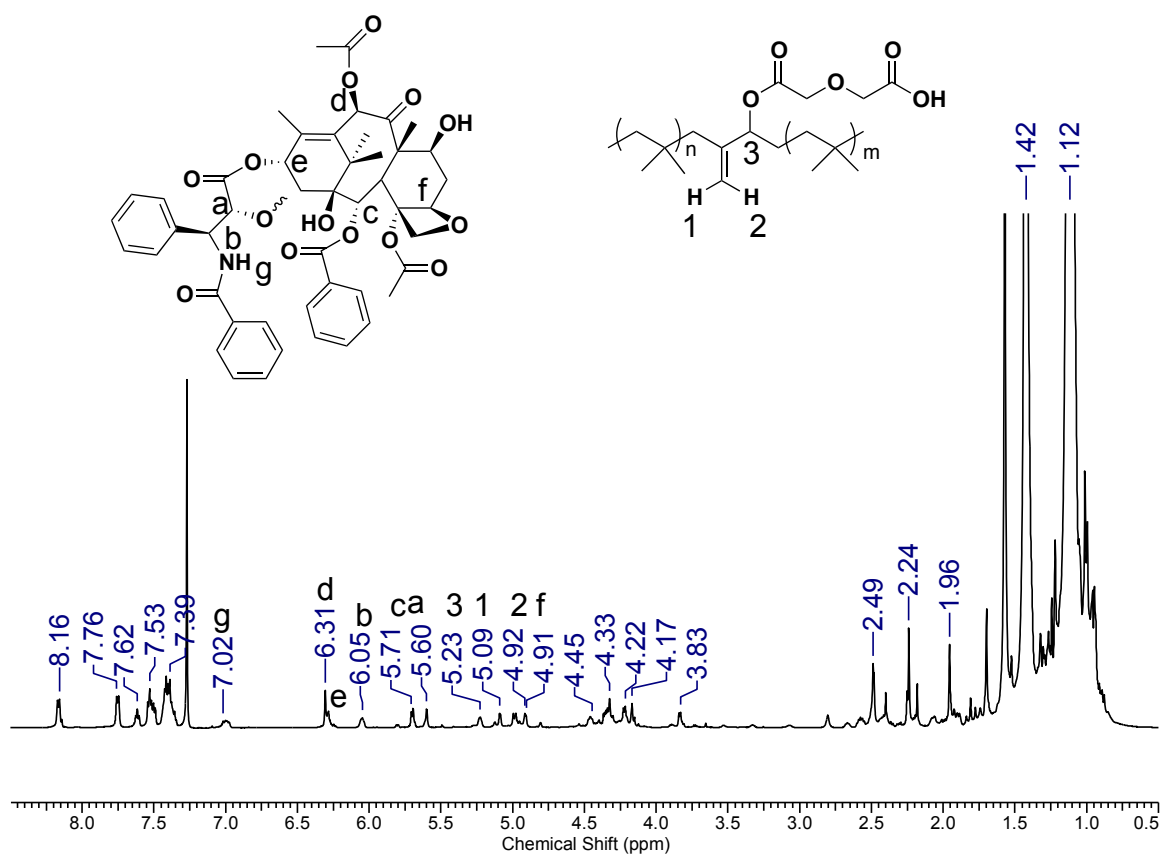


Figure 4.2.1 ^1H NMR spectra of the 4.3a showing all the peaks corresponding to both PTx and RB, the key peaks are assigned for PTx.

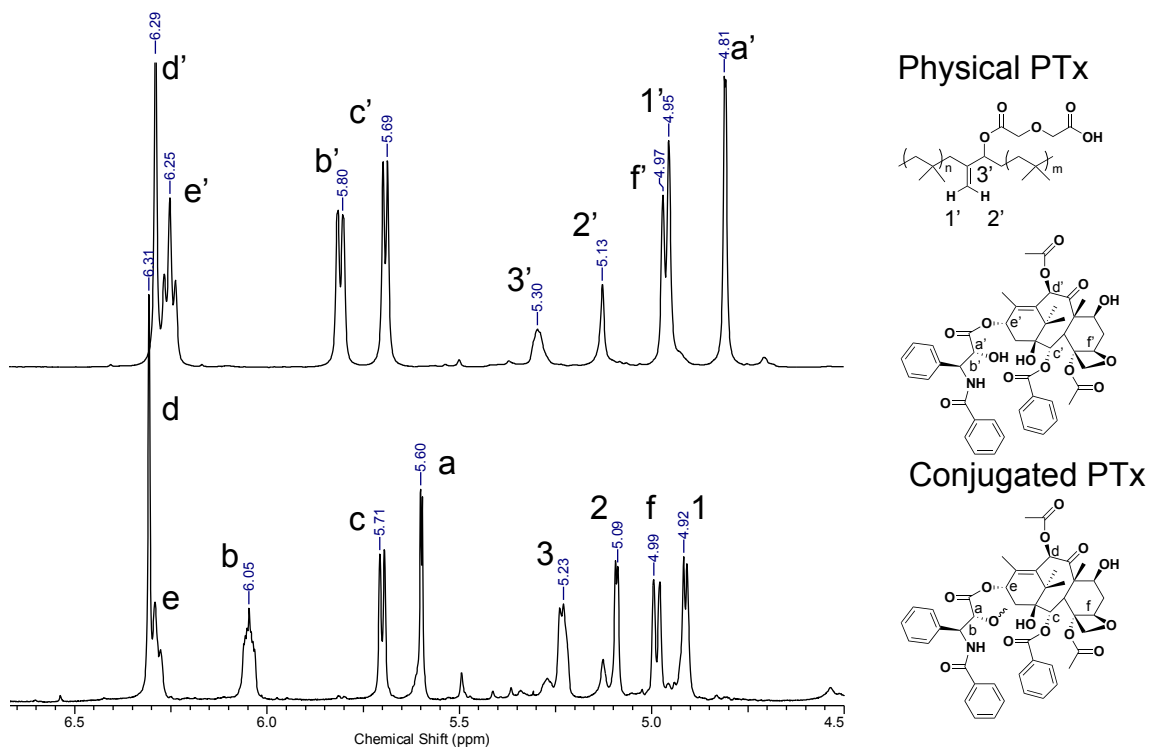


Figure 4.2.2 ^1H NMR spectra illustrating the key peak changes observed a) a mixture of PTx with 4.2a/b b) after conjugation of PTx to 4.3a/b.

Once PTx was confirmed to be on the RB backbone, the release profiles were of specific interest for DES. Thin films of the polymer were coated on polished stainless steel plates via drop casting. In addition to the conjugates 4.3a and 4.3b, containing different wt.% of PTx, several controls were also prepared. To demonstrate the effect of covalent conjugation, 4.2a and 4.2b were physically mixed with 24 and 48 wt% of PTx respectively and the mixtures were cast on the stainless steel. These physical mixtures are denoted 2P and 7P respectively. Also, two examples of SIBS with different amounts of styrene content (S1-10% and S2-20%) and 24 wt.% of physically encapsulated PTx were used as a comparison with the other systems (Table 4.2.1). The release studies were carried out using literature protocols^{7, 22, 23}. Briefly, the release medium was pH controlled at 7.4 and contained Tween, which is a surfactant known to help solubilize PTx. The Tween ensures the PTx does not adhere to the glass during the release study. The medium was removed from each sample every 7 days for analysis and was replaced with fresh medium.

Table 4.2.1 Description of the samples used in the release study.

Sample Name	Polymer Composition	PTx wt.%	PTx immobilization
2C	4.3a	~24	Covalent
7C	4.3b	~48	Covalent
2P	4.2a	24	Physical
7P	4.2b	48	Physical
S1	SIBS- 10% styrene	24	Physical
S2	SIBS- 20% styrene	24	Physical

The release rates of PTx from the different films were studied by HPLC. The HPLC procedure was adapted from literature protocols²⁴. The limit of detection for the HPLC study was 0.2 µg/mL. As a result of this limit of detection, all the samples of the release medium had to be concentrated from 10 mL to 2 mL. Water was removed via lyophilization and then the samples were reconstituted in water and acetonitrile. It was found during this study that a portion of acetonitrile was needed to solubilize the PTx. The release profile can be seen in Figure 4.2.3. The profile is shown in cumulative mass of PTx released and it should be noted that some degradation products of PTx were also seen in the HPLC trace such as the known epimer²⁵. As expected, the covalently bound PTx samples showed a very sustained, slow release in comparison to the physically immobilized samples. The covalently bound PTx samples also showed slower release in comparison to the SIBS examples. As observed in other studies, the introduction of hydrophilic blocks increases the bursts release of PTx but in the examples where it was covalently bound, it is the contrary. This is a very encouraging sign for applications of these materials. The slow sustained release exhibited by the conjugated PTx samples eliminates the burst release of drug that limits the application of such polymers in DES.

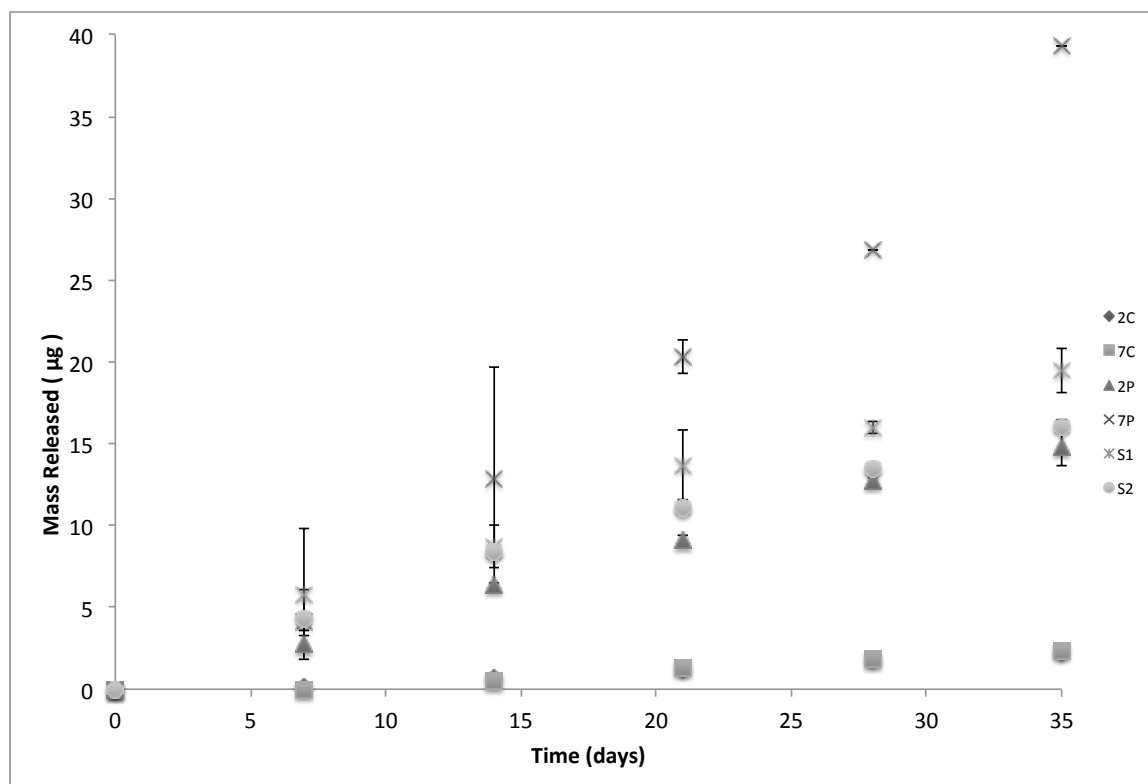


Figure 4.2.3 Release study of PTx from the polymeric substrates completed using HPLC. Note: 2C and 7C overlap for much of the study.

The covalently bound samples also exhibited enhanced film adhesion to the metal substrate in comparison to the controls. As seen in Figure 4.2.4 the delamination of the physically immobilized samples and the SIBS examples was observed over the 35 day incubation period. Since the PTx is covalently bound to the RB there appears to be no phase separation (Figure 4.2.6 c/e) as seen with the physically encapsulated samples so there is no interference at the polymer-metal interface. The phase separation can clearly be seen in Figure 4.2.6 a/g for the S1 and 2P samples. The increased adhesion could also be attributed to the incomplete conjugation of PTx to the RB backbone. The incomplete conjugation would leave residual carboxylic acid groups that would increase the adhesion to the stainless steel plate.

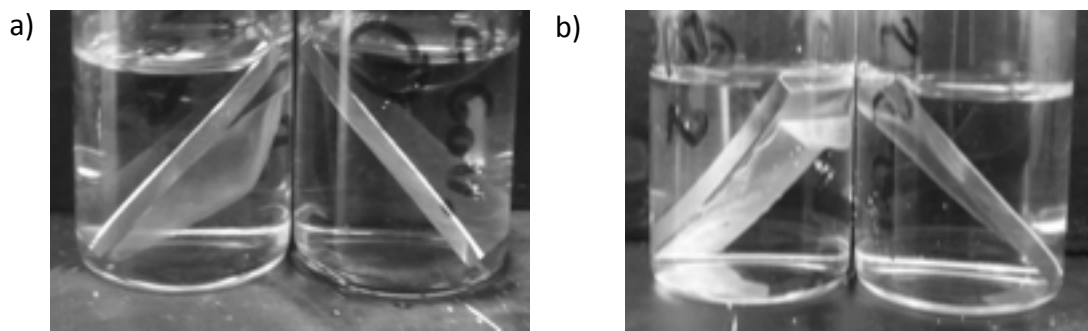


Figure 4.2.4 a) left- S1 after 35 days showing delamination right- 2C at 35 days showing little or no delamination b) left- 2P at 35 days showing slight delamination right- 2C at 35 days showing resilience with no or little delamination.

The films were imaged by SEM (Figure 4.2.5) and AFM (Figure 4.2.6) to investigate their integrity throughout the release study. The SIBS example can be seen in Figure 4.2.5a&b. As shown by SEM, the initial film was very smooth and uniform. After 35 days in the release medium, the film's integrity had decreased drastically. The surface became non-homogenous with what appeared to be a rippling of the film itself. When comparing it to the physically immobilized examples, again at the beginning a uniform film was observed but after 35 days the film integrity was much different (4.2.5d). There were cracks in the polymer surface that could be visualized all over the surface. Finally, when observing the covalently bound examples, the results were quite different. The initial films were smooth as in the other cases, but after 35 days there were tiny holes throughout the film, which is believed to be indicative of release (Figure 4.2.5 f&h). This was confirmed by observing the AFM topography images. AFM also showed hole formation in the polymer film (Figure 4.2.6 d/f).

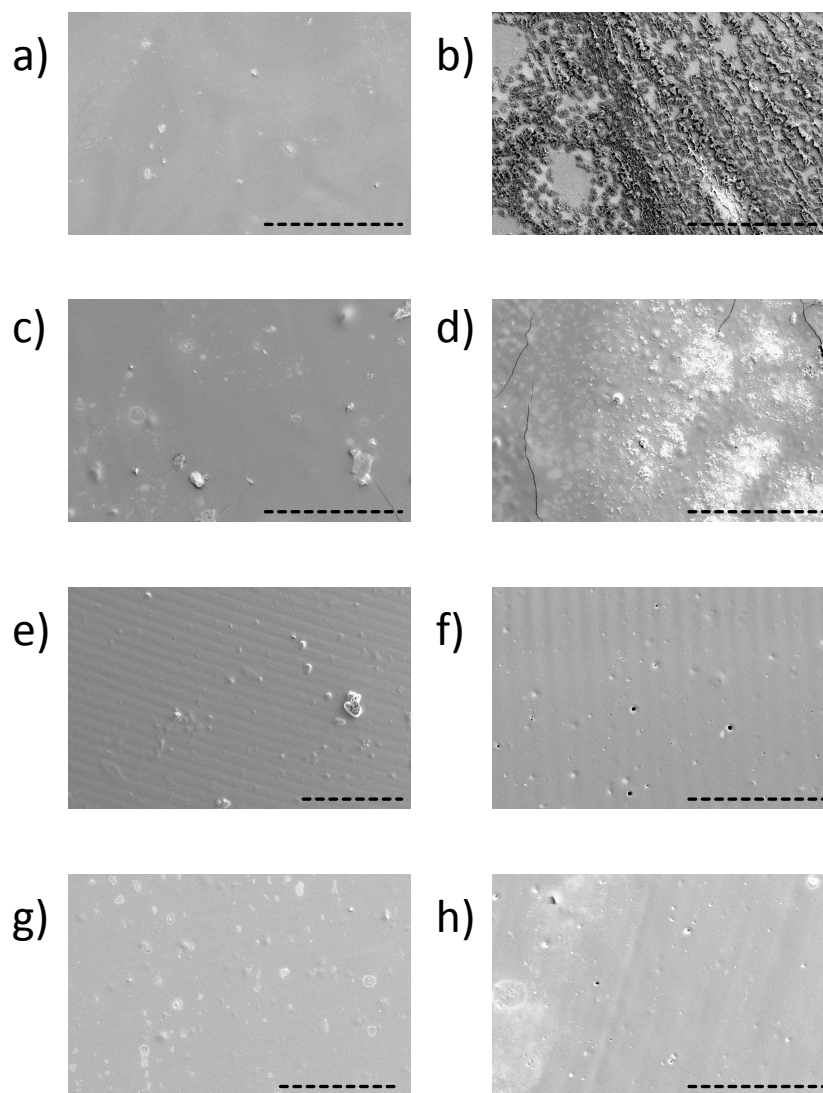


Figure 4.2.5 SEM images of polymer surfaces before and after the degradation study: a) S1 before degradation; b) S1 at 35 days; c) 2P before degradation; d) 2P at 35 days; e) 7C before degradation; f) 7C at 35 days; g) 2C before degradation; h) 2C at 35 days. All scale bars correlate to 500 μm.

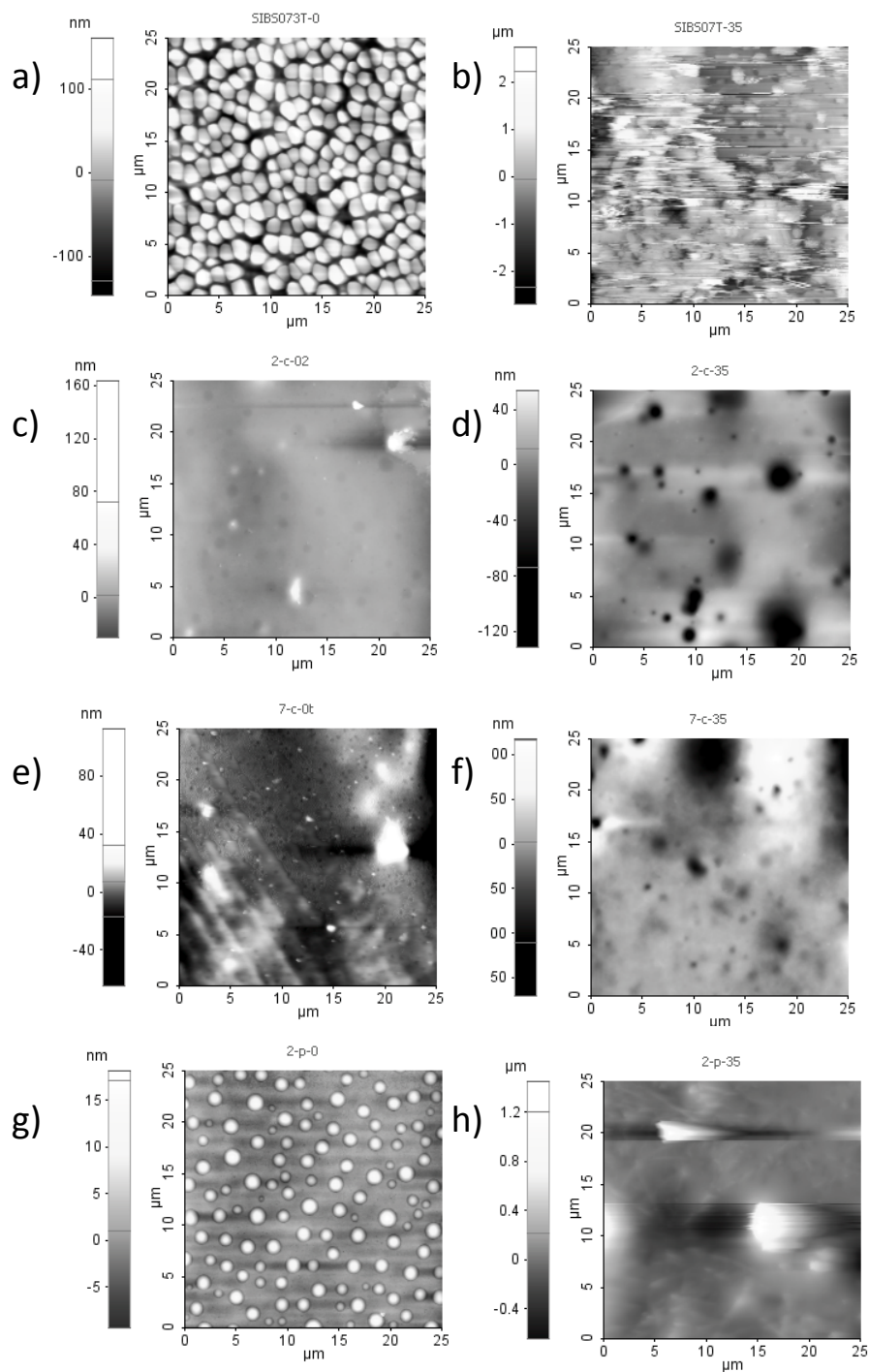


Figure 4.2.6 AFM topography images of polymer surfaces before and after the degradation study: a) S1 before degradation; b) S1 at 35 days; c) 2C before degradation; d) 2C at 35 days; e) 7C before degradation; f) 7C at 35 days; g) 2P before degradation; h) 2P at 35 days.

Toxicity studies were also performed to evaluate whether these surfaces would release toxic levels of PTx during a defined incubation period in cell culture media. First, each surface was incubated in cell culture medium at 37 °C for 24 hours. This medium was then added to cells at serial 2-fold dilutions. As a known non-toxic control, high-density polyethylene (hdpe) was the negative control. Sodium dodecyl sulfate was used as a positive control and toxicity was detected at 0.2 µg/mL, demonstrating the efficacy of the assay in detecting toxicity. In addition, to detect the leaching of any potentially toxic molecules from the starting acid functionalized rubbers, 4.2a and 4.2b, and SIBS without PTx, these were also included in the study. As shown in Figure 4.2.7, most of the materials did not lead to any detectable toxicity, with only a few of the films exhibiting modest toxicity at the highest leachate concentrations. These surfaces were the physically immobilized PTx materials as well as the SIBS materials, which released PTx the most rapidly in the release study. It should be noted that although PTx is a very toxic drug, the amounts of PTx released over the 24-hour incubation period would still be extremely small. The controls did not exhibit any toxicity in this assay. This again supports the use of these materials for biomedical applications.

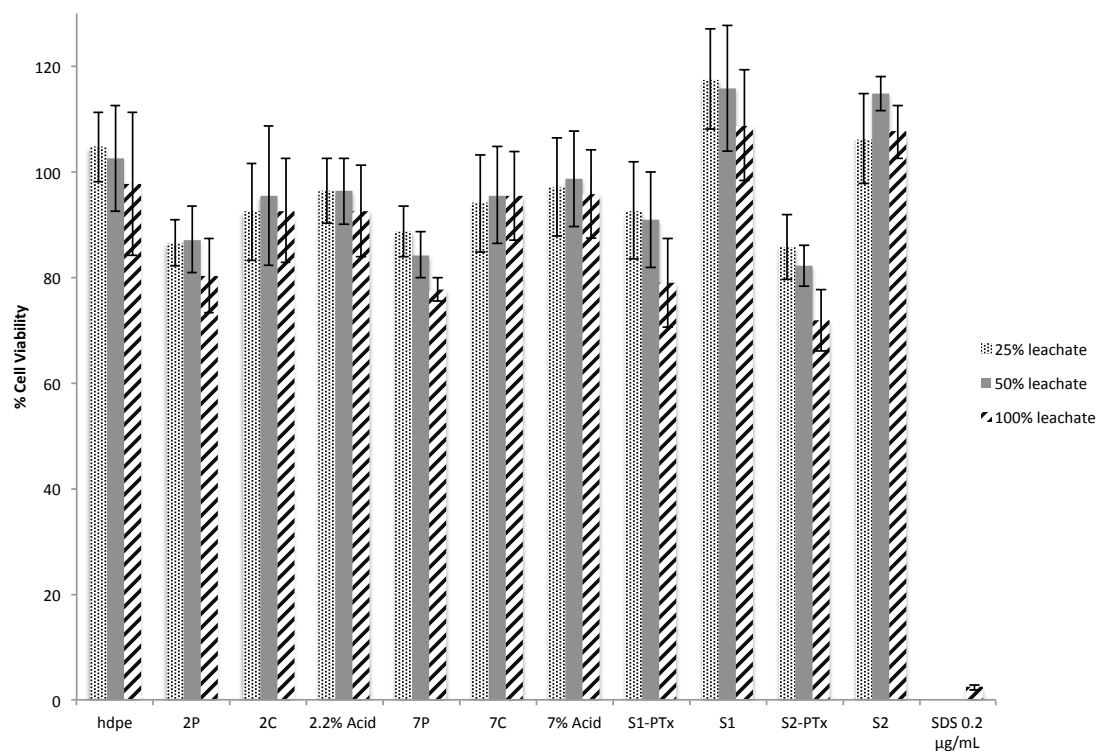


Figure 4.2.7 MTT assay in evaluation of the toxicity of the polymeric surfaces.

4.3 Conclusions

The successful conjugation of PTx to acid functionalized RB was described and the release of PTx from films of the conjugates was studied. The release was followed using HPLC and various imaging techniques. The synthesized RB-PTx conjugates showed a substantial decrease in the burst release of PTx in comparison with previously reported systems. These polymers exhibited a much slower release than previously reported physical mixtures of drug and polymer. In addition, the RB-PTx covalent conjugates show enhanced integrity and adhesion to the metal substrate throughout the release study. Thus, this new PTx polymer conjugate serves a promising new stent coating material that warrants further investigation for the development of new medical devices.

4.4 Experimental

Synthesis of 4.3a

A dried sample of 4.2a prepared as described in chapter 2, was dissolved in dry toluene (10 g, 3.9 mmol of CO₂H) and put under inert conditions. A solution of 1-ethyl-3-(3-dimethylaminopropyl) carbodiimide) (EDC) (1.25 eq. per CO₂H, 4.9 mmol, 0.76g), and 4-dimethylaminopyridine (DMAP) (0.5 eq. per CO₂H, 1.95 mmol, 0.25g) were dissolved in dry CH₂Cl₂ and added to the 4.2a. The solution was allowed to stir for 10-20 minutes prior to the addition of Paclitaxel (PTx) (1.1 eq. per CO₂H, 4.29 mmol, 3.65g) dissolved in CH₂Cl₂. The solution was left at room temperature overnight. The reaction mixture was then stripped of CH₂Cl₂ via rotary evaporation and then washed with DI water, 1M HCl and 1M NaHCO₃, two times. Lastly the resultant solution was precipitated in ethanol and dried under vacuum. Conversion was calculated using ¹H NMR. ¹H NMR (400 MHz, CDCl₃) 8.16 (PTx, d, 2H), 7.76 (PTx, d, 2H), 7.62 (PTx, m, 1H), 7.42-7.52 (PTx, m, 4H), 7.28-7.41 (PTx, m, 8H), 6.90-7.02 (PTx, m, 1H), 6.31 (PTx, s, 2H), 6.05 (PTx, brs, 1H), 5.71 (PTx, d, 1H), 5.60 (PTx, s, 1H), 5.23 (RB, brs, 1.4H), 5.09 (RB, d, 1.4H), 4.99 (PTx, d, 1.2H), 4.92 (RB, d, 1.6H), 4.06-4.47 (PTx, m, H), 3.83 (PTx, d, 1H), 2.49 (PTx, s, 4H), 2.24 (PTx, s, 4H), 1.96 (PTx, s, 4H), 1.42 (RB, s, 316H), 1.12 (RB, s, 978H). SEC: M_w = 337000 g/mol, PDI = 1.47. IR 1232, 1367, 1390, 1475, 1670, 1737, 2960 cm⁻¹.

Synthesis of 4.3b

Conjugate 4.3b was prepared as described above for 4.3a except that this polymer contained 1.2 mmol per g of CO₂H and thus the amounts of EDC, DMAP and PTx were increased to retain these reagent ratios at 1.25, 0.5, and 1.1 equivalents per CO₂H respectively. ¹H NMR (400 MHz, CDCl₃) .16 (PTx, d, 2H), 7.76 (PTx, d, 2H), 7.62 (PTx, m, 1H), 7.42-7.52 (PTx, m, 4H), 7.28-7.41 (PTx, m, 8H), 6.90-7.02 (PTx, m, 1H), 6.31 (PTx, s, 2H), 6.05 (PTx, brs, 1H), 5.71 (PTx, d, 1H), 5.60 (PTx, s, 1H), 5.23 (RB, brs, 1.4H), 5.09 (RB, d, 1.4H), 4.99 (PTx, d, 1.2H), 4.92 (RB, d, 1.6H), 4.06-4.47 (PTx, m, H), 3.83 (PTx, d, 1H), 2.49 (PTx, s, 4H), 2.24 (PTx, s, 4H), 1.96 (PTx, s, 4H), 1.42 (RB, s,

111H), 1.12 (RB, s, 353H). SEC: $M_w = 501400$ g/mol, PDI = 2.66. IR 1232, 1367, 1390, 1475, 1670, 1737, 2960 cm^{-1} .

Preparation of Films

The substrate chosen was a stainless steel plate with dimensions of 3 cm X 1 cm. The surface was polished with a bench-top grinder to give a smooth surface. To prepare the film, a 100 mg/mL solution (in CH_2Cl_2) of polymer was prepared. For the physically encapsulated samples, the PTx was added next at the appropriate weight percentage. A 100- μL aliquot of each of the polymer solution was drop cast onto the stainless steel plate. The sample was dried under reduced pressure prior to the release study. Each sample was prepared and studied in triplicate.

Release Study

The release study was performed in 0.01 M phosphate buffered solution of pH= 7.4. The final buffer also contained 0.138 M NaCl and 0.0027 M KCl and also contained 0.05% Tween 20 as a surfactant. The stainless steel plates were placed into a vial containing 10 mL of buffered solution. The solution was maintained at 37 °C and the buffer was removed every 7 days for analysis of PTx and replaced with fresh medium. Due to the low concentrations of PTx released, the release medium was concentrated prior to HPLC analysis. The water was removed via lyophilization and the solid was redissolved in 2 mL of 80:20 water:acetonitrile.

HPLC protocol

The HPLC instrument was equipped with a Waters Separations Module 2695, a Photodiode Array Detector (Waters 2998) and a Nova-Pak C18 4 μm (3.9x150mm) column connected to a C18 guard column. The PDA detector was used to monitor PTx at 228 nm. PTx separation was obtained using a gradient method with Solvent A (5% acetonitrile in water) and Solvent B (80% acetonitrile, 0.1% H_3PO_4 in water) flowing at 1mL/min. Gradient of Solvent A 65% was decreased to 30% over 10 min, and increased back to 65% over the next 5 min where the column was allowed to equilibrate over another 5 min.

The calibration curve was obtained from Paclitaxel (LC Laboratories, >99%, P-9600) standard solutions. Stock solutions of 1000 µg/mL, 100 µg/mL and 50 µg/mL of PTx in acetonitrile were prepared. The stock solutions were used to make standard solutions of 25, 20, 15, 10, 7.5, 5, 2, 1, 0.5 µg/mL in 20:80 acetonitrile:PBS solution. Standards were filtered and injected at 100 µL using the above instrument method. Samples were prepared in a 20:80 acetonitrile:PBS solution, filtered through 0.2 µm filters and injected at 100 µL using the same conditions as described above. The limit of detection of PTx was determined to be 0.02 µg.

Atomic Force Microscopy

Surface morphologies of the samples were imaged with the dynamic force mode using a Park Systems XE-100 atomic force microscope. A rectangular-shaped silicon cantilever (T300, VISTA probes) was used, which has a nominal tip apex radius of 10 nm, spring constant of 40 N/m and resonant frequency of 300 kHz. The cantilever was vibrated around its resonant frequency and its reduced amplitude was used as the feedback parameter to image the sample surface. The measurements were carried out in air at room temperature. Image processing was completed using XEI software developed by Park Systems.

Scanning Electron Microscopy

In all cases, all stainless steel plates were mounted on aluminum stubs with carbon tape, then sputter coated with gold. The surface microstructure was then imaged by scanning electron microscopy (SEM) (S- 2600N, Hitachi, Japan).

Toxicity assay.

Preparation of leachate: Test samples were melt-pressed to a thickness of 0.4 mm as described above. The melt pressed film was then cut into squares of 1 cm × 1 cm. Samples were sterilized by washing with 70% ethanol and subsequently dried for 2 hours under UV light. They were placed in Petri dishes and incubated in 2 mL of Dulbecco's

Modified Eagle Medium (DMEM, Invitrogen) supplemented with 10% fetal bovine serum (Invitrogen) and supplemented with 1% Glutamax (100×) solution and 1% Penstrep (100×) in an incubator at 37°C for 24 hours. The leachate was then removed and passed through a 0.2 µm filter.

MTT assay: C2C12 mouse myoblast cells were seeded in a Nunclon® 96-well U bottom transparent polystyrol plate to obtain 10,000 cells/well in 100 µL of DMEM containing serum, glutamax and antibiotics as described above. The cells were allowed to adhere in a 5% CO₂ incubator at 37 °C for 24 hr. Next, the growth medium was aspirated and was replaced with either the positive control - sodium dodecyl sulfate (SDS) in the cell culture medium at concentrations of 0.2, 0.15, 0.10, or 0.05 mg/mL, serial two-fold dilutions of the leachate, or just the medium. The cells were then incubated at 37 °C (5% CO₂) for 24 h. The medium was then aspirated and replaced with 110 µL of fresh medium containing 0.5 mg/mL (3-(4,5-dimethylthiazol-2-yl)-2,5-diphenyltetrazolium bromide) (MTT) reagent. After 4 h of incubation (37 °C, 5% CO₂), the MTT solution was carefully aspirated and the purple crystals were dissolved by addition of 50 µL of spectroscopic grade dimethylsulfoxide (DMSO). After shaking (1 second, 2 mm amp, 654 rpm), the absorbance of the wells at 540 nm was read using an M1000-Pro plate reader (Tecan). The absorbance of wells not containing cells but treated by all of the above steps was subtracted as a background and the cell viability was calculated relative to wells containing cells that were exposed to just culture medium. No (0%) cell viability was detected for the cells exposed to the highest concentrations of the positive control sodium lauryl sulfate, confirming the sensitivity of the assay.

4.5 References

(1) Pinchuk, L.; Wilson, G. J.; Barry, J. J.; Schoephoerster, R. T.; Parel, J.; Kennedy, J. P. *Biomaterials* **2008**, *29*, 448.

- (2) Puskas, J.; Chen, Y.; Dahman, Y.; Padavan, D. *J. Polym. Sci., Part A: Polym. Chem.* **2004**, *42*, 3091.
- (3) Puskas, J.; Chen, Y. *Biomacromolecules* **2004**, *5*, 1141.
- (4) Gruentzig, A.; King, S.; Schlumpf, M.; Siegenthaler, W. *N. Engl. J. Med.* **1987**, *316*, 1127.
- (5) James, S. K.; Stenestrand, U.; Lindback, J.; Carlsson, J.; Schersten, F.; Nilsson, T.; Wallentin, L.; Lagerqvist, B. *N. Engl. J. Med.* **2009**, *360*, 1933.
- (6) Moreno, R.; Fernandez, C.; Sanchez-Recalde, A.; Galeote, G.; Calvo, L.; Alfonso, F.; Hernandez, R.; Sanchez-Aquino, R.; Angiolillo, D. J.; Villarreal, S.; Macaya, C.; Lopez-Sendon, J. L. *Eur. Heart J.* **2007**, *28*, 1583.
- (7) Strickler, F.; Richard, R.; McFadden, S.; Lindquist, J.; Schwarz, M. C.; Faust, R.; Wilson, G. J.; Boden, M. *J. Biomed. Mater. Res. A* **2010**, *92A*, 773.
- (8) Grube, E.; Mueller, R.; Schuler, G.; Hauptmann, K.; Schofer, J. *J. Am. Coll. Cardiol.* **2012**, *60*, B14.
- (9) Grube, E.; Schofer, J.; Hauptmann, K. E.; Nickenig, G.; Curzen, N.; Allocco, D. J.; Dawkins, K. D. *JACC Cardiovasc. Interv.* **2010**, *3*, 431.
- (10) Ranade, S.; Miller, K.; Richard, R.; Chan, A.; Allen, M.; Helmus, M. *J. Biomed. Mater. Res. A* **2004**, *71A*, 625.
- (11) Richard, R.; Schwarz, M.; Chan, K.; Teigen, N.; Boden, M. *J. Biomed. Mater. Res. A* **2009**, *90A*, 522.
- (12) Sipos, L.; Som, A.; Faust, R. *Biomacromolecules* **2005**, *6*, 2570.
- (13) Cho, J. C.; Cheng, G.; Feng, D.; Faust, R.; Richard, R.; Schwarz, M.; Chan, K.; Boden, M. *Biomacromolecules* **2006**, *7*, 2997.

- (14) Cadieux, P.; Watterson, J.; Denstedt, J.; Harbottle, R.; Puskas, J.; Howard, J.; Gan, B.; Reid, G. *Colloids Surf., B* **2003**, *28*, 95.
- (15) Ikeda, Y.; Kodama, K.; Kajiwara, K.; Kohjiya, S. *J. Polym. Sci., Part B: Polym. Phys.* **1995**, *33*, 387.
- (16) Fukushima, K.; Pratt, R. C.; Nederberg, F.; Tan, J. P. K.; Yang, Y. Y.; Waymouth, R. M.; Hedrick, J. L.. *Biomacromolecules* **2008**, *9*, 3051.
- (17) Guillen-Castellanos, S.; Parent, J.; Whitney, R.. *J. Polym. Sci., Part A: Polym. Chem.* **2006**, *44*, 983.
- (18) Bonduelle, C. V.; Gillies, E. R. *Macromolecules* **2010**, *43*, 9230.
- (19) Bonduelle, C. V.; Karamdoust, S.; Gillies, E. R. *Macromolecules* **2011**, *44*, 6405.
- (20) Zhang, X.; Li, Y.; Chen, X.; Wang, X.; Xu, X.; Liang, Q.; Hu, J.; Jing, X. *Biomaterials* **2005**, *26*, 2121.
- (21) Deutsch, H.; Glinski, J.; Hernandez, M.; Haugwitz, R.; Narayanan, V.; Suffness, M.; Zalkow, L. *J. Med. Chem.* **1989**, *32*, 788.
- (22) Sirianni, R. W.; Jang, E.; Miller, K. M.; Saltzman, W. M. *J. Controlled Release* **2010**, *142*, 474.
- (23) Sipos, L.; Som, A.; Faust, R. *Biomacromolecules* **2005**, *6*, 2570.
- (24) Goyal, N.; El Achchabi, A.; Goldberg, E.; Hochhaus, G. *J. Liq. Chromatogr. Rel. Technol.* **2008**, *31*, 1478.
- (25) Volk, K.; Hill, S.; Kerns, E.; Lee, M. *J. Chromatogr. B* **1997**, *696*, 99.

Chapter 5

5 Conclusions

5.1 Concluding remarks and future directions

The synthesis of functionalized butyl rubbers (RB) has significant importance in the expansion of its applications into different areas. As a result of these modifications, RB and its other copolymers can be utilized in the expanding field of biomaterials. The biomaterials market is currently expanding and RB should be a viable candidate for such applications. However, there are some limitations that can potentially be addressed through modification of the polymer backbone. In order to address some of these limitations, this thesis aimed at introducing carboxylic acid derivatives onto the RB backbone and using these to enhance the properties and application potential of RB.

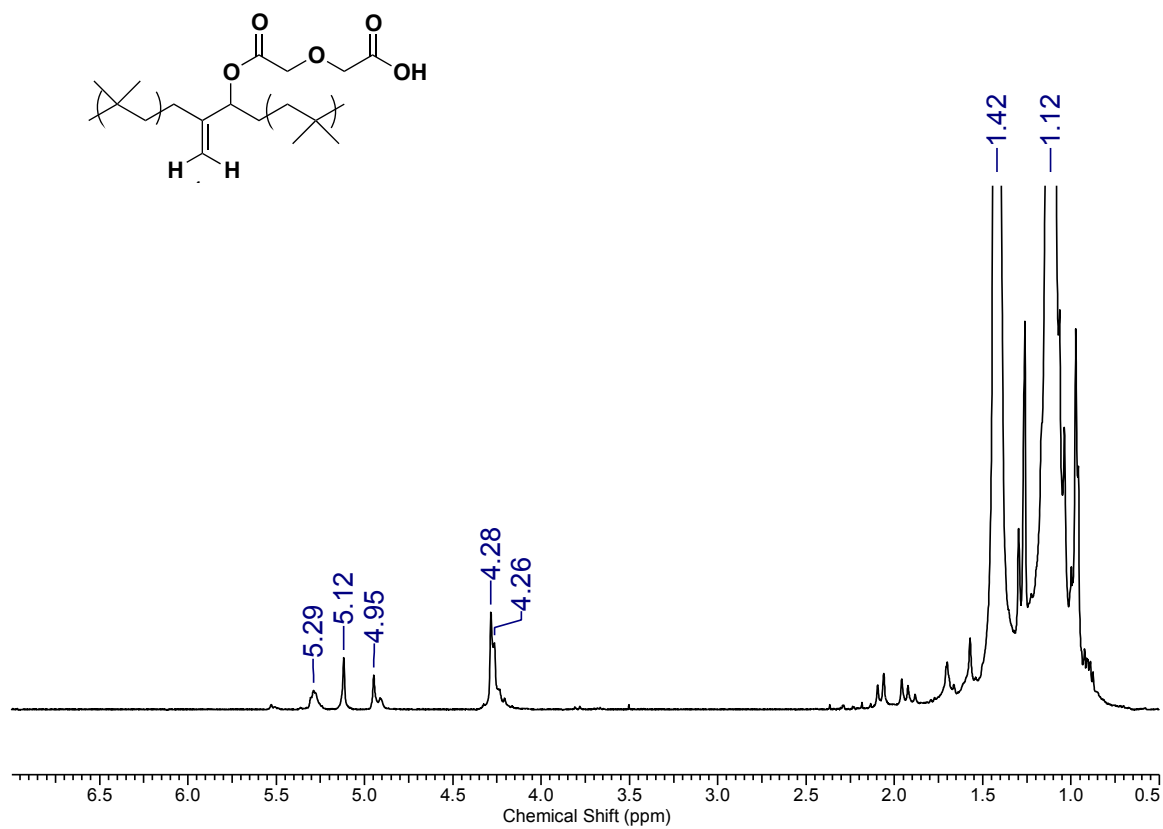
In Chapter 2, the chemical functionalization of RB with acid moieties was described. The ring opening of diglycolic anhydride was a successful method for introducing individual carboxylic acid moieties along the backbone and this was applied to RB containing different isoprene contents to achieve different degrees of carboxylic acid functionalization along the backbone. ATRP was a successful approach for the introduction of poly(carboxylic acid) arms along the backbone to achieve even higher acid content. On the other hand, despite its widespread use, thiol-ene chemistry proved unsuccessful for the functionalization of RB.

In Chapter 3, the acid functionalized RB synthesized using the cyclic anhydride route was examined as a compatibilizer for the deposition of hydrophilic polymers on RB and for increased surface adhesion. When applied to the preparation of poly(ethylene oxide) (PEO) films on RB, it was found to behave similarly to the hydroxylated and epoxidized RB samples, providing compatibilization and thus more uniform films. It also provided enhanced adhesion to stainless steel. When compared to commercial RB, the acid functionalized RB showed greater than two times the adhesion to the stainless steel substrate.

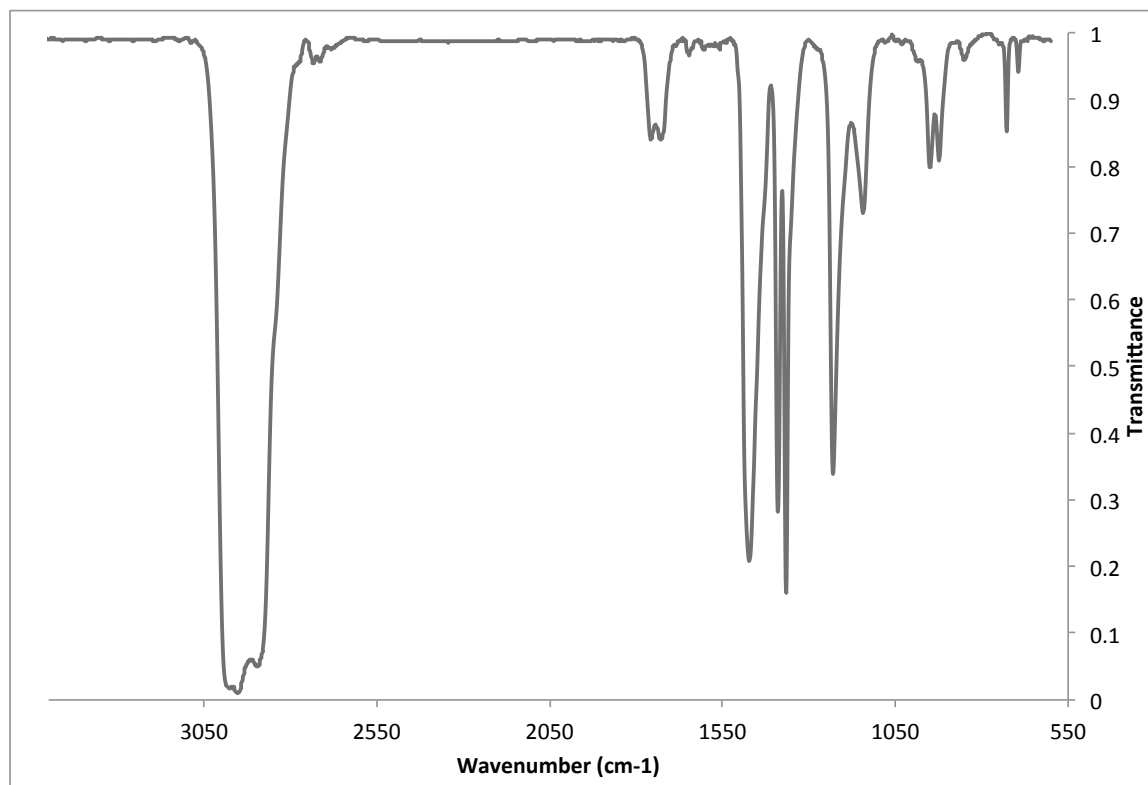
In Chapter 4, the use of carboxylic acid functionalized RB for the preparation of paclitaxel (PTx) conjugates was explored with the aim of slowing drug release for drug eluting stents. The acid functionalized via cyclic anhydride was conjugated with PTx via a carbodiimide coupling. Films on stainless steel substrates were prepared and compared with various controls that did not have the drug covalently conjugated. The conjugated samples showed very slow, sustained release in comparison to the other polymeric films used. Also it was observed that the conjugated samples showed increased adhesion to the stainless steel substrate suggesting the promise of these materials for further investigation.

With respect to future work, there are several aspects that warrant further investigation in the future. The PTx-RB conjugates were coated onto stainless steel plates in this study and it would be ideal to explore the coating on actual stents. The release of drug from the actual stents should then be studied. In addition, unlike the SIBS materials that are used clinically, the current materials are not thermoplastic elastomers and are not covalently cross-linked. Their physical properties should be studied and a means of cross-linking the materials may need to be investigated. The poly(carboxylic acid) functionalized RB, synthesized using ATRP should be tested for increasing surface adhesions as well as producing PTx conjugates. For the application to DES, this project should also be directed towards applying these chemical techniques to the arborescent versions of RB, which are also promising materials for stent coatings.

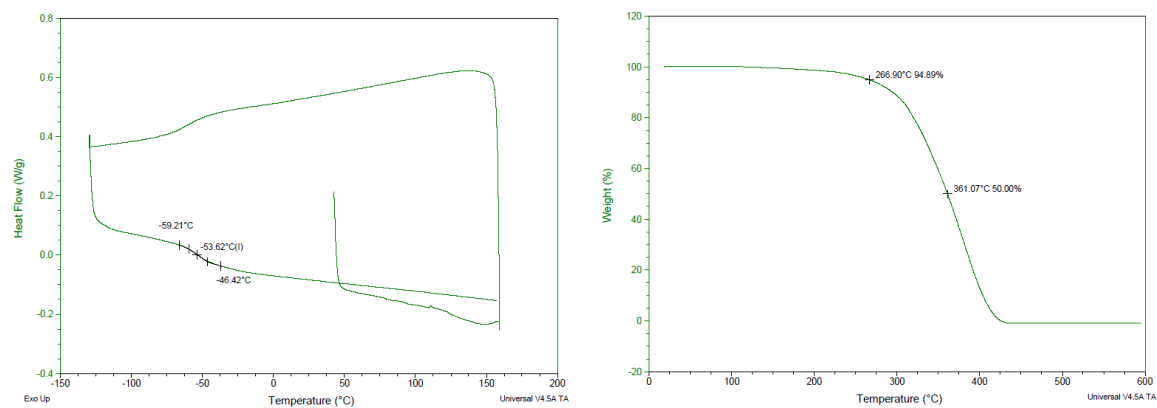
Appendices



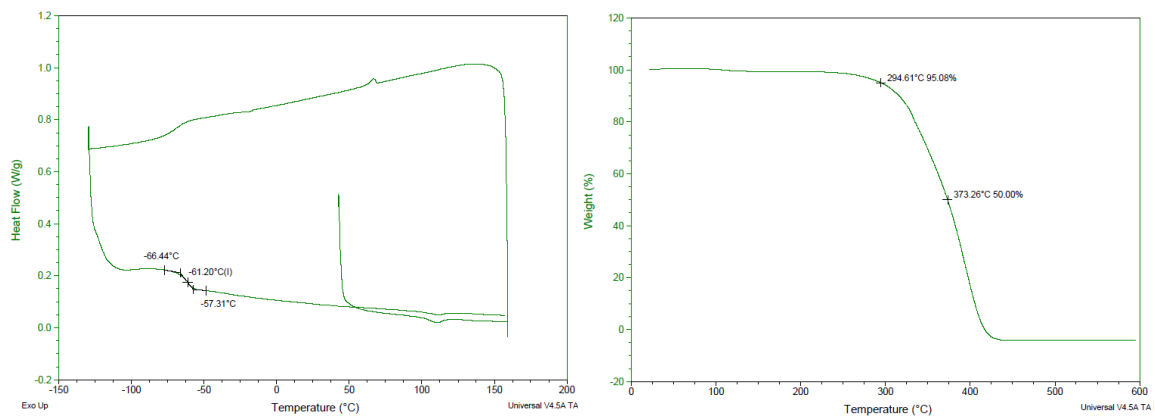
Appendix A ^1H NMR (400 MHz, CDCl_3) of polymer 2.4b with the 7.0% IP RB.



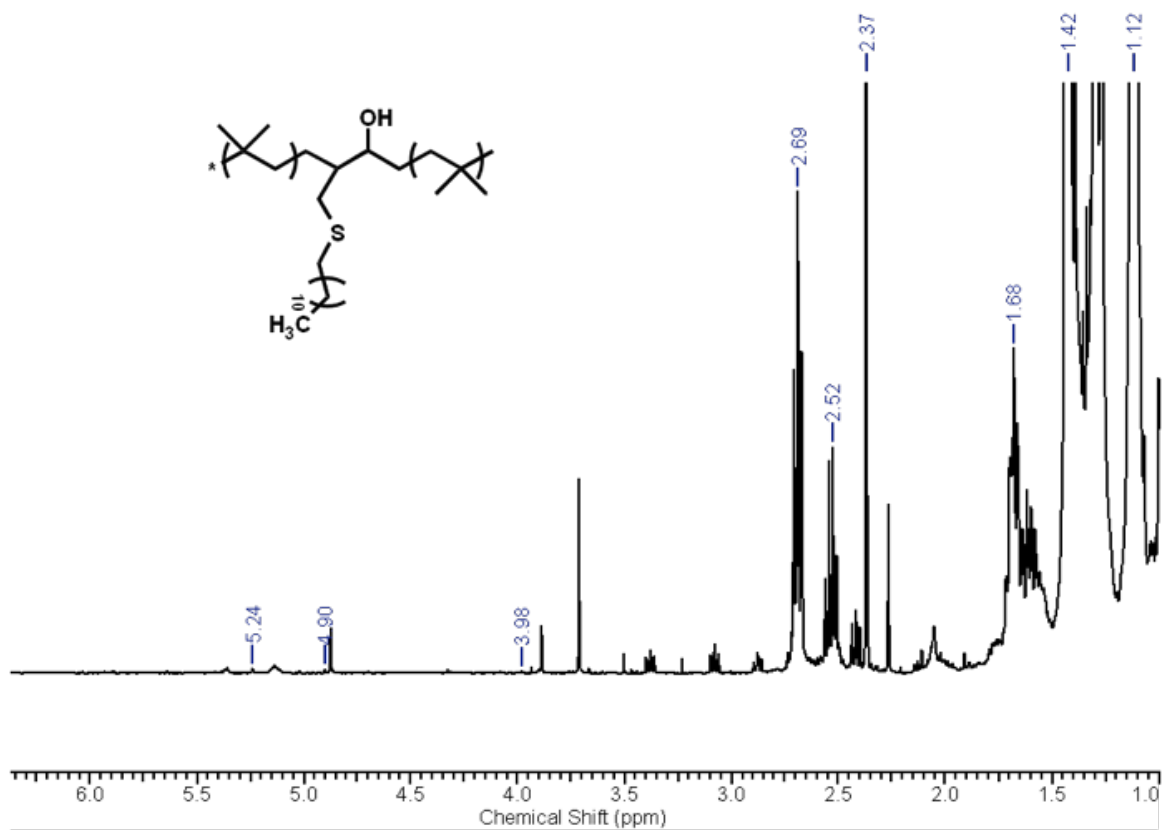
Appendix B IR trace for polymer 2.4b with higher IP content (7%) RB.



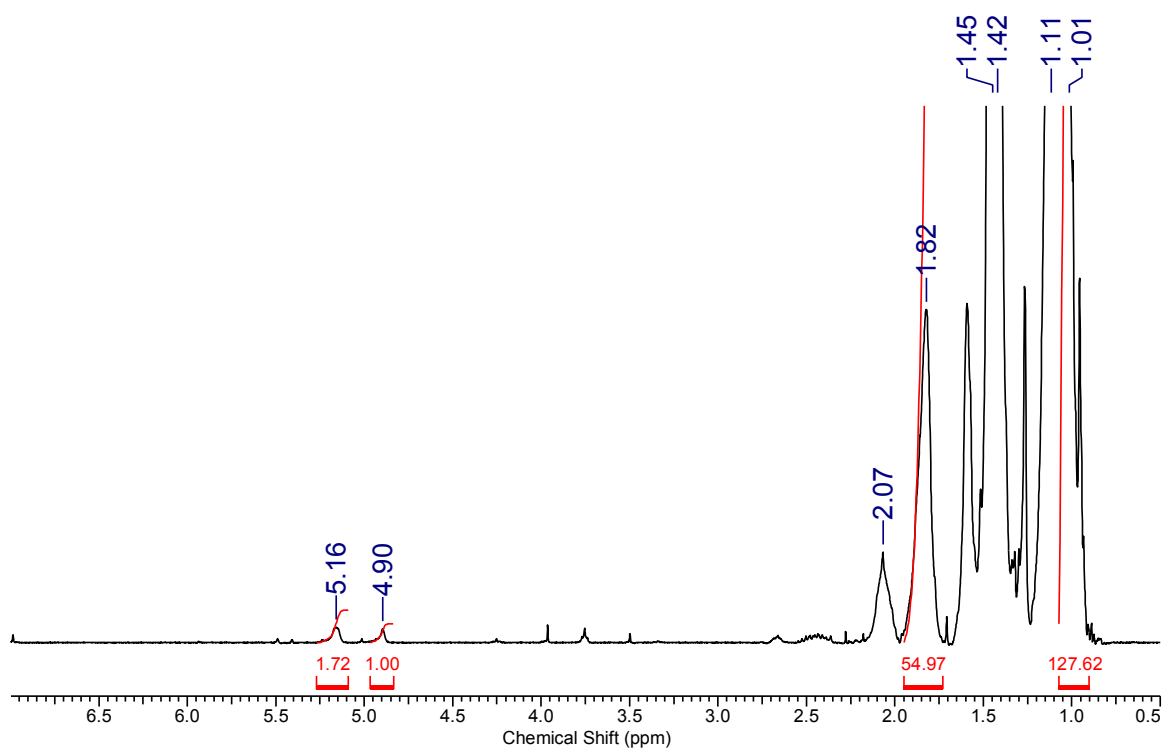
Appendix C left-DSC and right-TGA for polymer 2.4b.



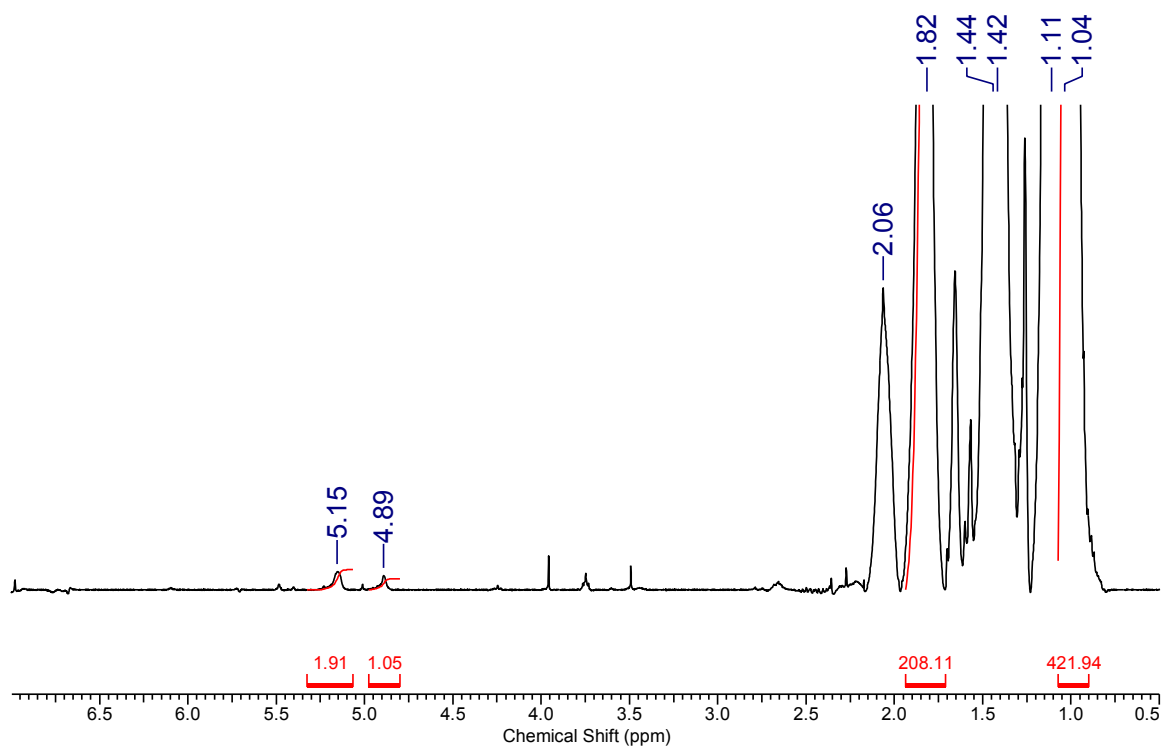
Appendix D left-DSC and right-TGA for polymer 2.4a.



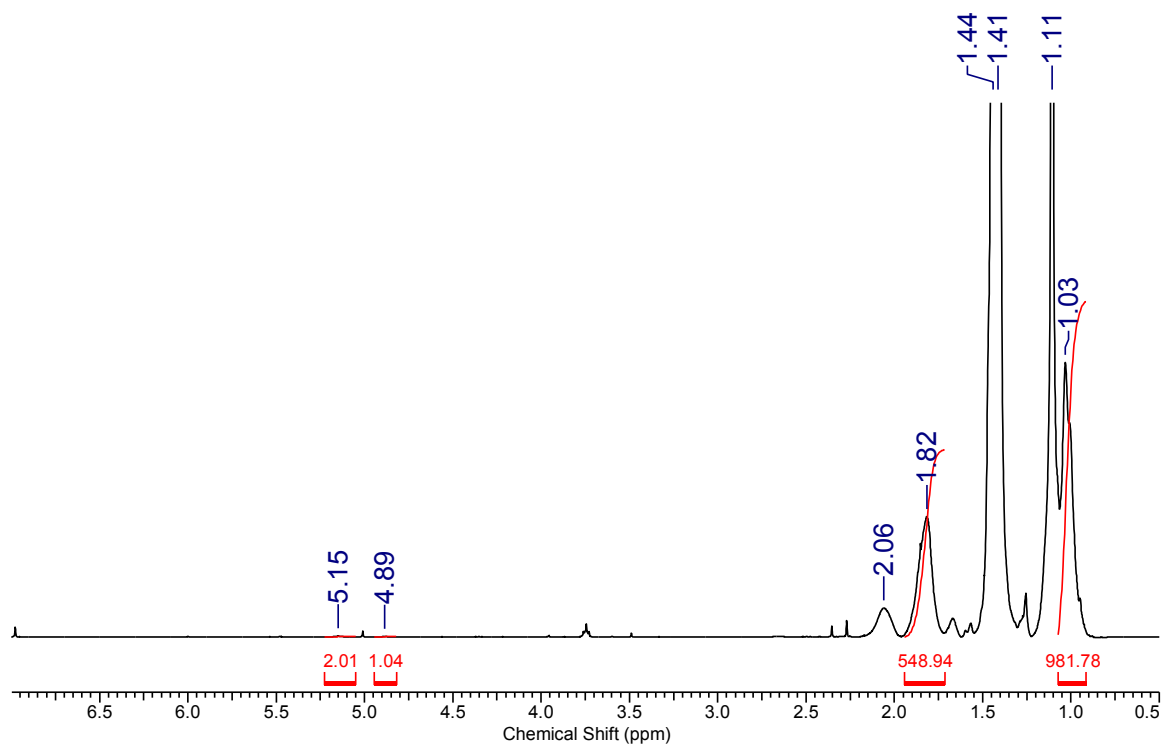
Appendix E ^1H NMR (400 MHz, CDCl_3) of thiol-ene attempts with dodecanethiol with polymer 2.3a.



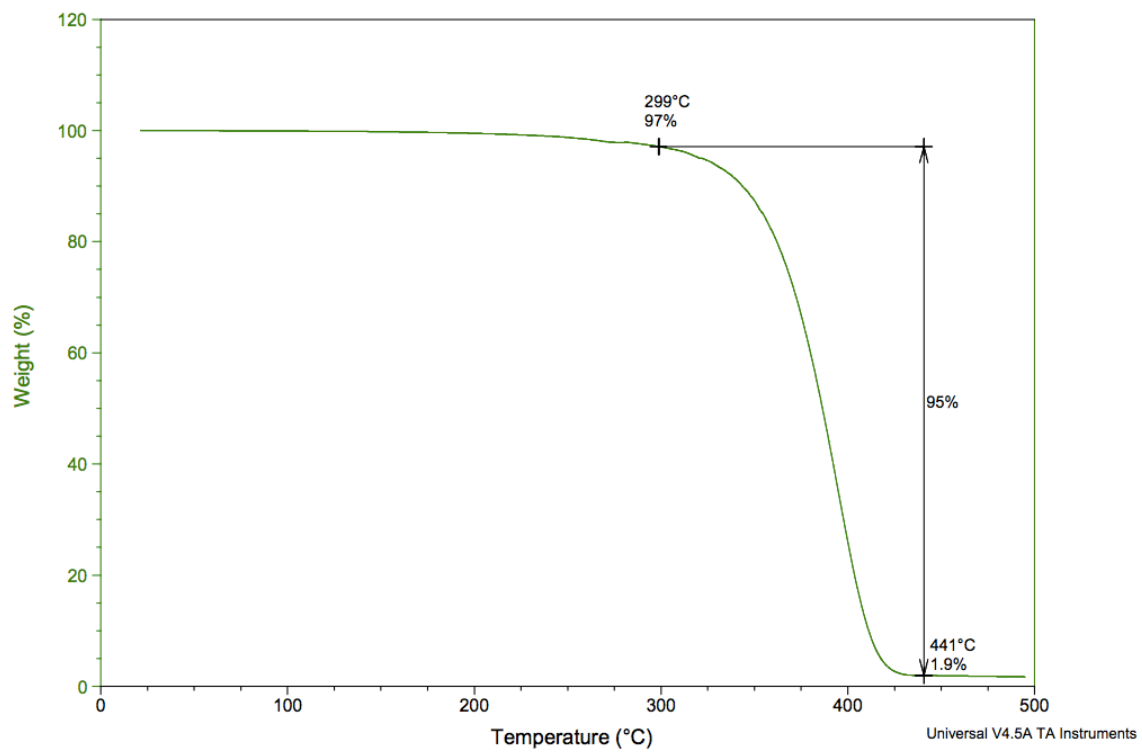
Appendix F ¹H NMR (400 MHz, CDCl₃) of copolymer 2.10.



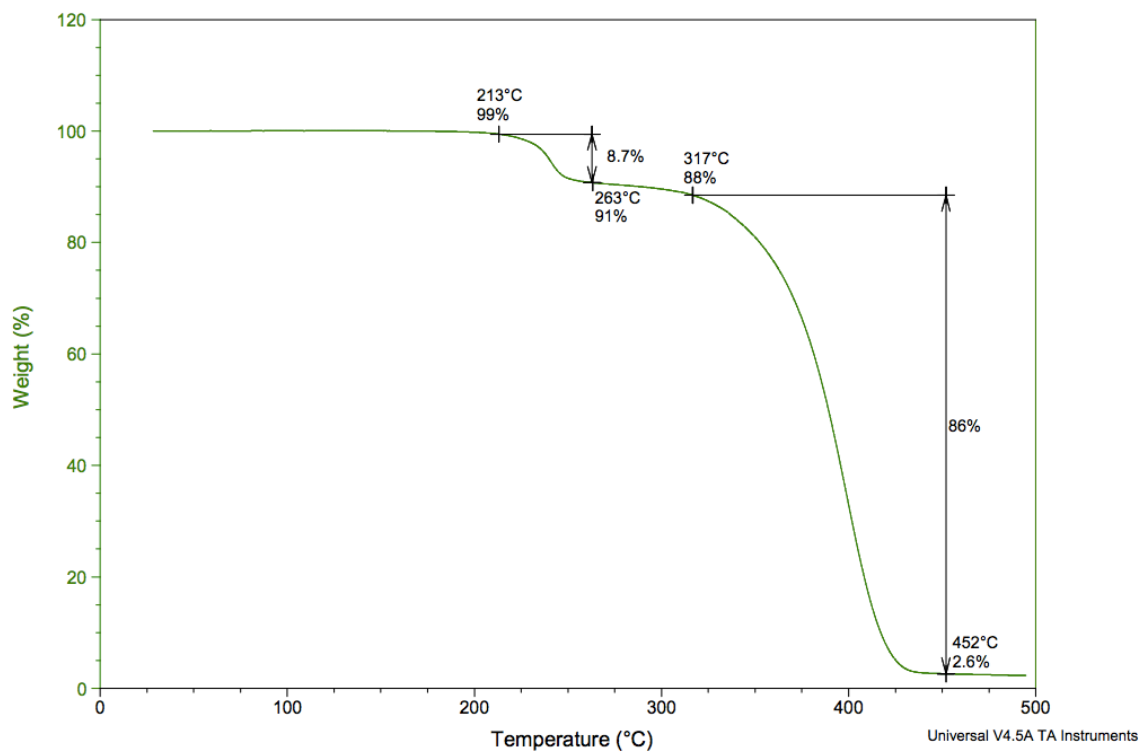
Appendix G ¹H NMR (400 MHz, CDCl₃) of copolymer 2.11.



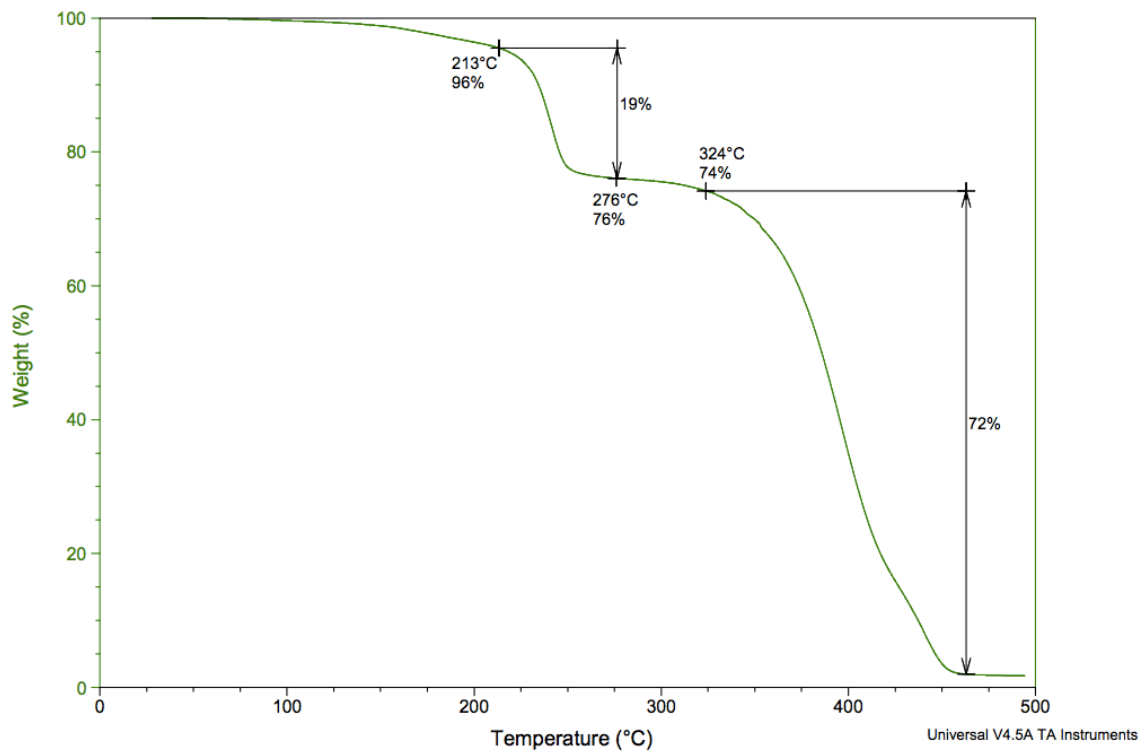
Appendix H ^1H NMR (400 MHz, CDCl_3) of copolymer 2.12.



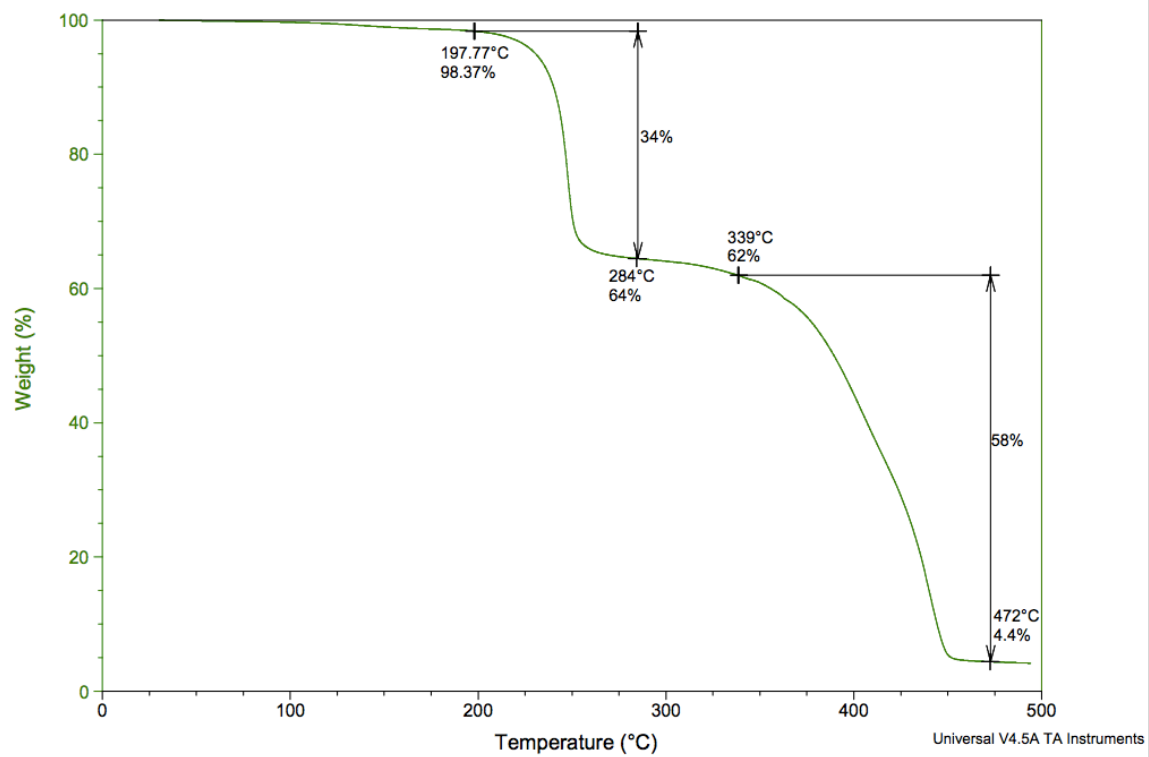
Appendix I TGA analysis of polymer 2.8.



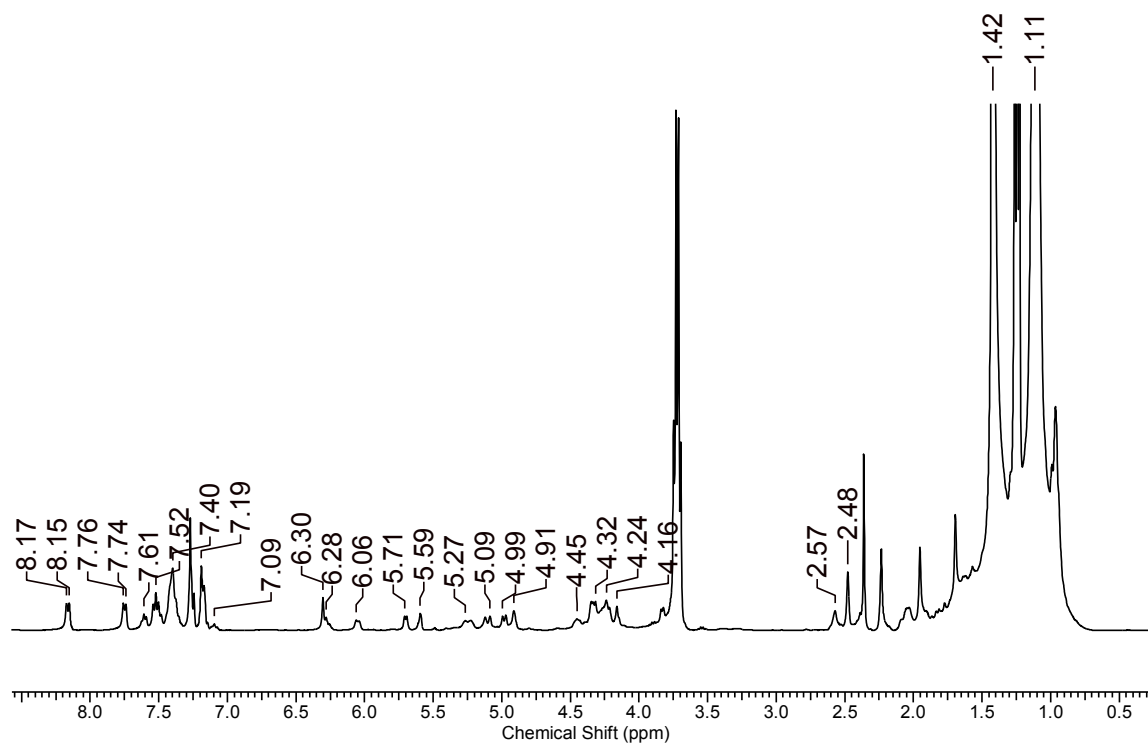
Appendix J TGA analysis of polymer 2.9.



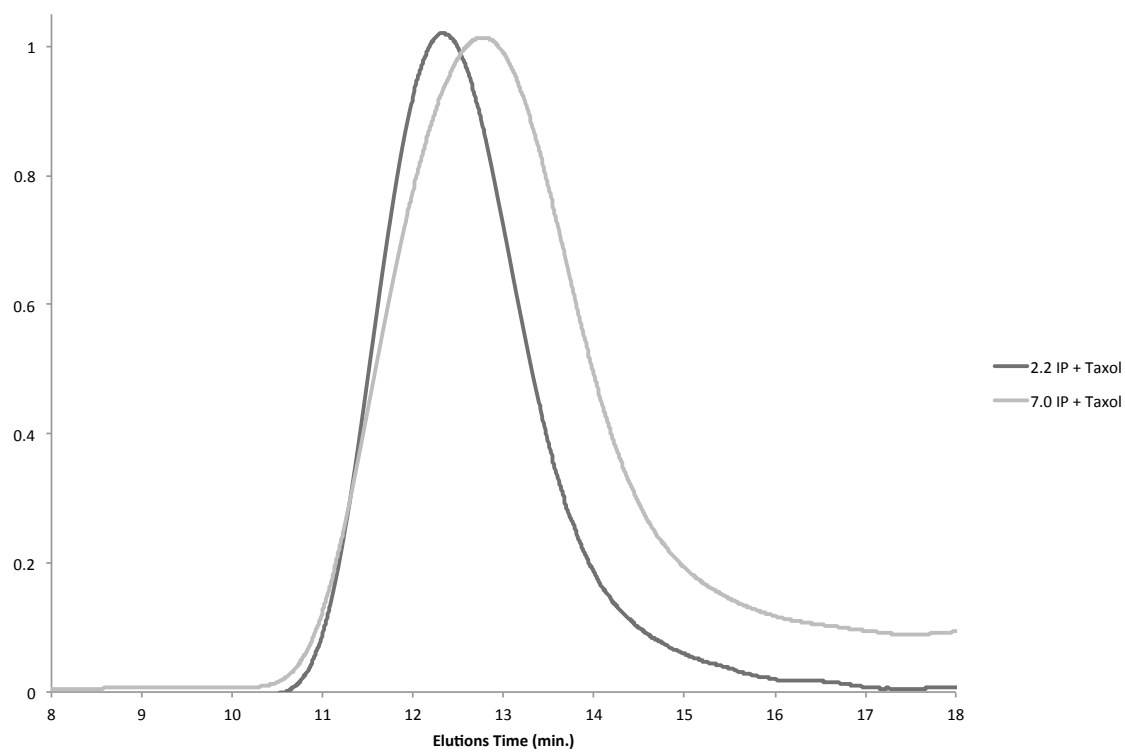
Appendix K TGA analysis of polymer 2.10.



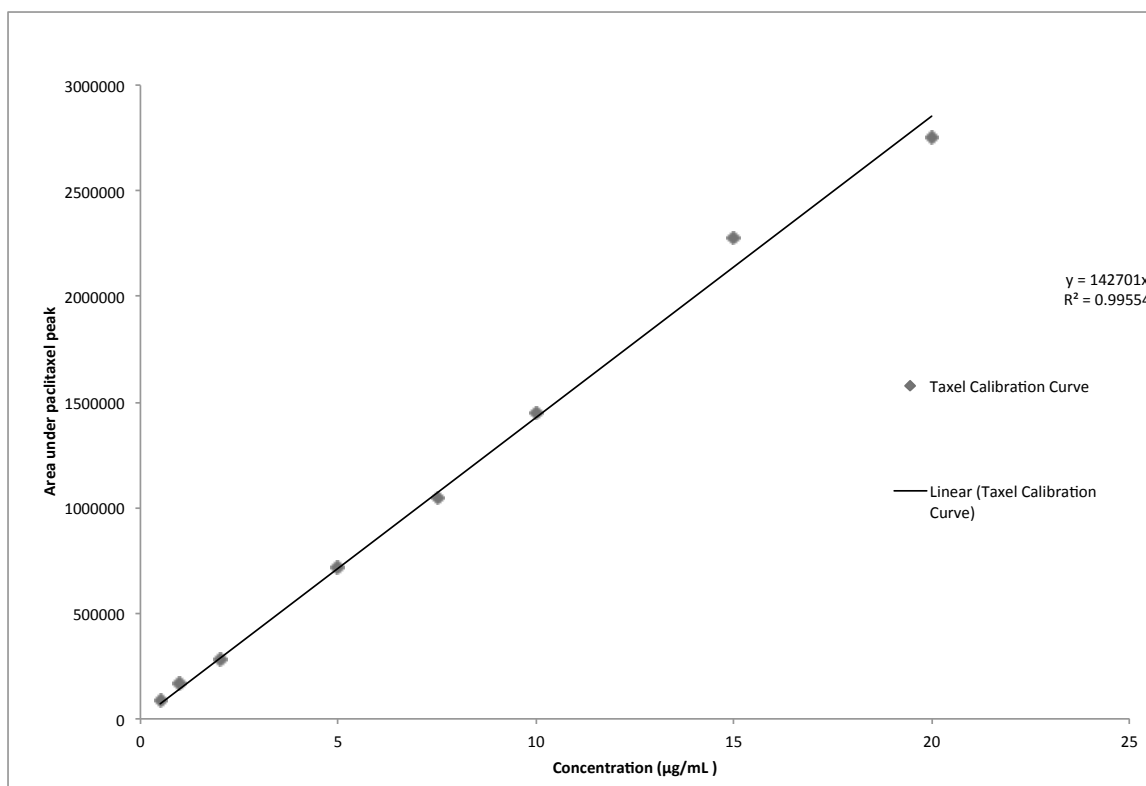
Appendix L TGA analysis of 2.11.



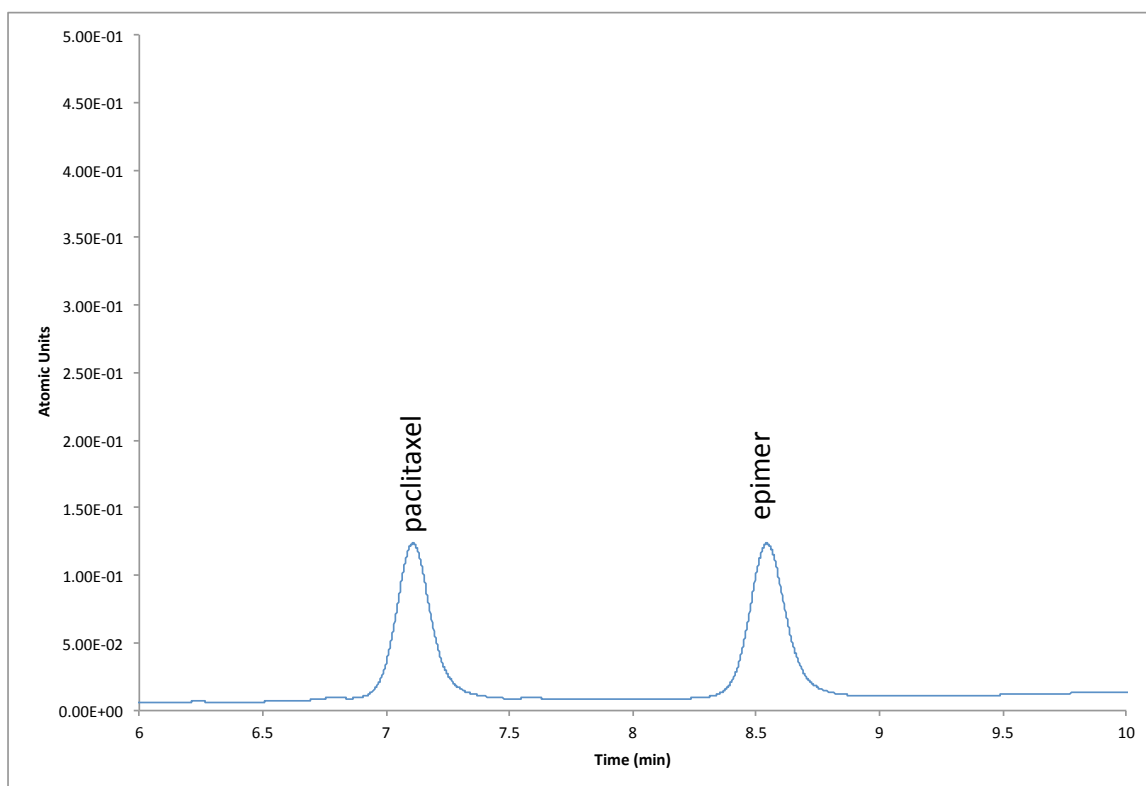
Appendix M ^1H NMR (400 MHz, CDCl_3) of polymer 4.3b.



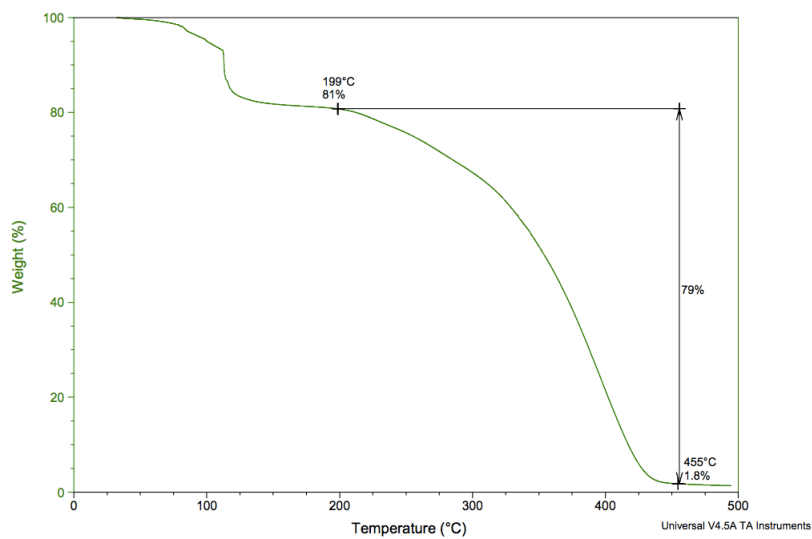
Appendix N SEC traces for the PTx conjugates 4.3a/b.



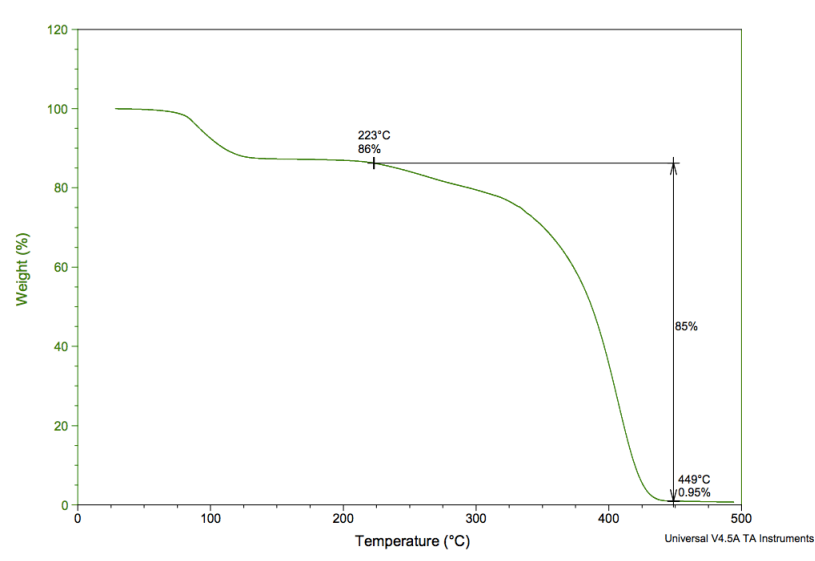
Appendix O Calibration curve for the release study of paclitaxel via HPLC.



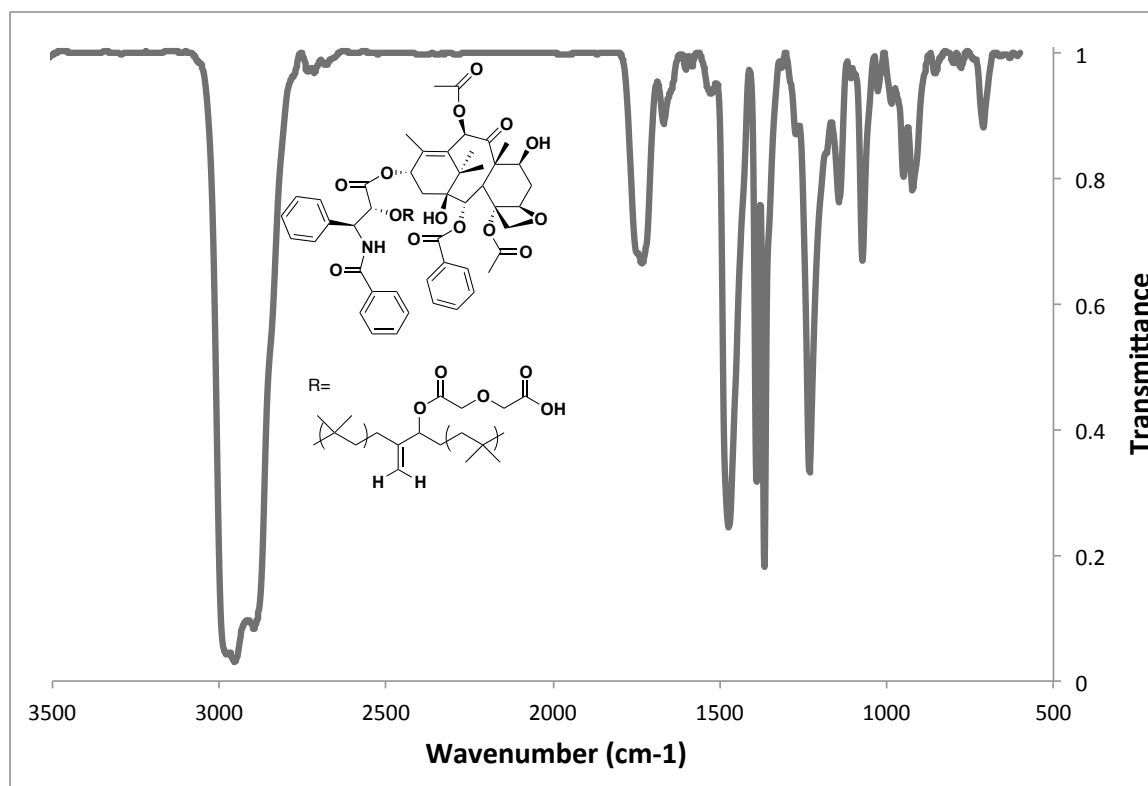
Appendix P Representative HPLC trace for release study.



Appendix Q TGA analysis of PTx conjugate 4.3b.



Appendix R TGA analysis of PTx conjugate 4.3a.



Appendix S IR trace of PTx conjugate of 4.3a.

Curriculum Vitae

Name: MATTHEW J. McEACHRAN

EDUCATION

- 01/2011 – 01/2013 **The University of Western Ontario**, London, Ontario, Canada, M.Sc. in Organic Chemistry
Research advisor: Prof. E.R. Gillies
- 09/2006 – 04/2010 **Wilfrid Laurier University**, Waterloo, Ontario, Canada, H.B.Sc. in Chemistry minor in Biology
Undergraduate honours supervisor: Dr. V. Kitaev

RESEARCH EXPERIENCE

- **Wilfrid Laurier University**, Department of Chemistry (2008-2009)
Summer research assistant
Research advisor: Dr. V. Kitaev
Project: Synthesis of novel Ag and Au nanoparticles

TEACHING EXPERIENCE

- **Teaching Assistant**, University of Western Ontario (2011 – 2013)
Laboratory instructor and help room assistant for
Chemistry 1100 and Chemistry 1200
- **Teaching Assistant**, Wilfrid Laurier University (2008 – 2010)
Laboratory instructor for Chemistry 111 and Chemistry 121

PUBLICATIONS and PATENTS

- Bonduelle, C.; **McEachran, M**; Karamdoust, S.; Gillies, E., R. "An oxygenated rubber derivative as a compatibilizer for the preparation of polymer films." *Journal of Coatings Technology and Research*, 2013, Accepted
- Gillies, E.; Bonduelle, C.; **McEachran, M.**; Arsenault, G.; Stojcevic, G. "Functionalized Copolymers of Isoolefins and Diolefins and their use as Compatibilizers." WO 2012/019303A1, Published 16 Feb. 2012
- Thompson, D.; Trebicky, T.; Crewdson, P.; **McEachran, M.**; Stojcevic, G.; Arsenault, G.; Woon, L.; Gillies, E., R. "Functional Polymer Laminates from Hyperthermal Hydrogen Cross-Linking." *Langmuir*, 2011, **27**, 14820
- **McEachran, M.**; Keogh, D.; Pietrobon, B.; Cathcart, N.; Gourevich, I.; Coombs, N.; Kitaev, V. "Ultrathin Gold Nanoframes through Surfactant-Free

Templating of Faceted Pentagonal Silver Nanoparticles” *J. Am. Chem. Soc.*, 2011, **133**, 8066

- Pietrobon, B.; **McEachran, M.**; Kitaev, V. “Synthesis of Size-Controlled Faceted Pentagonal Silver Nanorods with Tunable Plasmonic Properties and Self-Assembly of These Nanorods” *ACS Nano*, 2009, **3**, 21
- **McEachran, M.**; Kitaev, V. “Direct structural transformation of silver platelets into right bipyramids and twinned cube nanoparticles: morphology governed by defects” *Chem. Commun.*, 2008, 5737

ORAL and POSTER PRESENTATIONS

- **McEachran, M.**; Bonduelle, C.; Karmadoust, S.; Gillies, E.; Ferrari, L.; Stojcevic, G. 95th Annual Canadian Chemistry Conference and Exhibition, Calgary, Alberta (2012), *Oral Presentation*
- **McEachran, M.**; Kitaev, V.; 93rd Annual Canadian Chemistry Conference and Exhibition, Toronto, Ontario (2010), *Poster*
- **McEachran, M.**; Kitaev, V.; 39th Annual Southern Ontario Undergraduate Student Chemistry Conference, London, Ontario (2010), *Oral Presentation*
- **McEachran, M.**; Kitaev, V.; 92nd Annual Canadian Chemistry Conference and Exhibition, Hamilton, Ontario (2009), *Poster*
 - Placed third in poster competition; inorganic division
- **McEachran, M.**; Kitaev, V.; 38th Annual Southern Ontario Undergraduate Student Chemistry Conference, St. Catharines, Ontario (2009), *Oral Presentation*